

# **OTRA Based Multiple Input Single Output Shadow Filter**

A DISSERTATION

SUBMITTED IN FULFILMENT OF THE REQUIREMENTS FOR THE  
AWARD OF THE DEGREE OF

**MASTER OF TECHNOLOGY  
IN  
VLSI DESIGN & EMBEDDED SYSTEMS**

Submitted by:

**SURUCHI**

**2K20/VLS/22**

Under the supervision of:

**Dr. NEETA PANDEY**

**Professor**



**ELECTRONICS & COMMUNICATION  
ENGINEERING**

**DELHI TECHNOLOGICAL UNIVERSITY**

(Formerly Delhi College of Engineering)

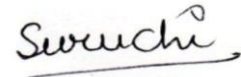
Bawana Road, Delhi-110042

**2021-2022**

## CANDIDATE'S DECLARATION

I, Suruchi, Roll No. 2K20/VLS/22 student of M.Tech (VLSI & Embedded systems), hereby declare that the work presented in this thesis designated “**OTRA Based Multiple Input Single Output Shadow Filter**” is done by me and submitted to the Department of Electronics and Communication Engineering, Delhi Technological University, Delhi in fractional fulfilment of the prerequisite for the award of the degree of Master of Technology.

This is an original research work and not copied from any source without acknowledge them with proper citation and has not previously published anywhere for the award of any Degree, Diploma Associate ship, Fellowship or other similar title or recognition.

A handwritten signature in black ink that reads "Suruchi". The signature is written in a cursive style and is positioned above a horizontal line.

Place: Delhi

(**Suruchi**)


Date: May 2022

## **CERTIFICATE**

I hereby certify that the Project Dissertation titled “**OTRA Based Multiple Input Single Output Shadow Filter**” which is submitted by Suruchi, **2K20/VLS/22**, to the Department of Electronics & Communication Engineering, Delhi Technological University, Delhi in partial fulfilment of the prerequisite for the award of the degree of Master of Technology, is a record of the project work carried out by the student under my supervision. To the best of my knowledge this work has not been submitted in part or full for any Degree or Diploma to this University or elsewhere.

Place: Delhi

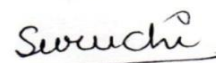
Date: May 2022

  
**PROF. NEETA PANDEY**  
**Department of ECE**  
**Delhi Technological University**

## **ACKNOWLEDGEMENTS**

It gives me immeasurable pleasure to express my deepest sense of gratitude and sincere appreciation to my supervisor, Professor Neeta Pandey, who has the substance of an intellect. She persuasively encouraged and guided me to be professional and do the work in a proper manner. The objective of this project would not have been completed without her persistent help. Her useful suggestions during this whole work and supportive behaviour are sincerely acknowledged.

I would like to acknowledge the support of my family and friends. They helped me a lot directly and indirectly during this project work.

A handwritten signature in black ink that reads "Suruchi". The signature is written in a cursive style with a small flourish at the end. It is positioned above a horizontal line.

Date: May 2022

**SURUCHI**

2K20/VLS/22

## **ABSTRACT**

A shadow filter is a second order filter with an external amplifier in the feedback path, & the characteristics of filters are regulated by adjusting the gain(G) of external amplifier. Authors propose new voltage-mode electronically tunable Low-pass controlled low pass , Low-pass controlled Band-pass filter, Low-pass controlled High- pass filter, Low-pass controlled notch filter, Band-pass controlled Low-pass filter, Band-pass controlled Band-pass filter, Band-pass controlled High- pass filter, Band-pass controlled notch filter, High- pass controlled Low-pass filter, High- pass controlled Band-pass filter, High- pass controlled High- pass filter, High- pass controlled notch filter, notch-controlled Low-pass filter, Notch controlled Band-pass filter, Notch controlled High- pass filter and Notch controlled notch filter shadow filters. The operational transconductance amplifier is built into the filters (OTRA). OTRA uses CMOS technology to provide an electronic tuning capability for its transresistance gain by adjusting its bias current or voltage. The OTRA-implemented circuits do not require a resistor, making them ideal for any integrated circuit implementation. In every case, the gain of an external amplifier built around the operational transresistance amplifier can be adjusted electronically to control one or more filter parameters. The shadow filter is implemented using the MISO configuration, which eliminates the need for an external summing amplifier. Component-matching conditions are not required to implement filter functions. To verify the presented theory, the proposed shadow filter is simulated using the LTspice simulator with a 180nm CMOS process.

## TABLE OF CONTENTS

<b>Candidate's Declaration</b>	ii
<b>Certificate</b>	iii
<b>Acknowledgement</b>	iv
<b>Abstract</b>	v
<b>Contents</b>	vi
<b>List of Figures</b>	viii
<b>List of Table</b>	x
<b>1. INTRODUCTION</b>	<b>1-4</b>
1.1. Background	1
1.2. Objective	4
1.3. Organization of Thesis	4
<b>2. OPERATIONAL TRANSRESISTANCE AMPLIFIER</b>	<b>5-10</b>
2.1. OTRA Basics	5
2.2. Differential OTRA	6
2.2.1. CMOS Realization of OTRA	7
2.2.2. Simulation Results	8
2.3. Summary	10
<b>3. OTRA BASED APPLICATIONS</b>	<b>11-24</b>
<b>3.1. PROPORTIONAL CONTROLLER</b>	<b>11</b>
3.1.1. Introduction	11
3.1.2. Simulation results	12
3.2. PD Controller	15
3.2.1. Circuit realization	16

3.2.2. Simulation results	17
3.3. PI CONTROLLER	19
3.3.1. Circuit realization	17
3.3.2. Simulation results	20
3.4. PID CONTROLLER	22
3.4.1. Circuit realization	23
3.4.2. Simulation results	24
3.5. Summary	24
<b>4. LITERATURE SURVEY</b>	<b>25-29</b>
4.1. Introduction	25
4.2. Available topologies of Shadow filter	25
4.3. Available literature	27
4.4. Summary	31
<b>5. MULTIPLE INPUT SINGLE OUTPUT SHADOW FILTER</b>	<b>31-61</b>
5.1. Introduction	31
5.2. Proposed OTRA MISO Shadow filter	32
5.2.1. Positive feedback	35
5.2.2. Negative feedback	47
5.3. Summary	59
<b>6. SIMULATION AND RESULT</b>	<b>62-54</b>
6.1. Simulation result	62
6.2. Summary	64
<b>7. CONCLUSION AND FUTURE WORK</b>	<b>65</b>
<b>REFERENCES</b>	<b>66-68</b>

## **LIST OF FIGURES**

- Fig.2.1 Symbol of OTRA  
Fig 2.2 Small Signal AC Equivalent of OTRA  
Fig 2.3 Symbol of Differential OTRA  
Fig 2.4 Small Signal AC Equivalent of Differential OTRA  
Fig 2.5 CMOS Realization of Differential OTRA Proposed in [33].  
Fig 2.6 OTRA implementation  
Fig 2.7: Output Characteristics of OTRA  
Fig 2.8: Transient response of OTRA  
Fig. 3.1 Control System with P-controller  
Fig. 3.2 OTRA based P-Controller  
Fig. 3.3 Transient response of the P Controller  
Fig. 3.4 Frequency and phase Response of P controller  
Fig. 3.5 Frequency and phase Response of MOS-C implementation of P controller  
Fig. 3.6 Closed Loop Control System using P controller  
Fig. 3.7: (a) Step Response of a second order system without P controller  
(b) Step Response of a second order system with P controller  
Fig. 3.8 Control System with PD-controller  
Fig. 3.9 OTRA based Proposed PD Controller  
Fig. 3.10 Transient response of the PD Controller  
Fig. 3.11 Frequency and phase Response of PD controller  
Fig. 3.12 Control System with PI-controller  
Fig. 3.13 OTRA based Proposed PI Controller  
Fig. 3.14 Transient response of the PI Controller  
Fig. 3.15 Frequency and phase Response of PI Controller  
Fig. 3.16 Block diagram of PID Controller  
Fig. 3.17 OTRA based Proposed PID Controller  
Fig. 3.18 Transient response of the PID Controller  
Fig.4.1. Second order voltage mode shadow filter  
Fig.4.2 Voltage mode shadow filter with amplifier feedback  
Fig 4.3: OTRA based shadow filter configuration.  
Fig: 4.4 OTRA controlled multi output shadow filter.  
Fig 5.1: Second Order MISO filter  
Fig 5.2: Signal flow graph of MISO filter  
Fig 5.3: (a) Block diagram of proposed shadow filter using MISO universal filter.  
(b) Schematic of MISO shadow filter  
Fig 5.4: (a) LP filter (b) BP filter, (c) HP filter, (d) Notch filter  
Fig 5.5: Signal flow graph of Low pass controlled Low pass shadow filter  
Fig 5.6: Signal flow graph of Band-pass controlled Band pass shadow filter  
Fig 5.7: Signal flow graph of High pass controlled High pass shadow filter  
Fig 5.8: Signal flow graph of Notch controlled notch shadow filter  
Fig 5.9: Signal flow graph of Band pass controlled Low pass shadow filter  
Fig 5.10: Signal flow graph of High pass controlled Low pass shadow filter  
Fig 5.11: Signal flow graph of Notch controlled Low pass shadow filter  
Fig 5.12: Signal flow graph of Low pass-controlled Band pass shadow filter  
Fig 5.13: Signal flow graph of High pass-controlled Band pass shadow filter  
Fig 5.14: Signal flow graph of Notch controlled Band pass shadow filter  
Fig 5.15: Signal flow graph of Low pass controlled High pass shadow filter  
Fig 5.16: Signal flow graph of Band pass controlled High pass shadow filter  
Fig 5.17: Signal flow graph of Notch controlled High pass shadow filter



Fig 5.18: Signal flow graph of Low pass-controlled Notch shadow filter  
Fig 5.19: Signal flow graph of Band-pass controlled Notch shadow filter  
Fig 5.20: Signal flow graph of High pass-controlled Notch shadow filter  
Fig 5.21: Signal flow graph of Low pass controlled low pass shadow filter  
Fig 5.22: Signal flow graph of Band-pass controlled band pass shadow filter  
Fig 5.23: Signal flow graph of High pass controlled high pass shadow filter  
Fig 5.24: Signal flow graph of Notch controlled notch shadow filter  
Fig 5.25: Signal flow graph of Band pass controlled Low pass shadow filter  
Fig 5.26: Signal flow graph of High pass controlled Low pass shadow filter  
Fig 5.27: Signal flow graph of Notch controlled Low pass shadow filter  
Fig 5.28: Signal flow graph of Low pass-controlled Band pass shadow filter  
Fig 5.29: Signal flow graph of High pass-controlled Band pass shadow filter  
Fig 5.30: Signal flow graph of Notch controlled Band pass shadow filter  
Fig 5.31: Signal flow graph of Low pass controlled High pass shadow filter  
Fig 5.32: Signal flow graph of Band pass controlled High pass shadow filter  
Fig 5.33: Signal flow graph of Notch controlled High pass shadow filter  
Fig 5.34: Signal flow graph of Low pass-controlled Notch shadow filter  
Fig 5.35: Signal flow graph of Band-pass controlled Notch shadow filter  
Fig 5.36: Signal flow graph of High pass-controlled Notch shadow filter

## **LIST OF TABLES**

Table 2.1: Transistor aspect ratio utilised in OTRA

Table 5.1: Characteristic Features of Positive Feedback MISO Shadow Filter

Table 5.2: Characteristic Features of Negative Feedback MISO Shadow Filter

Table 5.3: Signal Flow Graph and Frequency Response of Filters

# **CHAPTER 1**

## **INTRODUCTION**

### **1.1. BACKGROUND**

This is a digital age, and everything employs digital components to some extent, such as computers, communications, and broadcasting. Though digital systems have numerous advantages over analogue systems, they must be interfaced with the real world. If undesired aliasing effects are not to be created, digital signal processing, for example, gives an advantage only if it is performed on bandlimited signals. After going through the reconstruction filter, the signals are returned to the real analogue environment. The analogue filters that work in continuous time are both bandlimited and reconstruction filters. Continuous time filters are used in any system that interacts with the actual world [1].

Analog filters were once used to process analogue signals in real time, as opposed to digital filters, which filter digital representations of signals samples infrequently in real time. Then, in the 1970s, sampled data filters became popular. Sampled data filters operate on the samples themselves rather than digital representations of sampled signals. The best example of this strategy is the switched capacitor filter, which filters data using switches, capacitors, and active devices. Due to the switching that occurs in these circuits, the time of these filters is discontinuous. As a result, constant band limitations and reconstruction filters were required [1]. The advantages of switched capacitor filters for integrated circuit implementation led to a lot of study in the 1970s and 1980s. When capacitor filters failed to give all of the solutions, traditional procedures gained popularity, and the term "continuous time filter" was established to differentiate them from their digital and sampled data equivalents.

The classic LCR filters, which use inductors, capacitors, and resistors, are widely used, but they are unsuitable for use in integrated circuits because no satisfactory method for making inductors on chip has been discovered [1]. This is why active continuous time filters have attracted so much interest over the years. Active filters allow complex filters to be integrated on a chip while avoiding the problems that bulky, lossy, and expensive filters have.

For a long time, active filters have been used to overcome the drawbacks of passive filters. Sallen & Key is a popular active RC filter that has been around for over 40 years. Voltage amplifiers, resistors, and capacitors are used. However, active filter research continues to this day, with thousands of research papers published on the subject over the years. There are numerous reasons for this, but two stand out in particular. First, due to changes in technology, a new approach was required, so the inexpensive and readily available OP-AMPs replaced their discrete circuit counterparts. As a result, large numbers of OP-AMPs can now be used to implement filter circuits, resulting in a new improved architecture. Similarly, the development of the operational trans resistance amplifier, or OTRA, resulted in new filter configurations. Second, as the world of electronics and communications has progressed, the demand for filter circuits has increased. The OTRA is a crucial basic component found in many analogue circuits with linear input-output characteristics. The OTRA (Operational Trans Resistance Amplifier) is a voltage output amplifier with a high gain current input. Because its input terminals are essentially grounded, OTRA inherits the benefits of current mode processing and is free of parasitic input capacitances and resistances because it is a current mode building block. As a result, non-ideality issues in circuits using OTRA are reduced. The use of OTRA-based controllers has yet to be documented.

Noise has a particularly noticeable effect in low-power analogue applications. Analogue IC designers generally develop their circuitry as differential rather than single-ended designs to reduce the effect of noise on circuits.

In light of the foregoing, this dissertation introduces Differential Operational Transresistance Amplifier-based controllers. Second order closed loop system with Low Pass Filter of second order is used to verify the theoretical analysis of these controllers, and the controllers are designed and simulated using LTspice.

OTRA is the foundation for a wide range of current, voltage, and mixed mode applications. The first OTRA CMOS circuit was introduced by J. J. Chen, H. W. Tsao, and C. C. Chen in 1992 [4]. Because OTRA have virtually grounded input terminal, circuits designed with it are insensitive to stray capacitances [5]. Salama and Ahmed M. Soliman published a simple CMOS implementation of OTRA [6] in 1999, which relied on a cascaded MDCC and a common source amplifier. They suggested a novel circuit in [7], which uses the same cascaded connection of modified differential current conveyor (MDCC) and a common source amplifier as in [6, but with better performance and fewer transistors. The circuit described in [8] uses the same input stage as the OTRA presented in [7], but rather than a single common source amplifier, it uses a differential gain stage with a compensation circuit to correct for the difference in the two-input transistor drain voltages. In literature, there are several other CMOS implementations of OTRA [10-12]. A voltage buffer is

utilized in circuit [10], accompanied by a differential current controlled current source (DCCCS), whereas  $R_m$  cell, output driver, and feedback network are employed in circuit [11]. The circuit presented in [12] uses a low voltage regulated cascode load as well as a low voltage regulated cascode current mirror. OTRA is a commercially available current differencing or Norton amplifier from several manufacturers [13-15].

There are numerous OTRA applications in the literature. Filters based on OTRA are proposed in [5-6, 16-21], oscillators and multi vibrators in [21-27], and Schmitt trigger is presented in [28]. [29-31] describes immittance realizations using OTRA.

A new method for electronic adjustment of the filter parameters has been incorporated in a recently proposed family of second-order filters known as the shadow filters [17]. This type of filter necessitates the use of an external amplifier in the feedback loop, and the filter's properties are altered by raising the external amplifier's gain ( $A$ ). Shadow filters are gaining in popularity [17]-[27]. This is due to its ability to change various filter parameters, such as bandwidth, over a wide range by simply adjusting the gain from outside the filter, without disturbing any active or passive component of the filter. On the other hand, the transition between the two continuous centre frequencies will become extremely fast. Both voltage-mode and current-mode circuits can benefit from the shadow filter theory. The shadow filter was created with a variety of blocks, including the second-generation current controlled conveyor (CCCII), operational transresistance amplifier (OTRA), differential difference current conveyor (DDCC), and others, but not the OTA. A new OTRA-based Multiple Input Single Output Shadow Filter is proposed in this thesis. The benefit of this suggested shadow filter is that it does not require component-matching requirements to implement the filter functions, as well as not requiring a summing amplifier, which is required in current mode shadow filters.

## **1.2. OBJECTIVE**

In light of the foregoing discussion, the thesis focuses on the following goals for creating voltage-mode OTRA-based shadow filters:

1. OTRA research and characterization
2. Examining and implementing OTRA-based applications
3. Construction of an OTRA-based shadow filter

LTspice simulators with 180nm m CMOS are used for all simulations.

## **1.3. ORGANIZATION OF THESIS**

**Chapter 1:** The first chapter provides a brief overview of filters and their significance in the operation of various electronic circuits. The motivation and goal of the work are also discussed in this chapter.

**Chapter 2:** Provides a brief overview of OTRA, as well as studies and simulations. It's also characterized for DC and transient responses, and simulations are used to extract various performance parameters.

**Chapter 3:** Some existing OTRA applications are being implemented and verified. Proportional (P), proportional-derivative (PD), proportional integrator (PI), and proportional integral and derivative (PID) differentiators are among the applications.

**Chapter 4:** A review of the shadow filter literature and its structure, as well as a look at different multi-input single-output voltage-mode universal filters that use OTRAs.

**Chapter 5:** A new single-feedback shadow filter structure is proposed, as well as various single-feedback shadow filter configurations such as band pass controlled low pass shadow filter, high pass controlled low pass shadow filter, and low pass controlled low pass shadow filter, which are implemented and simulated in both positive and negative feedback configurations to compare simulation results to theoretical values. The filter responses are simulated to ensure that the proposed filter is functional.

**Chapter 6:** This chapter summarizes the work presented in this thesis as well as discussing future work.

## CHAPTER 2

### OPERATIONAL TRANSRESISTANCE AMPLIFIER

The fundamentals of OTRA as well as Differential OTRA are covered in this chapter. The CMOS implementation of Differential OTRA [9], as well as the simulation results, are discussed here. The controllers proposed in this paper are designed using this simulated Differential OTRA.

#### 2.1 OTRA Basics

The OTRA (Operational Trans-resistance Amplifier) is a voltage output amplifier with a high gain current input [4]. Figure 2.1 depicts the OTRA symbol. The matrix equation for OTRA, a three-terminal device, is:

$$\begin{bmatrix} V_p \\ V_n \\ V_o \end{bmatrix} = \begin{bmatrix} 0 & 0 & 0 & 0 \\ 0 & 0 & 0 & 0 \\ R_m & -R_m & 0 & 0 \end{bmatrix} \begin{bmatrix} I_p \\ I_n \\ I_o \end{bmatrix}$$

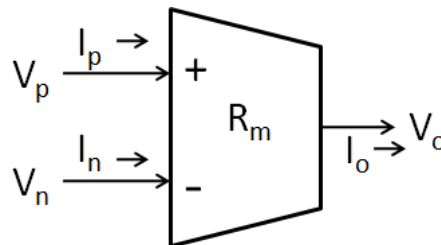


*Fig. 2.1 OTRA Symbol*

The input and output terminals have low impedance, removing response constraints imposed by capacitive time constants, as shown in the above equation. The circuits are impervious to stray capacitances because the input terminals are practically grounded [5]. External negative feedback should be used to force the input currents,  $I_p$  &  $I_n$ , to equalise [6]. The ideal value for  $R_m$  is infinity. As a result, OTRA must rely on negative feedback to function. In practise, transresistance gain is limited & should be considered. Frequency constraints imposed by OTRA must also be considered. If the transresistance gain in a single-pole model is represented by  $R_m$  [6,] then:

$$R_m(s) = \left( \frac{R_0}{1 + s/\omega_0} \right) \quad (2.2)$$

For high frequency applications transresistance gain ( $R_m(s)$ ) can be expressed as follows:

$$R_m(s) \approx \left( \frac{1}{sC_p} \right) \quad (2.3a)$$

where

$$C_p = \frac{1}{R_0\omega_0} \quad (2.3b)$$

The DC open loop transresistance gain is  $R_0$ , while the transresistance cut off frequency is  $\omega_0$ . Figure 2.2 shows the small signal AC equivalent of OTRA.

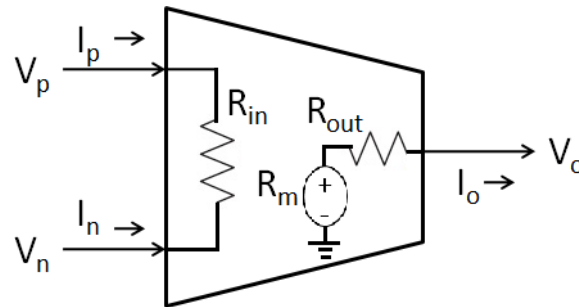


Fig. 2.2 OTRA's Small Signal AC Equivalent

## 2.1 Differential OTRA

The dynamic range and power supply rejection of single-ended signal processing are lower than those of differential signal processing. In low-power circuits, these parameters are especially important. Differential circuits also have lower harmonic distortion and are less susceptible to common-mode noise signals.

Differential OTRA is defined as a four-terminal device using the matrix equation [39].

$$\begin{bmatrix} V_+ \\ V_- \\ V_o \end{bmatrix} = \begin{bmatrix} 0 & 0 & 0 \\ 0 & 0 & 0 \\ R_m & -R_m & 0 \end{bmatrix} \begin{bmatrix} I_+ \\ I_- \\ I_o \end{bmatrix}$$



Figures 2.3 and 2.4 illustrate the differential OTRA symbol and tiny signal ac equivalents, respectively. [32].

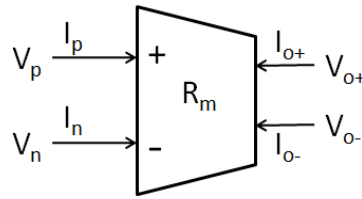


Fig. 2.3 OTRA Differential Symbol [39]

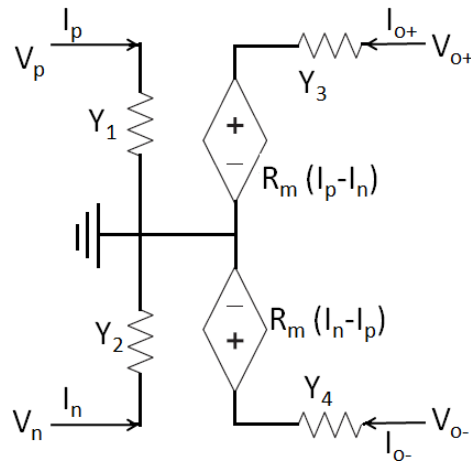


Fig. 2.4 Differential OTRA Small Signal AC Equivalent [39].

### 2.2.1 Differential OTRA realization using CMOS

A CMOS implementation of the differential OTRA proposed in [9] is shown in Figure 2.5. A differential gain stage and a Modified Differential Current Conveyor (MDCC) are connected in a cascade [40].

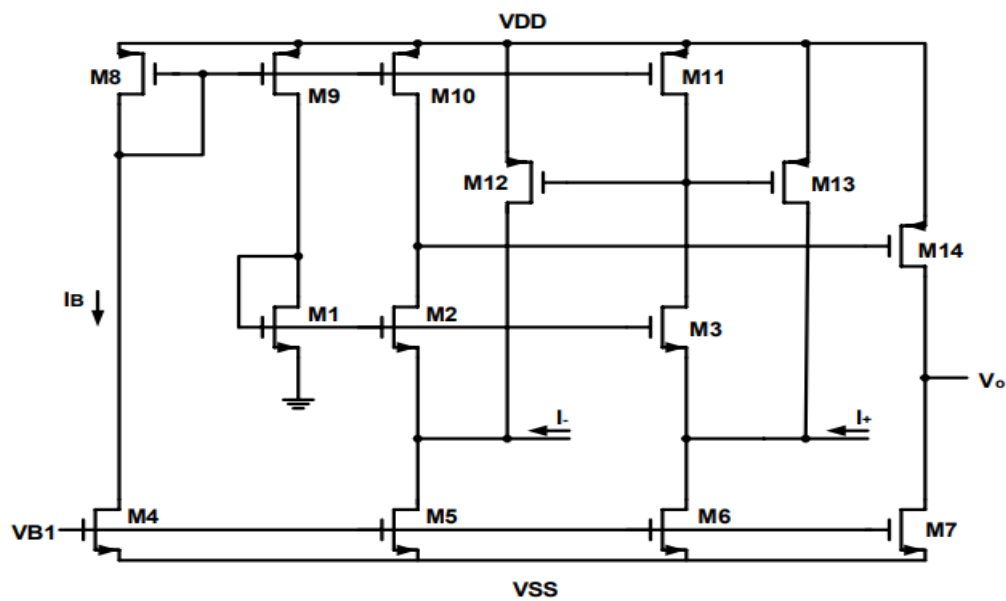


Fig. 2.5 Differential OTRA realization using CMOS Proposed in [33].

Figure 2.5 depicts the proposed low-power wide-band OTRA's CMOS implementation. A cascaded Modified Differential Current Conveyor (MDCC) and a common source amplifier form the basis of the system. Assume that transistor groups M1-M3, M5 and M6, M8-M11, and M12 and M13 are all matched. The circuit works as follows, assuming that all of the transistors are in the saturation region.

Equal currents ( $I_B$ ) are forced in transistors M1, M2, and M3 by current mirrors (M8-M11). This operation effectively grounds the two input terminals by making the gate to source voltages of M1, M2, and M3 equal.

The current mirrors generated by the transistor pairs (M10 and M11) and (M12 and M13) offer current differencing, while the common source amplifier provides the high gain stage (M14). The Salama and Soliman OTRAs have fewer current mirrors than the modified OTRA, resulting in less transistor mirror mismatch and increased frequency capabilities. Furthermore, the proposed OTRA has fewer transistors, which means less power is dissipated.

The table below shows the transistor aspect ratios.  $I_B$  is the biasing current in Amperes.  $V_{B1}$ , or -0.5 V, is the biasing voltage. The input differential current range is -50A to 50A. 0.1A is the current offset.

### 2.2.2 Differential OTRA Simulation Results

The CMOS implementation of differential OTRA presented in [9] is used for simulation. LTspice 180nm CMOS process parameters and 1.5 V supply voltages are used in the SPICE simulation. Table 2.1 shows the aspect ratios of transistors.

**Table 2.1** Aspect ratios of the transistors in the circuit shown in Fig.2.5.

<i>Transistors</i>	<b>W(<math>\mu\text{m}</math>)</b>	<b>L(<math>\mu\text{m}</math>)</b>
<i>M1-M3</i>	100	2.5
<i>M4</i>	10	2.5
<i>M5, M6</i>	30	2.5
<i>M7</i>	10	2.5
<i>M8-M11</i>	50	2.5
<i>M12, M13</i>	100	2.5
<i>M14</i>	50	0.5

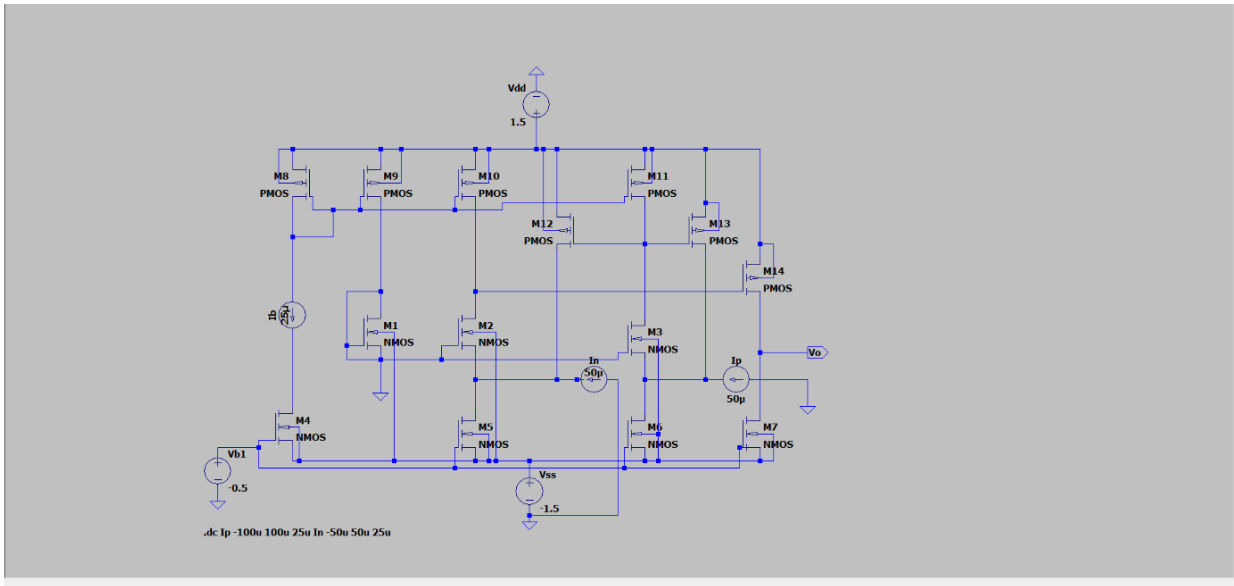


Fig.2.6 OTRA implementation

## DC RESPONSE

For -0.5V to +0.5V and a transresistance of 8.335Mohms, the DC characteristics in Figure.2.3 show a linear relationship between output current & input differential voltage (V1 V2).

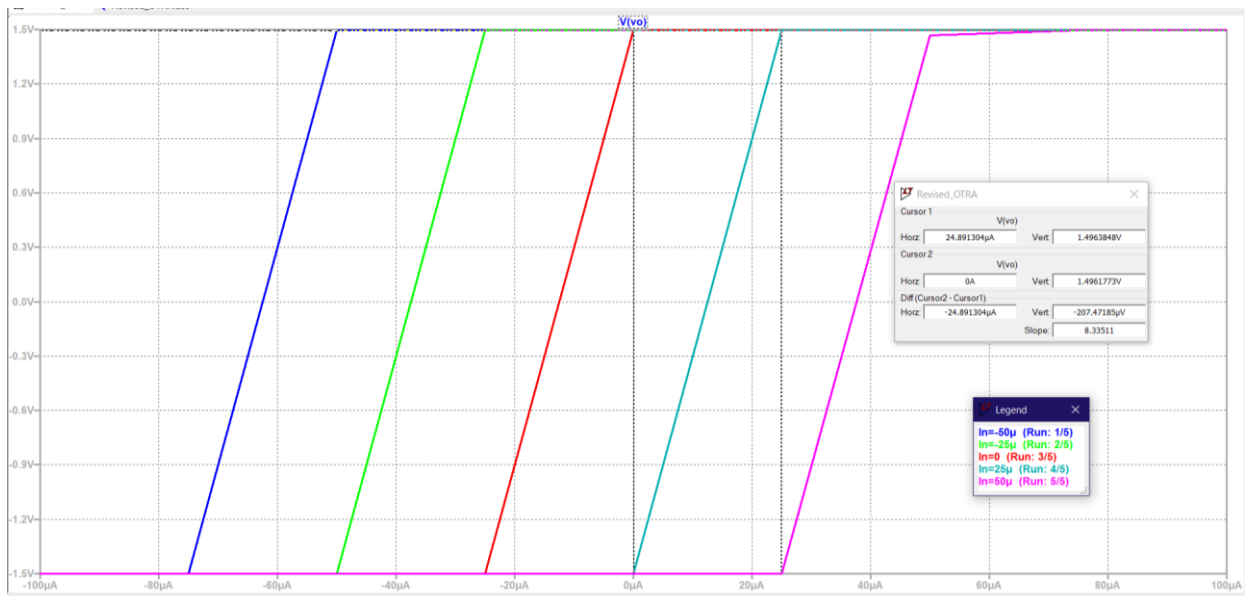
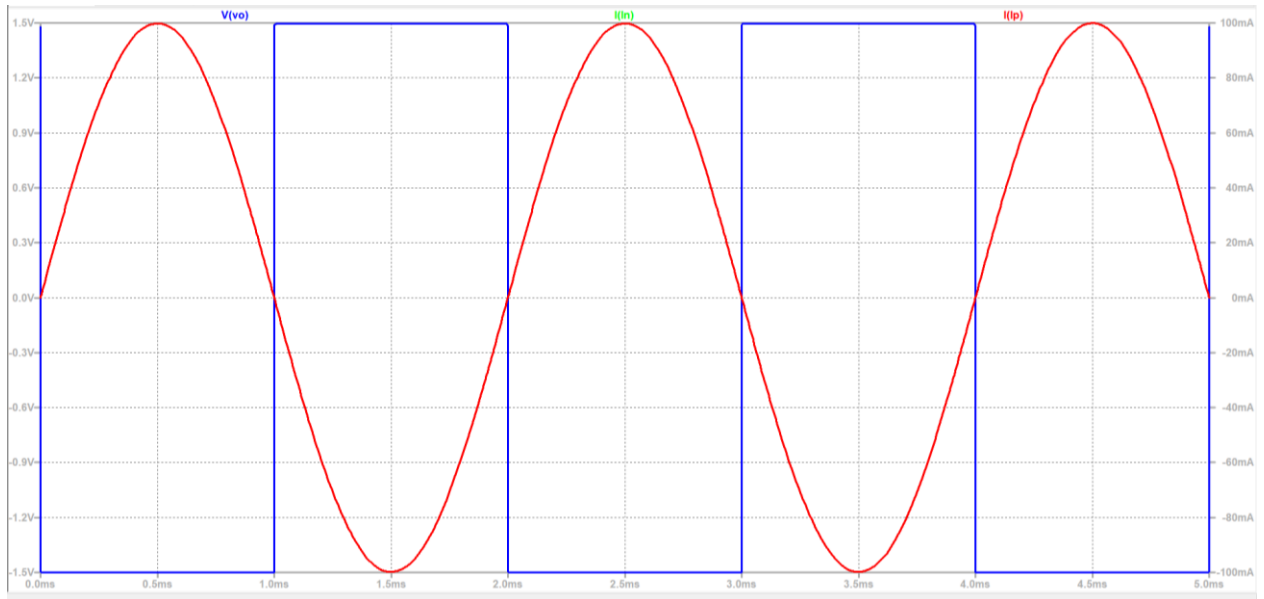


Fig 2.7: Output Characteristics of OTRA

## **TRANSIENT RESPONSE**

V2 is grounded, and V1 is provided with a Sinusoidal source of 0.2 V amplitude with a frequency of 50 KHz, and the transient response is simulated for time 0 ms to 5 ms. V1 is grounded, and V2 is given a Sinusoidal source of 0.2 V amplitude with a frequency of 50 KHz as the input condition for the transient response of Figure 2.7.



*Fig 2.8: Transient response of OTRA*

## **SUMMARY**

This chapter covers the OTRA's preliminary steps. The terminal characteristics of the OTRA symbol are presented first, followed by its characterization. The current study employs OTA as an active block in the development of various filter circuits.

## CHAPTER 3

### OTRA BASED APPLICATIONS

This chapter covers traditional controllers like proportional (P), proportional-derivative (PD), proportional integrator (PI), and proportional integral and derivative (PID) differentiators. The operation of these circuits was verified using SPICE simulation. Theoretical and observed results are found to be nearly identical, indicating that OTA-based applications work.

### 3.1. PROPORTIONAL CONTROLLER

#### 3.1.1. INTRODUCTION

The instantaneous value of the control error  $E(s)$  determines  $U(s)$ , the actuating signal of a proportional controller [42]. Any stable plant can be controlled by a proportional controller, but its performance is limited and its steady state errors are nonzero. It has this limitation because its frequency response is bounded for all frequencies. Figure 3.1 shows a block diagram of a second-order unity feedback control system with a P-controller.

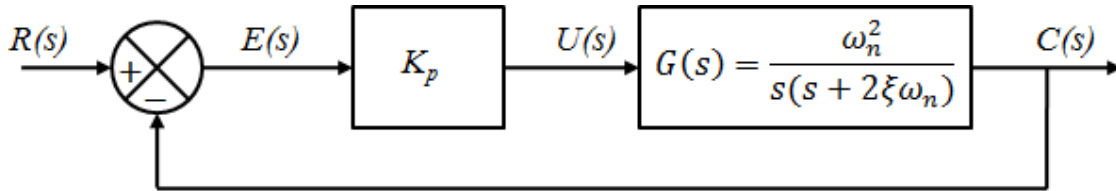


*Fig. 3.1 Control System with P-controller*

Mathematically,

$$U(s) = K_p E(s)$$

So, Transfer function is as follow

$$G_c(s) = K_p$$

where,  $K_p$  is constant of proportionality.

#### 3.1.2 P-CONTROLLER WITH SECOND ORDER SYETEM

The transfer function of the complete system can be deduced from the Fig. 3.1,

$$T_p(s) = \frac{K_p \omega_n^2}{s^2 + 2\xi \omega_n s + K_p \omega_n^2}$$

$$\omega_n' = \omega_n \sqrt{K_p}$$

$$\xi' = \frac{\xi}{\sqrt{K_p}}$$

From the above comparison, it is clear that natural frequency,  $\omega_n$  increases while damping ratio,  $\xi$  decreases by  $\sqrt{K_p}$ , this results in following merits and demerits:

- Rise time gets shorter.
- The peak period shrinks.
- The maximum peak overshoot increases.
- The settling time is unaffected.
- Error in steady state is reduced.

- *OTRA based P-Controller*

Figure 3.2 depicts a proportional controller, which is essentially a voltage-controlled voltage source.

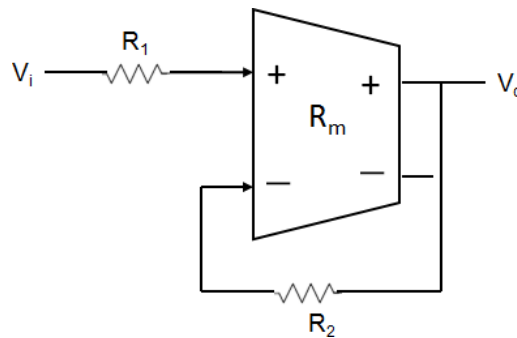


Fig. 3.2 OTRA based P-Controller

For Ideal case,  $R_m = \infty$

$$I_p = I_n$$

So, Transfer function will be

$$K_p = \frac{V_o(s)}{V_i(s)} = \frac{R_2}{R_1}$$

The non-saturation region of MOS transistors can be used to implement linear passive resistors, allowing these parameters to be electronically tuned. Using different gate voltages, the resistance value can be changed.

### Simulation Results of P Controller

The values of the passive components for the OTRA-based P controller shown in Fig. 3.2 are  $R_1=10K$  and  $R_2=20K$ . A 3mV, 2.5 MHz sinusoidal input voltage is used for time domain analysis. Figure 3.3 shows both ideal and simulated results. Figure 3.4 depicts frequency domain characteristics. The gate voltages are set to  $V_{a1}= V_{a2} = 1.2V$  and  $V_{b1} =0.59V$ ,  $V_{b2} =0.64V$ , resulting

in resistance values of  $R1 \approx 10K\Omega$  and  $R2 \approx 20K\Omega$ . Fig. 3.3 depicts the transient response, while Fig. 3.4 depicts the frequency domain characteristics of the MOS-C implementation of the P controller.

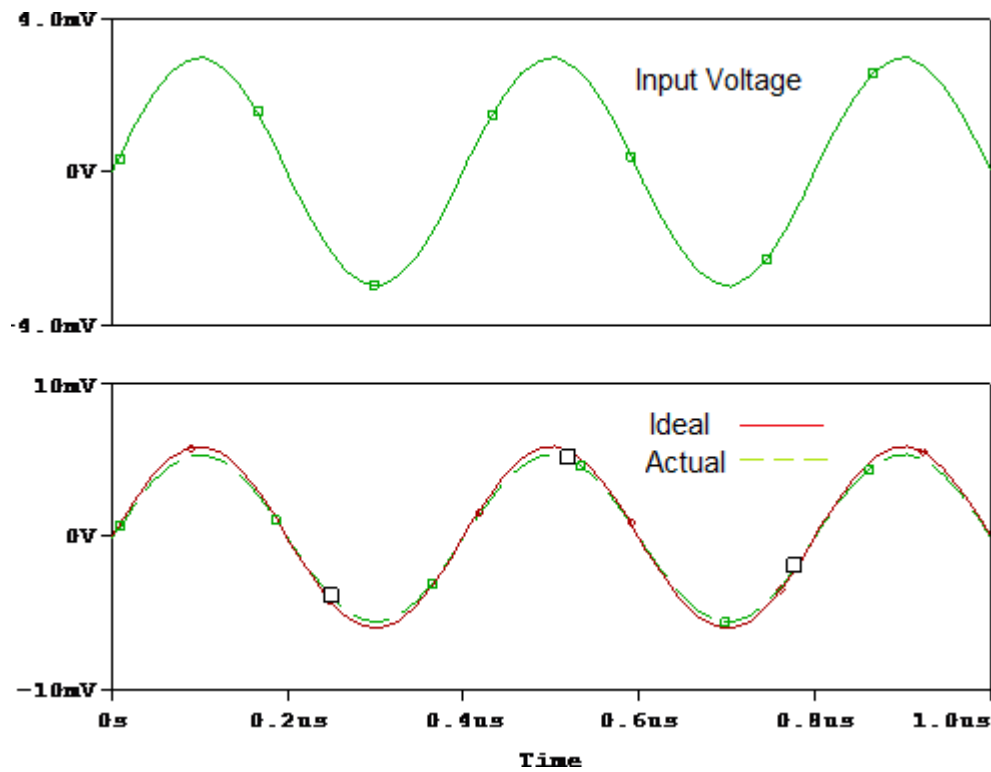


Fig. 3.3 Transient response of the P Controller

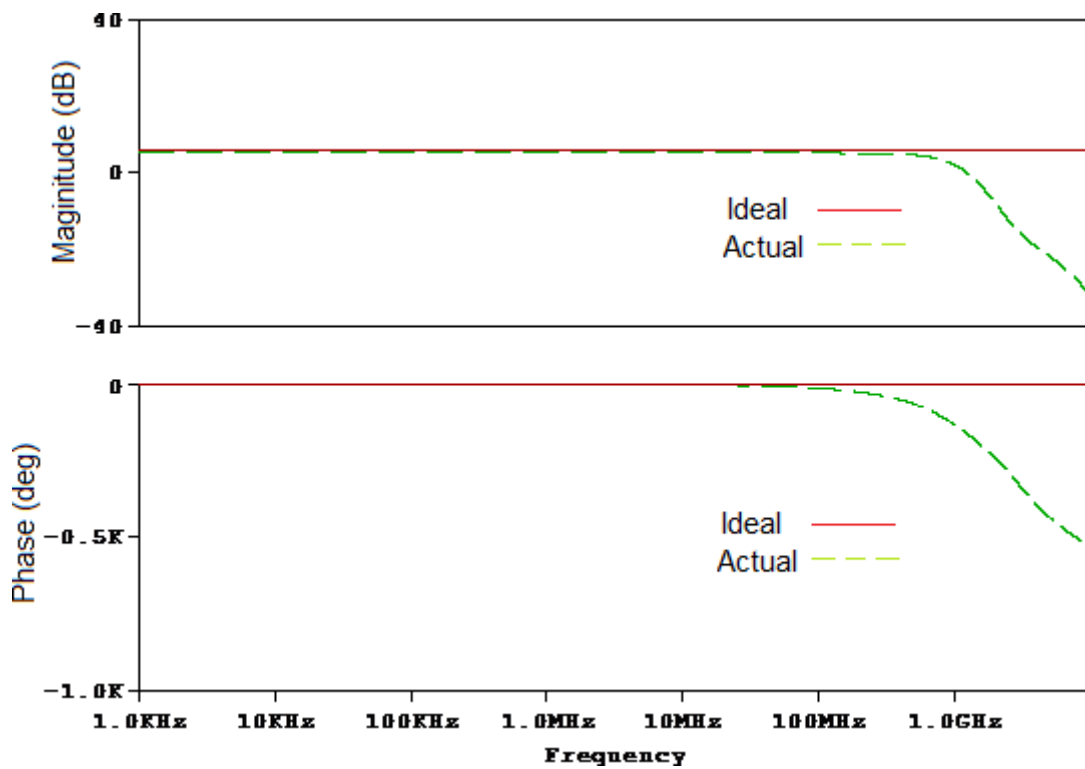


Fig. 3.4 Frequency and phase Response of P controller

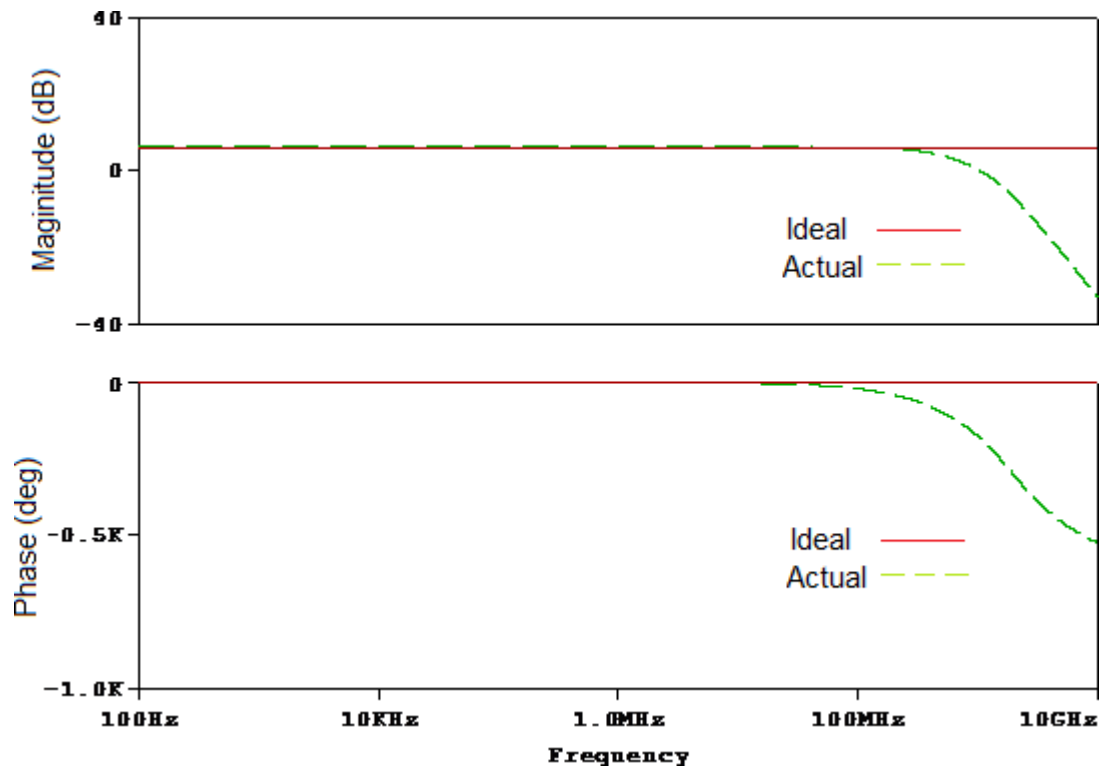


Fig. 3.5 Frequency and phase Response of MOS-C implementation of P controller

A closed loop control system based on the suggested P controller and a second order low-pass filter is shown in Figure 3.6. (LPF). Figure 3.7a shows the step response of a Low-pass filter without the P controller for a 50mV step input, while Figure 3.7b shows the step response of a closed loop system with the P controller effect. Figure 3.6 depicts the effect of altering  $K_p$  on the second order system, showing that as  $K_p$  grows, rise time decreases but peak overshoot increases.

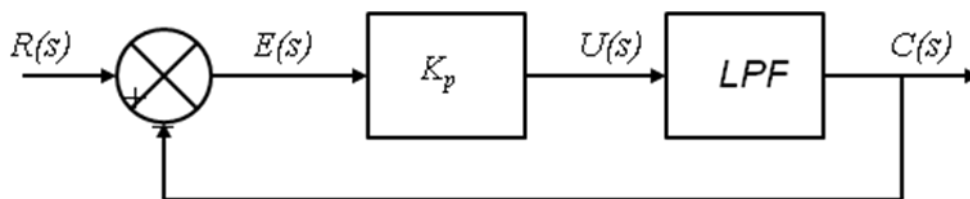


Fig. 3.6 Closed Loop Control System using P controller



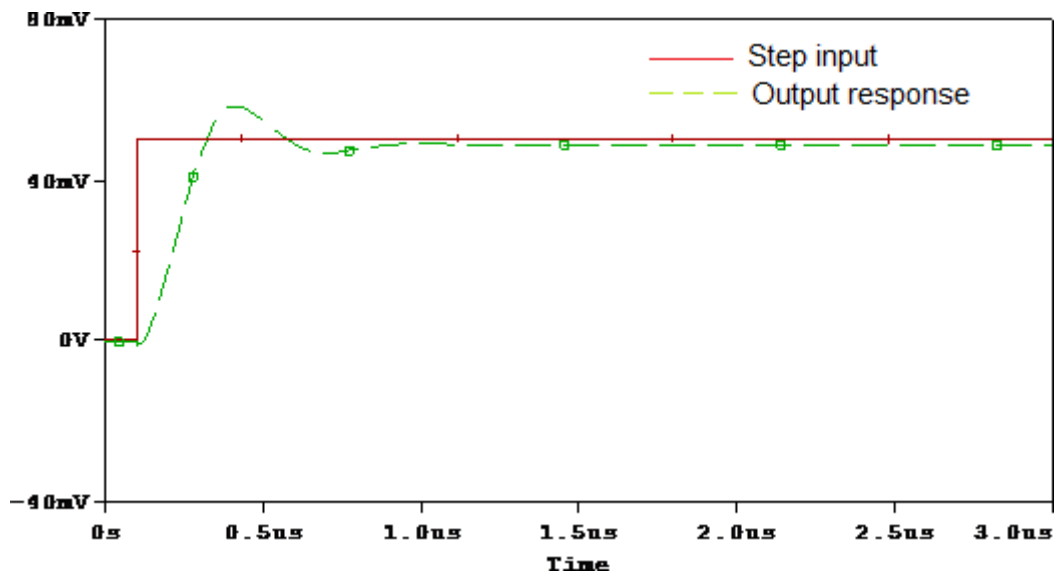


Fig. 3.7a Step Response of a second order system without P controller

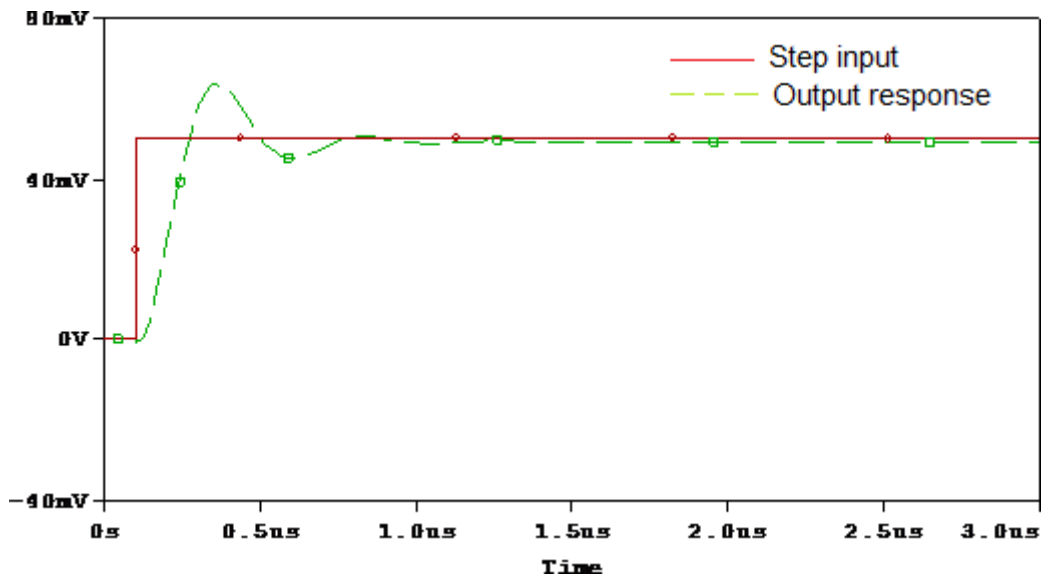


Fig. 3.7b Step Response of a second order system with P controller

## 3.2 PD CONTROLLER

### 3.2.1 INTRODUCTION

In a PD controller, the actuating signal  $U(s)$  is the sum of proportional to the error signal  $E(s)$  and its rate of change. If the error is large or changing rapidly, the control will result in a faster response from the system. It's a quick mode that fades away when faced with constant errors. Based on the error trend it is also known as predictive mode. The derivative mode's main drawback is its proclivity for producing large control signals in response to high frequency control errors, such as measurement noise or set point changes, when viewed in isolation. Figure 3.8 shows the block diagram of a second order unity feedback control system using a PD-controller.

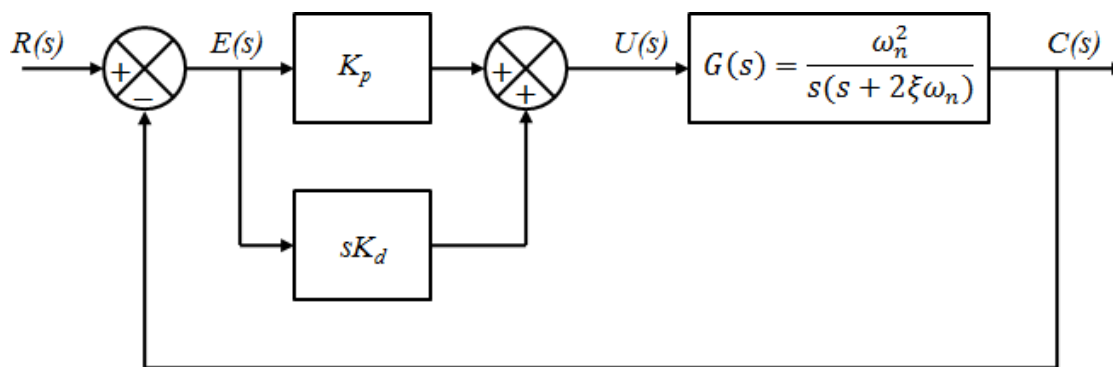


Fig. 3.8 Control System with PD-controller

Proportional-derivative (PD) type controller's transfer function is as following:

$$G_c(s) = K_p + K_d s$$

The proportional and derivative constants, respectively, are  $K_p$  and  $K_d$ .

#### PD-Controller with Second order system

From the Figure. 3.8 the transfer function of the complete system can be calculated as,

$$T_{pd}(s) = \frac{(K_p + sK_d)\omega_n^2}{s^2 + (2\xi\omega_n + K_d\omega_n^2)s + K_p\omega_n^2}$$

On comparing it with standard second order equation, For  $K_p = 1$ ,

From the above results, it is clear that natural frequency,  $\omega_n$  does not change while damping

$$\omega_n' = \omega_n$$

$$\xi' = \xi + \frac{K_d\omega_n}{2}$$

ratio,  $\xi$  increases, this result in following merits and demerits:

- Peak overshoot is reduced as the damping improves.

- Rise time gets reduces.
- The peak period reduces.
- The time it takes to settle decreases.
- Stable state error is unaffected.

### OTRA based Proposed PD-Controller

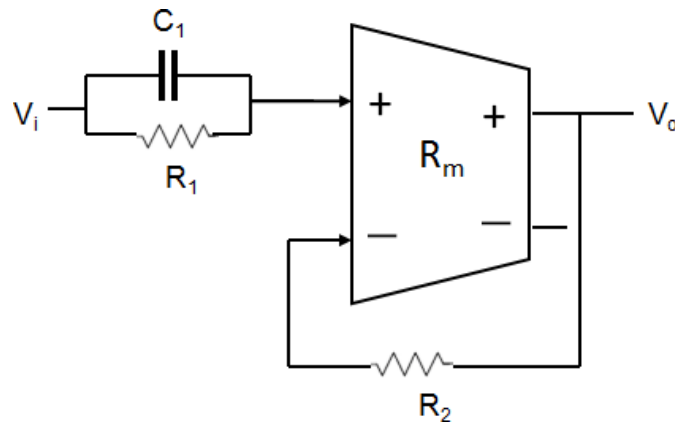


Fig. 3.9 OTRA based Proposed PD Controller

Figure 3.9 depicts the proposed PD-Controller. Using OTRA's terminal equations and assuming OTRA to be ideal, i.e.  $R_m = \infty$ , a routine analysis of this controller yields.

$$V_i \left( \frac{1}{R} + sC \right) = \frac{V_{o^+}}{R_f}$$

$$\frac{V_{o^+}}{V_i} = \frac{R_f}{R} + sCR_f$$

### Simulation Results of PD Controller

The values of passive elements for the OTRA-based proposed PD controller shown in Fig. 3.8 are  $R_1 = 10K$ ,  $R_2 = 20K\Omega$ , and  $C_1 = 20pF$ . A triangular input voltage of 3mV peak is used for time domain analysis, and both ideal and simulated results are shown in Figure. 5.8. The input signal's frequency domain characteristics are shown. For the square input waveform, the integrator acts as a low pass filter and generates a sawtooth waveform. Integrators are commonly found in wave shaping, ramp generators and analogue-to-digital converters.

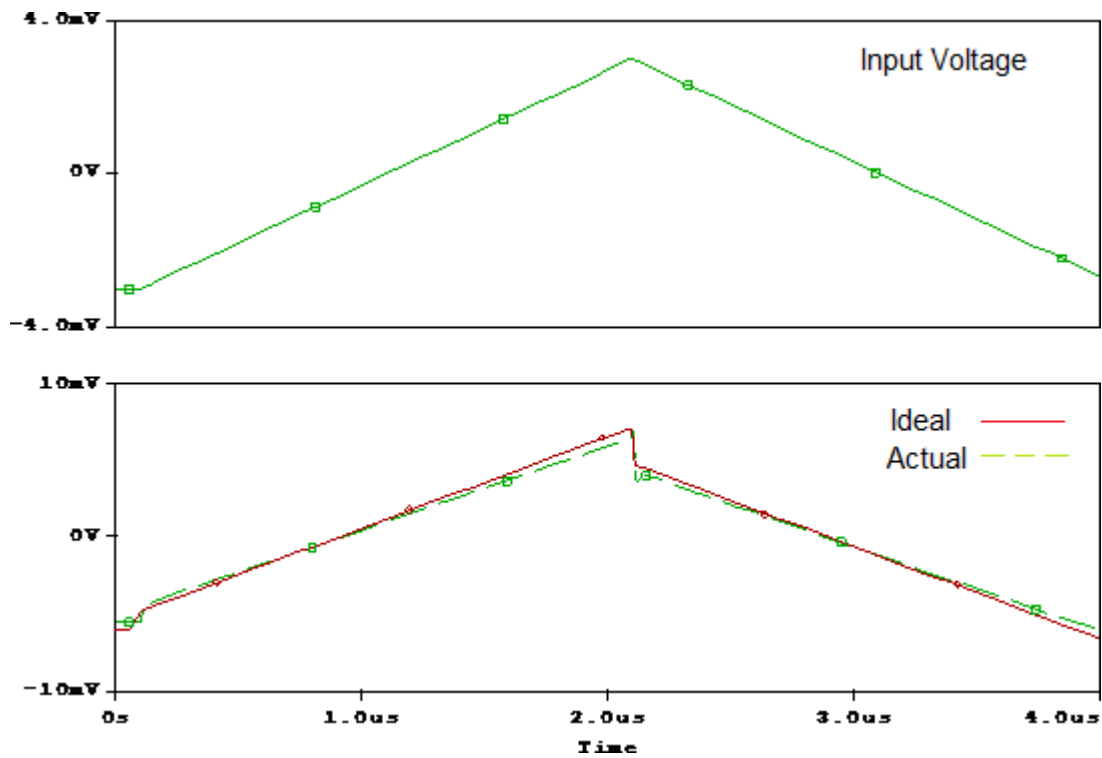


Fig. 3.10 Transient response of the PD Controller

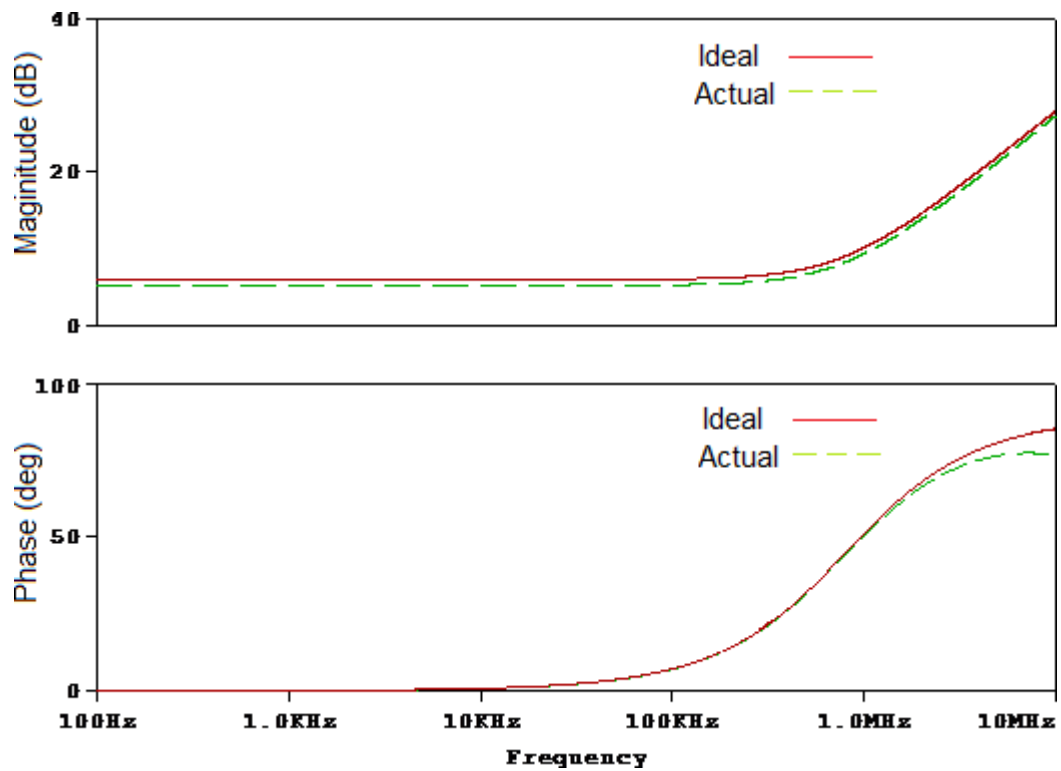


Fig. 3.11 Frequency and phase Response of PD controller

### 3.3 PI CONTROLLER

#### 3.3.1 INTRODUCTION

The actuating signal of PI, a weighted sum of the error signal and the integral of that value is used by the controller to control the plant, implying that the control mode is slow reaction. This is reflected in its low pass frequency response. In order to achieve perfect plant inversion, the integral mode  $\omega$  must be set to 0. In the presence of a step reference and disturbance, the steady state error is driven to zero. When seen in isolation, the integral mode has two main flaws: its pole at the origin causes the undesirable effect known as wind-up (in the presence of actuator saturation) & degrades loop stability.

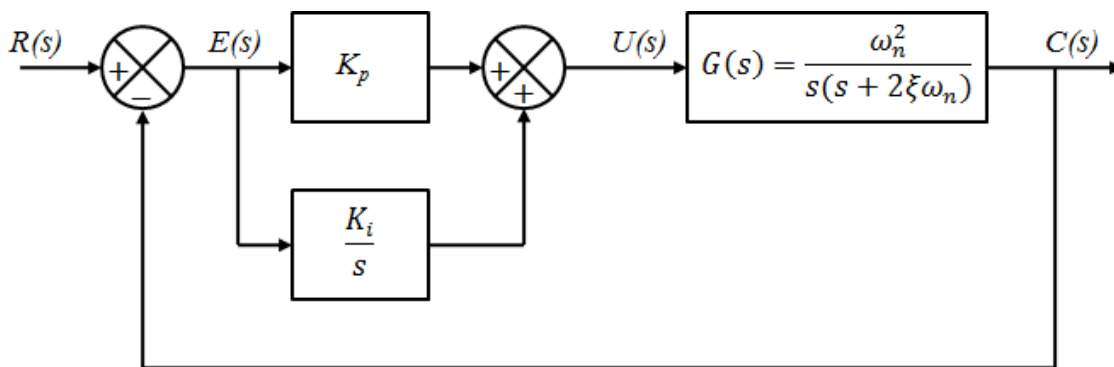


Fig. 3.12 Control System with PI-controller

The transfer function of proportional-integrator (PI) controller is,

$$G_c(s) = K_p + \frac{K_i}{s}$$

The proportional and integral constants, respectively, are  $K_p$  and  $K_i$ .

#### PI-Controller with Second order system

From the Figure. 3.12 the system's complete transfer function can be calculated as,

$$T_{pi}(s) = \frac{(K_i + sK_p)\omega_n^2}{s^3 + 2\xi\omega_n s^2 + K_p\omega_n^2 s + K_i\omega_n^2}$$

For  $K_p = 1$ , Error signal is given by

$$E(s) = R(s) \frac{s^2(s + 2\xi\omega_n)}{s^3 + 2\xi\omega_n s^2 + \omega_n^2 s + K_i\omega_n^2}$$

The steady state error is given by step input,  $e_{ss} = 0$

For ramp input,  $e_{ss} = 0$

For parabolic input,  $e_{ss} = \frac{2\xi}{K_i\omega_n}$

As a result, the benefits and drawbacks of PI-Controller can be summarised as follows:

- By lowering the steady state error, it improves steady state response.
- Rise time lengthens
- It improves the system's type and order

### *OTRA based Proposed PI-Controller*

Proposed PI-Controller is shown in Fig. 3.13.

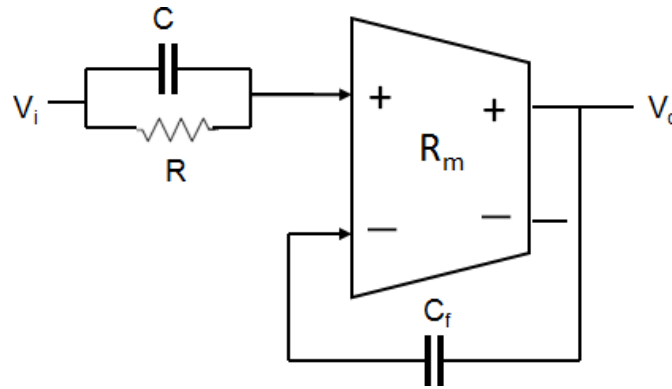


*Fig. 3.13 OTRA based Proposed PI Controller*

The following voltage transfer function gives the routine analysis of this controller:

$$\frac{V_{o+}}{V_i} = \frac{C}{C_f} + \frac{1}{sC_f R}$$

$$K_p = \frac{C}{C_f}, \quad K_i = \frac{1}{C_f R}$$

### **Simulation Results of PI Controller**

The values of the passive element for the proposed OTRA-based PI controller shown in Figure. 3.13 are  $R_1 = 10\text{K}\Omega$ ,  $R_2 = 20\text{K}\Omega$ , and  $C_1 = 20\text{pF}$ . A  $3\text{mV}$  step input voltage with a  $20\text{ns}$  rise time is used for time domain analysis, and both ideal and simulated results are shown in Figure. 3.14. Figure 3.15 shows the frequency domain characteristics.

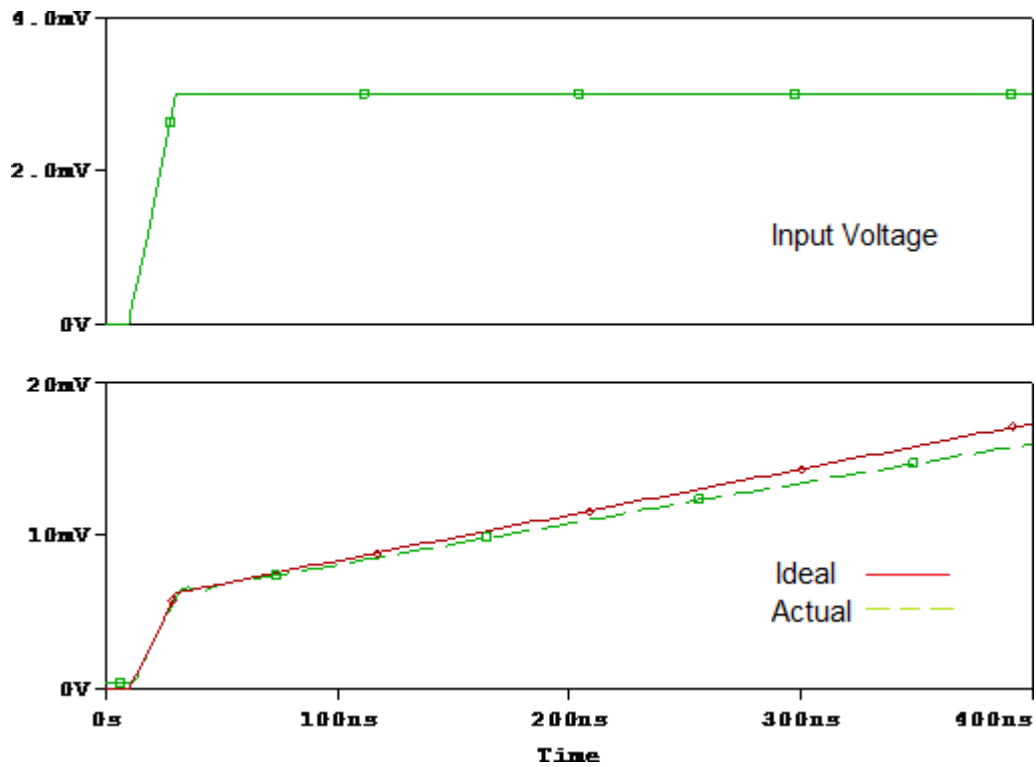


Fig. 3.14 Transient response of the PI Controller

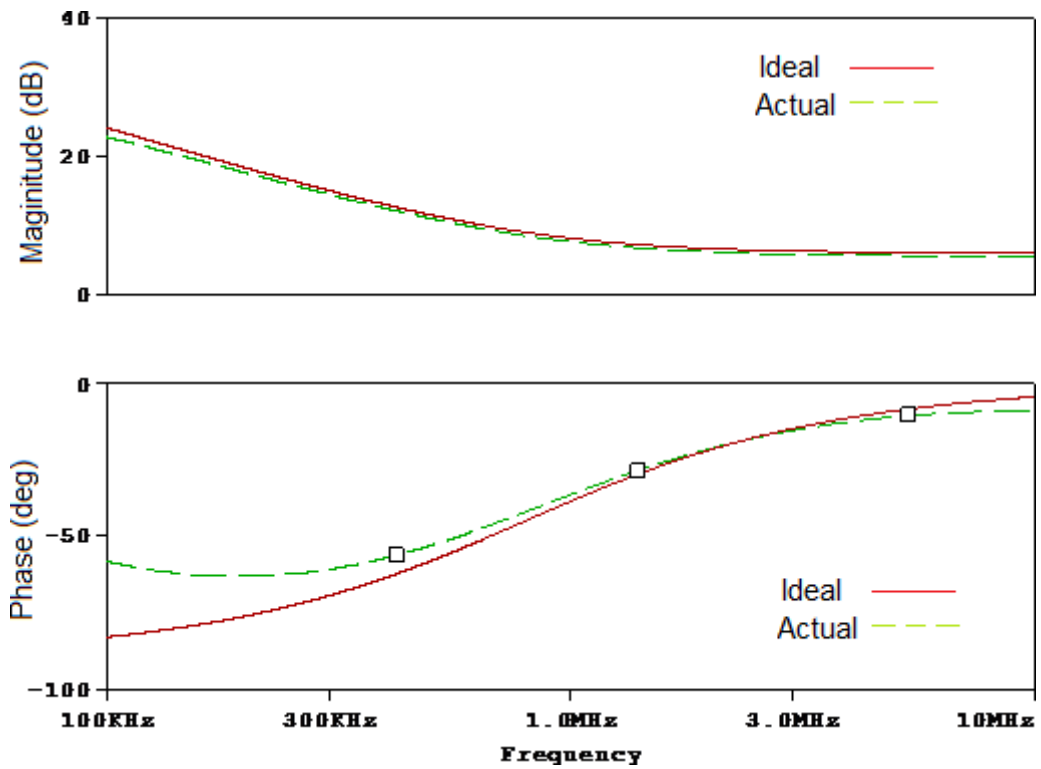


Fig. 3.15 Frequency and phase Response of PI Controller

## 3.4 PID CONTROLLER

### 3.4.1 INTRODUCTION

The PD controller improves system damping but has no effect on steady-state response. The PI controller simultaneously improves steady-state error & relative stability, but the rise time is also increased. As a result, none of them can completely improve a system's performance on their own. This motivates the use of a PID controller to take advantage of the best characteristics of both the PI and PD controllers. The block diagram of a second order unity feedback control system using a PID controller is shown in Figure 3.16.

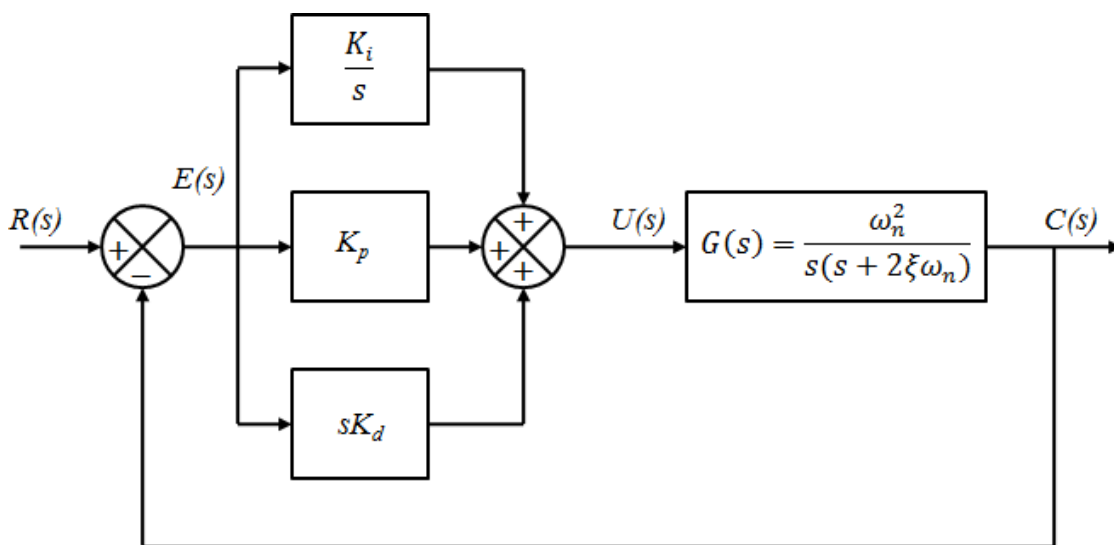


Fig. 3.16 Block diagram of PID Controller

Transfer function of PID Controller is given by

$$G_c(s) = K_p + K_d s + \frac{K_i}{s}$$

Where, proportional, derivative, and integral constants, respectively, are  $K_p$ ,  $K_d$ , and  $K_i$ .

Advantages of PID controller:

- High speed.
- High accuracy.
- High stability.
- No offset problem.

*OTRA based Proposed PID-Controller*

Proposed PID-Controller is shown in Fig. 3.17.



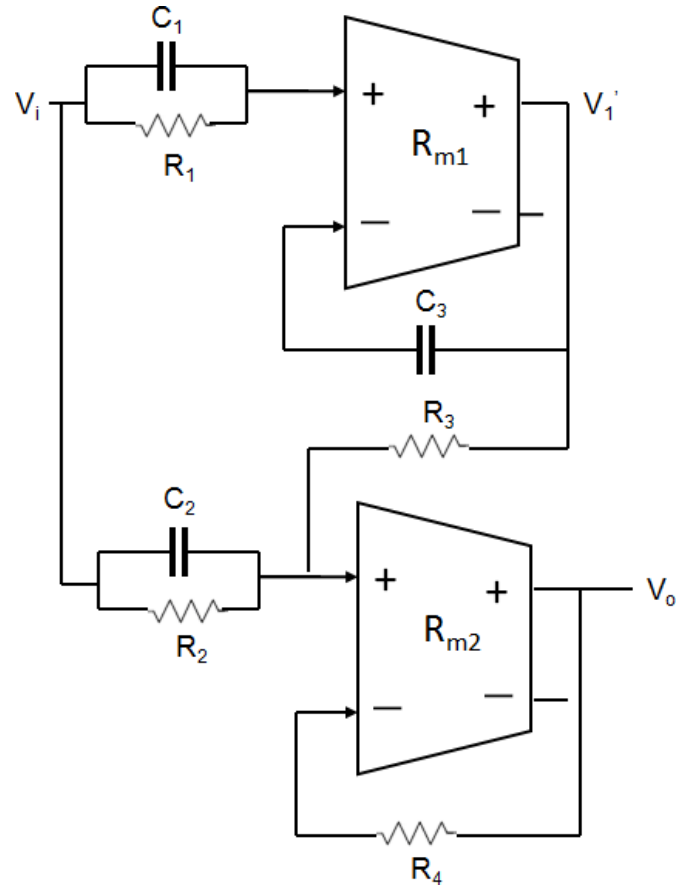


Fig. 3.17 OTRA based Proposed PID Controller

PID is made up of PI and PD controllers, as shown in Figure. 3.17. The first OTRA acts as a PI controller, while the second acts as a PD controller and an adder. The circuit's analysis reveals that

$$\frac{V_1'}{V_i} = \frac{C_1}{C_3} + \frac{1}{sC_3R_1}$$

$$V_o = V_i \left( \frac{R_4}{R_2} + sC_2R_4 \right) + V_1' \frac{R_4}{R_3}$$

$$\frac{V_o}{V_i} = \left( \frac{R_4}{R_2} + sC_2R_4 \right) + \frac{R_4}{R_3} \left( \frac{C_1}{C_3} + \frac{1}{sC_3R_1} \right)$$

$$K_p = \frac{R_4}{R_3} \times \frac{C_1}{C_3} + \frac{R_4}{R_2}, \quad K_d = C_2R_4 \quad \& \quad K_i = \frac{R_4}{R_3} \times \frac{1}{C_3R_1}$$

Component choice of  $R_4 = R_3$ ,  $R_2 = \infty$ , results in

$$K_p = \frac{C_1}{C_3}, \quad K_d = C_2R_4 \quad \& \quad K_i = \frac{1}{C_3R_1}$$

For  $R_4 = R_3$ ,  $C_1 = 0$ , we get

$$K_p = \frac{R_4}{R_2}, \quad K_d = C_2R_4 \quad \& \quad K_i = \frac{1}{C_3R_1}$$

### Simulation Results of PID Controller

$R1 = R2 = R3 = R4 = 50K$ ,  $C1 = C3 = 10pF$ , and  $C2 = 0.05pF$  are the values of passive elements in the differential OTRA-based proposed PID controller shown in Figure. 3.17. A 3mV step signal with a 10ns rise time is used for time domain analysis, and both ideal and simulated results are shown in Figure. 3.18

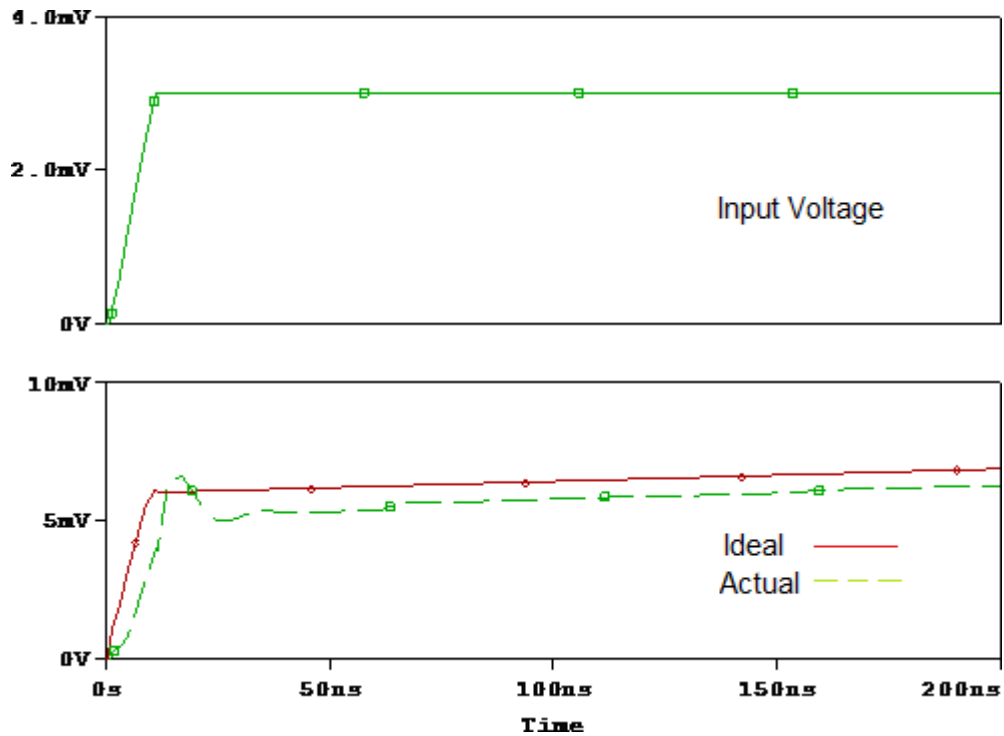


Fig. 3.18 Transient response of the PID Controller

### 3.5 SUMMARY

In this chapter, the SPICE simulator is used to implement and verify some existing OTRA applications. Proportional (P), proportional- derivative (PD), proportional integral (PI), and proportional integral derivative (PID) controllers are among the applications.

## **CHAPTER 4**

### **LITERATURE SURVEY OF SHADOW FILTER**

#### **4.1. INTRODUCTION**

The characteristics of a filter, such as characteristic bandwidth, frequency and quality factor can be changed by altering the values of the passive components exercised in the design of the filter or by electronically adjusting the active block trans-conductance. A new method for electronic tuning of the filter parameters has been implemented in a recently proposed family of second-order filters known as the shadow filters [34]. An external amplifier is placed in the feedback path and its gain ( $G$ ) is varied to change the filter characteristics. The shadow filter is a popular term for this concept, which is gaining research interest [34]. The filter characteristics range from zero to infinity in these filters, but in practice they range from very low to very high. This is due to its ability to change various filter parameters, such as bandwidth, over a wide range by simply adjusting the gain using an amplifier. A quick transition between the two continuous center frequencies is possible. The shadow filter theory can be applied to either voltage-mode or current-mode circuits. In the past, various terminologies were used to describe shadow filters. The terminologies associated with shadow filters are reviewed in this chapter.

#### **4.2. AVAILABLE TOPOLOGIES OF SHADOW FILTER**

The generalized block diagram of a second order shadow filter with voltage inputs & outputs is shown in Fig.4.1 [35]. It's known as working in voltage mode. The band-pass transfer function  $H(s)$  and the low-pass transfer function  $H_1(s)$  are both second-order transfer functions with the same denominator and modified transfer function properties. The band-pass characteristics of  $H'(s) = V_o/V_{in}$  are preserved, but with a centre frequency is constant,  $Q$  is dynamic, and the product of centre frequency and  $Q$  is constant.

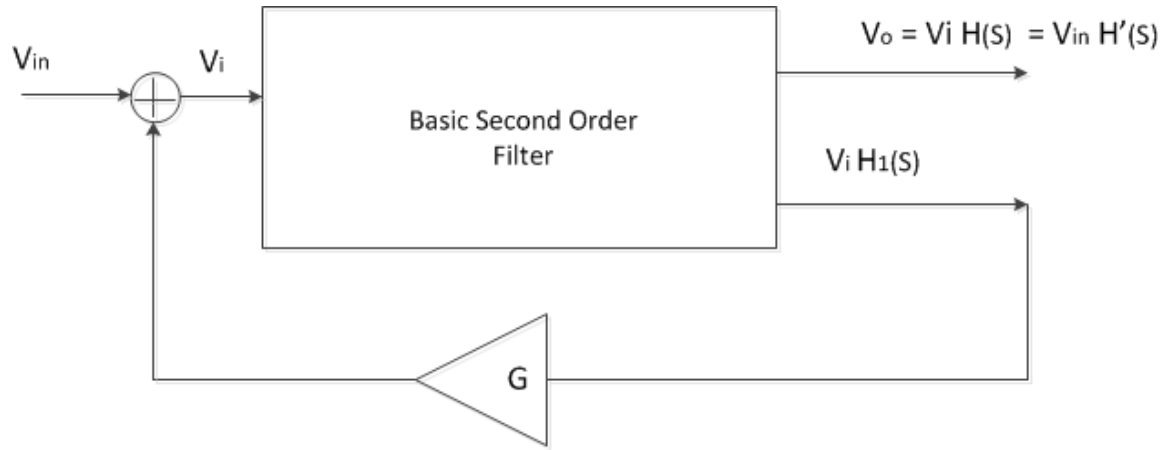


Fig.4.1. Second order voltage mode shadow filter

Any output, or a combination of outputs, can provide feedback in Fig.4.1. As a result,  $H(s)$  and  $H_1(s)$  are of forms:

$$H(s) = \frac{d + es + fs^2}{s^2 + \left(\frac{\omega_0}{Q_0}\right)s + \omega_0^2}$$

$$H_1(s) = \frac{a + bs + cs^2}{s^2 + \left(\frac{\omega_0}{Q_0}\right)s + \omega_0^2}$$

From Fig.4. 1  $H'(s)$  can be deduced as

$$H'(s) = \frac{H(s)}{1 - AH_1(s)}$$

When  $H(s)$  and  $H_1(s)$  are substituted in (3) the results is,

$$H'(s) = \frac{d + es + fs^2}{s^2(1 - Ac) + \left[\left(\frac{\omega_0}{Q_0}\right) - Ab\right]s + \omega_0^2 - Aa}$$

This can be expressed as

$$H'(s) = \frac{d' + e's + f's^2}{s^2 + \left(\frac{\omega'_0}{Q'_0}\right)s + \omega_0'^2}$$

Where,

$$(d', e', f') = \frac{d, e, f}{(1 - Ac)}, \omega'_0 = \sqrt{\frac{(\omega_0^2 - Aa)}{(1 - Ac)}}, Q'_0 = Q_0 \sqrt{\frac{(1 - Ac)(\omega_0^2 - Aa)}{(\omega_0 - AbQ)}}$$

## SPECIAL CASES

In [38] the authors contemplate  $b = 0$  and  $c = 0$  (it would be a mistake to consider  $b = c = 0$  because  $b$  and  $c$  are different dimensionally) so that

$$\omega'_0 = \omega_0 \sqrt{(1 - Aa/\omega_0^2)}; Q' = Q \sqrt{(1 - Aa/\omega_0^2)}$$

As a result, the centre frequency  $Q$  change proportionally, while the bandwidth  $\Delta\omega' = \omega'_0/Q'$  remains constant as per the basic bandwidth  $\Delta\omega = \omega_0/Q$ .

Taking the high-pass output of the basic second order cell for  $H_1(s)$ , i.e.  $a = 0$  and  $b = 0$ , yields an interesting variation of the circuit. Then we have

$$\omega'_0 = \omega_0 / \sqrt{(1 - Ac)}; Q' = Q \sqrt{(1 - Ac)}$$

In this case, the product of  $\omega_0$  and  $Q$  remains constant, implying that we receive higher  $Q$  at lower frequencies and vice versa. Due to the huge values of  $Q$  inductance and capacitance required, as well as the difficulties of constructing high priced high inductors,  $Q$  achieving high at low frequencies is a recurring challenge in passive filters. Active filters necessitate high resistor-to-capacitor ratios, which makes this difficult.

If the feedback signal is obtained directly from the bandpass output,

$$a = 0 \text{ and } c = 0$$

$$\omega'_0 = \omega_0; Q' = Q / (1 - AbQ/\omega_0)$$

In this scenario, a variable  $Q$  with a fixed centre frequency is obtained. The bandwidth required is given by,

$$\Delta\omega' = \Delta\omega (1 - Ab/\omega_0)$$

This case is also of practical significance. The shadow filter topology shown in Fig.4.1 does not allow for orthogonal tuning of filter characteristics.

Another topology available is of single input multiple output mode as shown in fig 4.2 [36]. In this topology multiple output are possible i.e., high pass, low pass, and band pass output using only one second order circuit. In this Voltage input is being summed by the feedback voltage output with feedback gain multiplied to it. This configuration requires another amplifier to be attached in the feedback loop.

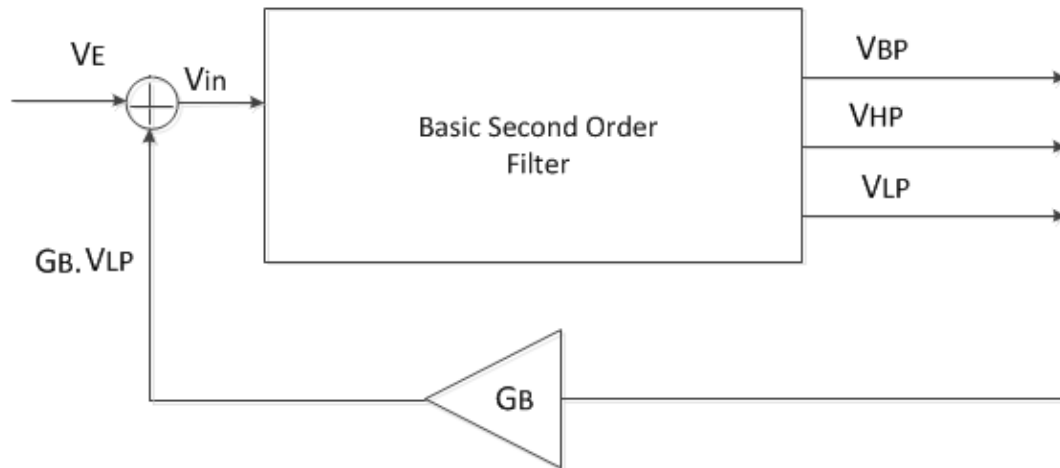


*Fig.4.2 Voltage mode shadow filter with amplifier feedback*

The topologies shown in Fig.4.1 and Fig.4.2 use an additional summer amplifier in their circuits to overcome this drawback. In this project report, a new topology is proposed that eliminates the need for the summer in the shadow filter circuit. Using only resistance as a feedback gain controller, both the centre frequency and bandwidth can be controlled simultaneously in this new topology.

### **4.3. AVAILABLE LITERATURE**

According to the literature, numerous active blocks have been used to implement shadow filters. The implementation of a second OTRA-based shadow is accomplished in [35]. Figure 4.3 shows a low-pass-controlled band pass structure. OTRA 1 and OTRA 2 are used to get the band pass and low pass responses, respectively. The OTRA 3 is an inverting amplifier and adder that adds the amplified low pass output to the applied input. By changing the value of Resistance, the inverting amplifier's gain  $A$  ( $A = -R_2/R_1$ ) can be changed.

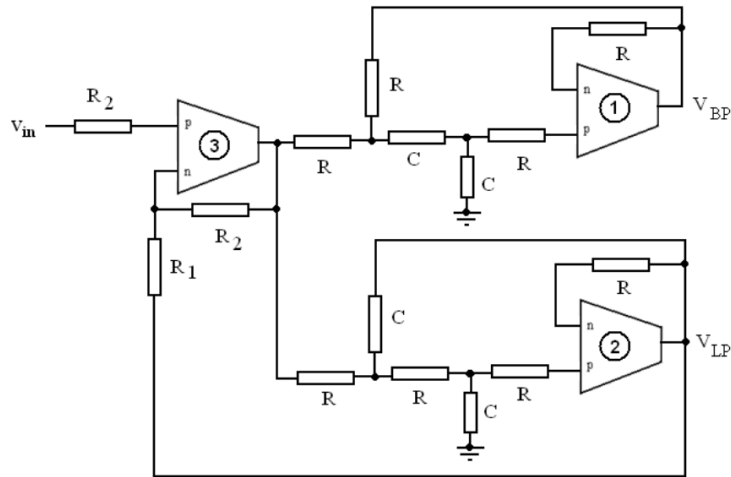


Fig 4.3: Configuration of a OTRA based shadow filter.

To get the controlled filter output, this implementation has limitations in that it requires a separate low pass filter structure & a separate summing amplifier. As a result, the monolithic size as well as the component requirements grow. This configurational circuit can also perform very limited controlled operations.

A second topology has been implemented in another literature [36] on OTRA based shadow filters, as shown in fig 4.4, in which a single input is fed to a second order filter that produces multiple outputs namely low pass, band pass and high pass simultaneously, & one of the output signals is then fed back through an OTRA based amplifier to produce a controlled filtered output. As a result, in addition to basic functions like low pass controlled low pass output, other configurations like LP controlled HP and BP, BP controlled LP and HP, and HP controlled LP and BP are also possible.

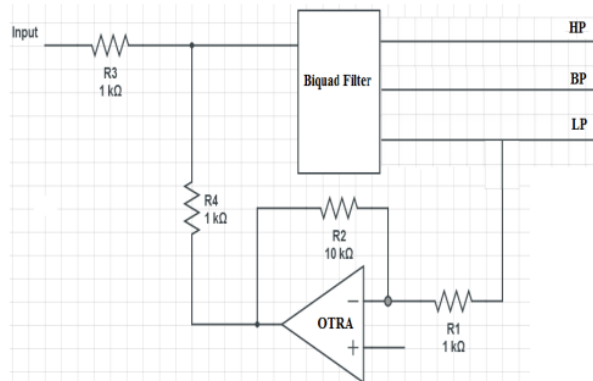


Fig: 4.4 OTRA controlled multi output shadow filter [36].

However, the above configuration necessitates the use of a feedback amplifier to control the gain, resulting in a larger chip size. This project report proposes a new topology that eliminates the need for the summer in the shadow filter circuit to overcome this drawback. Using only resistance as a

feedback gain controller, both the center frequency and bandwidth can be controlled simultaneously in this new topology.

#### **4.4. SUMMARY**

This chapter gives a short overview of the shadow filter. The shadow filter topologies that are currently available are discussed. An extensive survey of shadow filters has also been provided, as well as a classification of shadow filters based on class.



# CHAPTER 5

## MULTIPLE INPUT SINGLE OUTPUT SHADOW FILTER

### 5.1 PROPOSED OTRA MISO

The various configurations of Multiple Input Single Output Shadow Filter shadow filters such as Low pass controlled low pass filter, Low pass-controlled band pass filter, Low pass controlled high pass filter, Low pass-controlled notch filter, Band pass controlled low pass filter, Band pass controlled band pass filter, Band pass controlled high pass filter, Band pass controlled notch filter are proposed in this chapter. In this study, OTRA is used as an active block in the development of shadow filter circuits.

The active building block in a standard SIMO filter is an Operational Transresistance Amplifier (OTRA). Depending on the node(s) at which input current is given, the SIMO filter provides every filter response without changing any hardware configuration at a single input port.

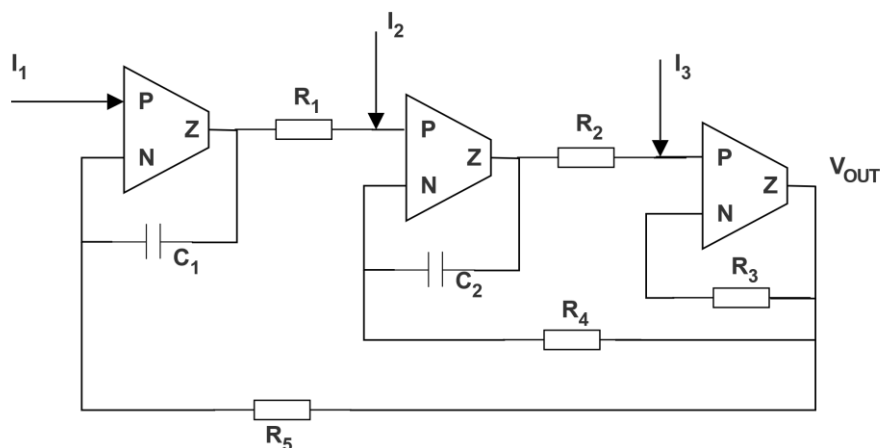


Fig 5.1: Second Order MISO filter

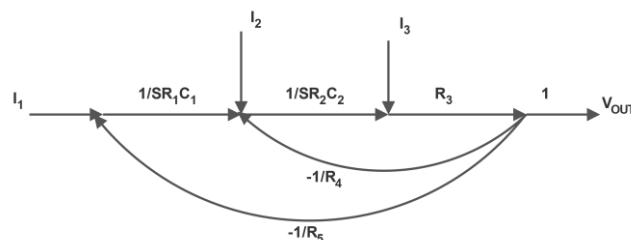


Fig 5.2: Signal flow graph of MISO filter

A universal filter with multiple inputs & single outputs and is based on integrated components of

the newly designed signal flow graph in Figure 5.2. The referenced MISO filter circuit shown in Figure 5.1 made using OTRA as an active structure.

The transfer function of the filter can be deduced by using the formula proposed by Samuel Jefferson Mason, proposed a method [8] to compute the transfer function of any signal flow graph (SFG) popularly known as Mason gain formula. Let,  $D(s)$  be the denominator of the transfer function and  $P_1, P_2$  and  $P_3$  be the forward path gain for input current at  $I_1, I_2$  and  $I_3$  respectively.

Therefore, transfer function of the SFG shown in figure 1(b) can be formulated as:

$$P_1 = \frac{R_3}{s^2 R_2 R_1 C_2 C_1}; \quad P_2 = \frac{R_3}{s R_2 C_2}; \quad P_3 = R_3$$

(Choosing Different path for different current input)

$$D(s) = 1 - \left[ \frac{-R_3}{s R_4 R_2 C_2} - \frac{R_3}{s^2 R_5 R_2 R_1 C_2 C_1} \right]$$

$$D(s) = \frac{s^2 R_5 R_4 R_2 R_1 C_2 C_1 + s R_5 R_1 C_1 R_3 + R_3 R_4}{s^2 R_5 R_4 R_2 R_1 C_2 C_1}$$

Hence for MISO filter Low pass (LP), Band pass (BP), and High pass (HP) responses are obtained at output terminal when input current is given at  $I_1, I_2$  and  $I_3$  respectively which is being obtained in equation (1), (2) and (3) discreetly. Notch output will be obtained when input currents are given at both  $I_1$  and  $I_3$ .

$$\frac{V_{out}}{I_1} = \frac{R_5 R_4 R_3}{s^2 R_5 R_4 R_2 R_1 C_2 C_1 + s R_5 R_1 C_1 R_3 + R_3 R_4} \quad (1)$$

$$\frac{V_{out}}{I_2} = \frac{s R_5 R_4 R_3 R_1 C_1}{s^2 R_5 R_4 R_2 R_1 C_2 C_1 + s R_5 R_1 C_1 R_3 + R_3 R_4} \quad (2)$$

$$\frac{V_{out}}{I_3} = \frac{s^2 R_5 R_4 R_3 R_2 R_1 C_2 C_1}{s^2 R_5 R_4 R_2 R_1 C_2 C_1 + s R_5 R_1 C_1 R_3 + R_3 R_4} \quad (3)$$

Angular frequency, Quality factor and Bandwidth of the MISO filter can be deduced as:

$$\text{Angular frequency, } \omega = \sqrt{\frac{1}{R_2 R_1 C_2 C_1} \frac{R_3}{R_5}}$$

$$\text{Quality factor, } Q = R_4 \sqrt{\frac{R_2 C_2}{R_1 C_1 R_3 R_5}}$$

$$\text{Bandwidth, } \frac{\omega}{Q} = \frac{1}{R_2 C_2} \frac{R_3}{R_4}$$

## 5.2. PROPOSED OTRA MISO SHADOW FILTER

The proposed circuit Figure 5.3 is of a MISO shadow filter. It consists of a Universal MISO filter using OTRA and  $R_6$  as a feedback amplifier. The gain of OTRA can be changed by changing the value of resistor  $R_6$ . As and on whichever input port feedback is required it can be altered to that position, so as to get the required filtration output. Angular frequency, gain, band-width and quality factor can be easily countercontrolled by altering the feedback gain values for all types of filters. Using a resistor instead of a summing amplifier provides an edge to the circuit as a MOS resistor can be easily cast-off on the hardware, resulting in lesser chip area required to realize the filter circuit. Characteristic features of a filter like angular frequency, bandwidth and quality factor can be controlled according to the requirement by using the appropriate configuration.

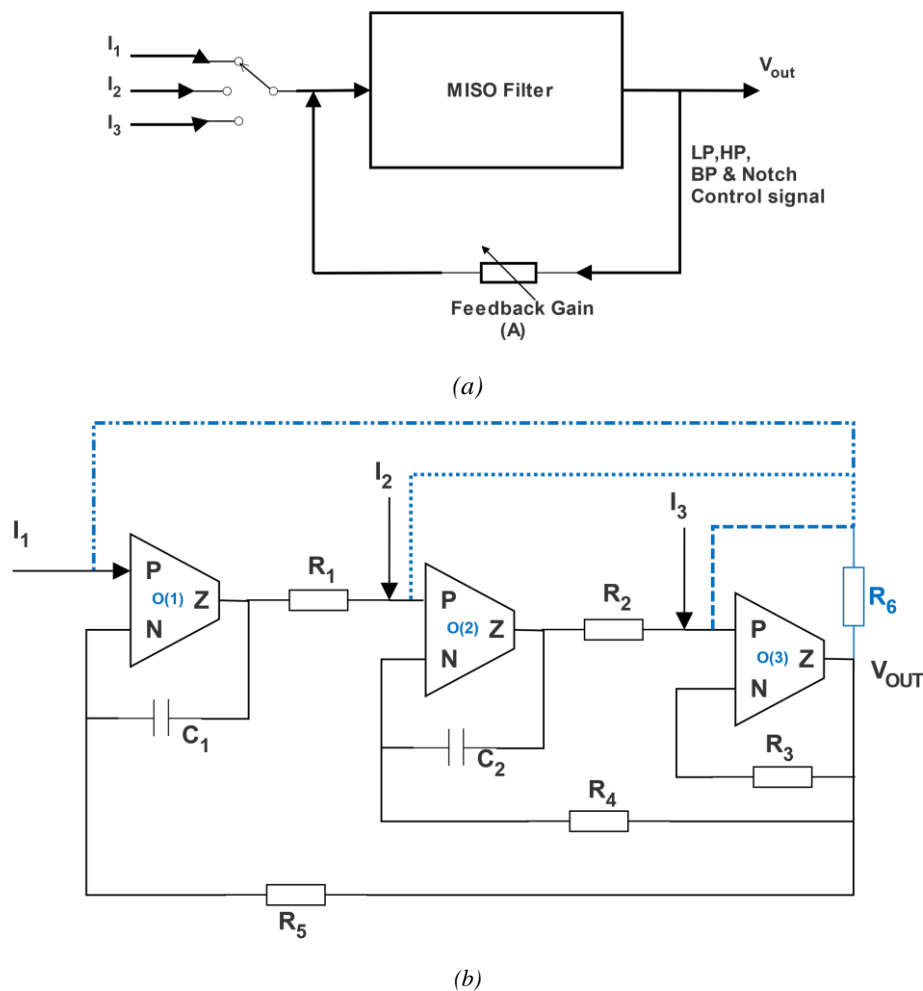


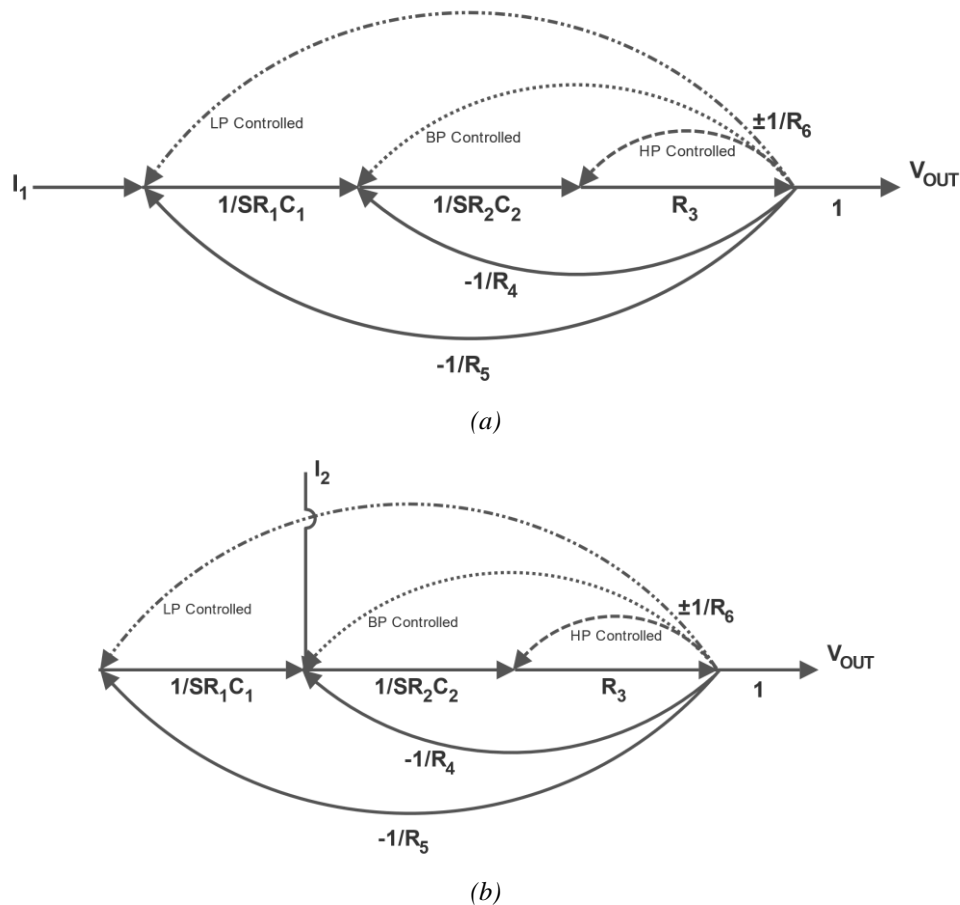
Fig 5.3: (a) Block diagram of proposed shadow filter using MISO universal filter. (b) Schematic of MISO shadow filter.

LP, BP, HP and notch-controlled output is obtained depending upon the position of feedback resistor ( $R_6$ ). In figure 5.3(b) when output is feedbacked to O(1), O(2) and O(3), LP, BP and HP controlled output is obtained respectively. While notch-controlled output is obtained when feedback

is positioned to O(1) and O(3) simultaneously. Henceforth four controlled configurations are viable i.e., LP, BP, HP and notch controlled filtered outputs.

Correspondingly, four configurations are attainable depending upon the input current position. In figure 5.4 when depending upon input current position LP, BP and HP filtered output is obtained while notch-filtered output is obtained when equal input current is given concurrently.

Therefore, sixteen plausible configurations are there based on the position of input current and resistance feedback i.e., LP controlled LP filter, LP controlled BP filter, LP controlled HP filter, LP controlled notch filter, BP controlled LP filter, BP controlled BP filter, BP controlled HP filter, BP controlled notch filter, HP controlled LP filter, HP controlled BP filter, HP controlled HP filter, HP controlled notch filter, notch-controlled LP filter, notch controlled BP filter, notch controlled HP filter and notch controlled notch filter.



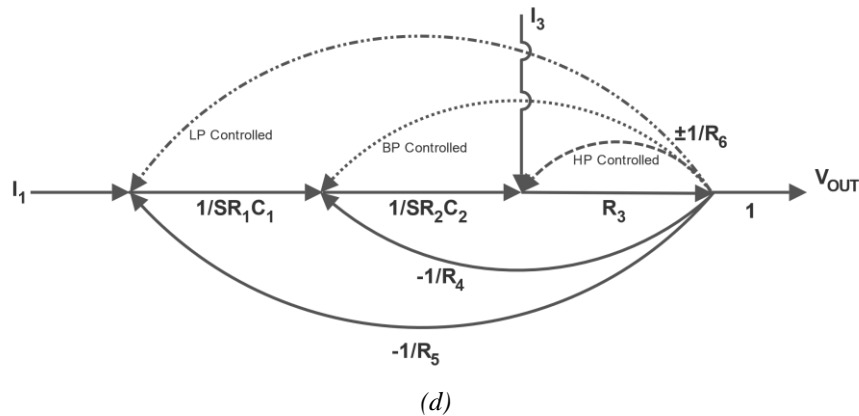
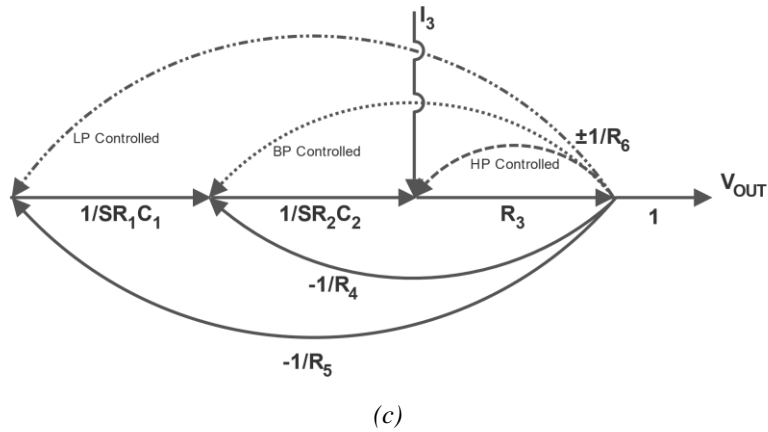


Figure 5.4:(a) LP filter, (b) BP filter, (c) HP filter, (d) Notch filter

Shadow filters can be used with both positive and negative feedback configurations. However, as the scale of the effective input signal increases in electronic and control systems, too much praise and positive feedback can create oscillatory circuit responses. Positive or regenerative feedback raises the gain and the risk of instability in a system, perhaps leading to self-oscillation.; thus, negative feedback shadow filters are used in conjunction with positive feedback in this paper, with the system's stability in mind. The signal flow graph of each case can be used to determine the transfer function and filter characteristic parameters.

### 5.2.1. Positive feedback:

- With  $I_1$  input current and with positive feedback resistance  $R_6$ , LP controlled LP shadow filter is obtained.

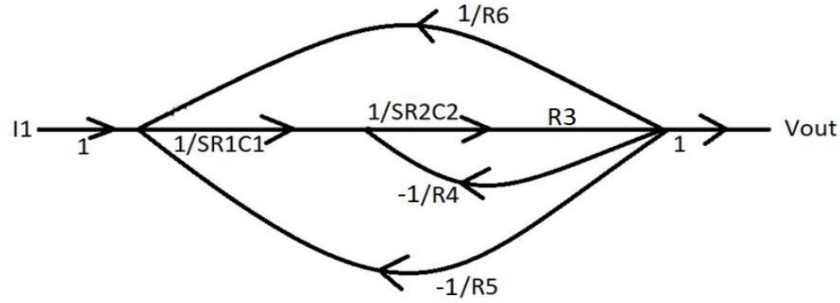


Fig 5.5: Signal flow graph of LP controlled LP shadow filter

$$\Delta_1 = 1 - \left[ \frac{-R_3}{SR_2C_2R_4} - \frac{R_3}{S^2R_5R_2R_1C_2C_1} + \frac{R_3}{S^2R_6R_2R_1C_2C_1} \right]$$

$$= 1 - \left[ \frac{-R_3}{SR_2C_2R_4} - \frac{R_3}{S^2R_2R_1C_2R_1} \left[ \frac{1}{R_5} - \frac{1}{R_6} \right] \right]$$

$$= 1 - \left[ \frac{-R_3}{SR_2C_2R_4} - \frac{R_3R_6 + R_3R_5}{S^2R_6R_5R_2R_1C_2S_1} \right]$$

$$\Delta_1 = \frac{S^2R_6R_5R_4R_2R_1C_2C_1 + BR_6R_5R_3R_1C_1 + R_3(R_5 - R_6)R_4}{S^2R_6R_5R_4R_2R_1C_2C_1}$$

$$\frac{V_{out}}{I_1} = \frac{R_6R_5R_4R_3}{S^2R_6R_5R_4R_2R_1C_2C_1 + SR_6R_5R_3R_1C_1 + R_3(R_5 - R_6)R_4} \quad \text{Eq (4)}$$

$$w = \sqrt{\frac{R_3 (R_5 - R_6)}{R_5 R_6 R_2 R_1 C_2 C_1}}$$

$$\frac{\omega}{Q} = \sqrt{\frac{R_3}{R_4 R_2 C_2}}$$

$$Q = R_4 \sqrt{\frac{(R_5 - R_6) R_2 C_2}{R_5 R_6 R_3 R_1 C_1}}$$

Equation (4) corresponds to LP controlled LP filter with R6 as positive feedback gain.

- With  $I_2$  input current with positive feedback Resistance  $R_6$ , BP controlled BP shadow filter is obtained.

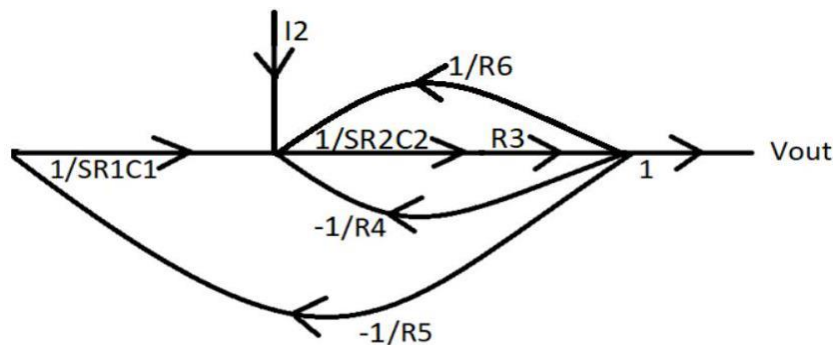


Fig 5.6: Signal flow graph of BP controlled BP shadow filter

$$\Delta_2 = 1 - \left[ \left[ -\frac{R_3}{SR_4R_2C_2} + \frac{R_3}{SR_6R_2C_2} \right] - \frac{R_3}{S^2R_5R_2R_1C_2C_1} \right]$$

$$\Delta_2 = \frac{S^2R_5R_6R_4R_2R_1C_2C_1 + SR_3R_5R_1C_1(R_6 - R_4) + R_3R_6R_4}{S^2R_6R_5R_4R_2R_1C_2C_1}$$

$$\frac{V_{out}}{I_2} = \frac{SR_6R_5R_4R_3R_1C_1}{S^2R_5R_6R_4R_2R_1C_2C_1 + SR_3R_5R_1C_1(R_6 - R_4) + R_3R_6R_4} \quad \text{Eq (5)}$$

$$\omega = \sqrt{\frac{1}{R_2R_1C_2C_1} \frac{R_3}{R_5}}$$

$$\frac{\omega}{Q} = \frac{R_3(R_6 - R_4)}{R_6R_4R_2C_2}$$

$$Q = \frac{R_6R_4}{(R_6 - R_4)} \sqrt{\frac{R_2C_2}{R_1R_3R_5C_1}}$$

Equation (5) corresponds to BP controlled BP filter with R6 as positive feedback gain.

- With  $I_3$  input current with positive feedback Resistance  $R_6$ , HP controlled HP shadow filter is obtained

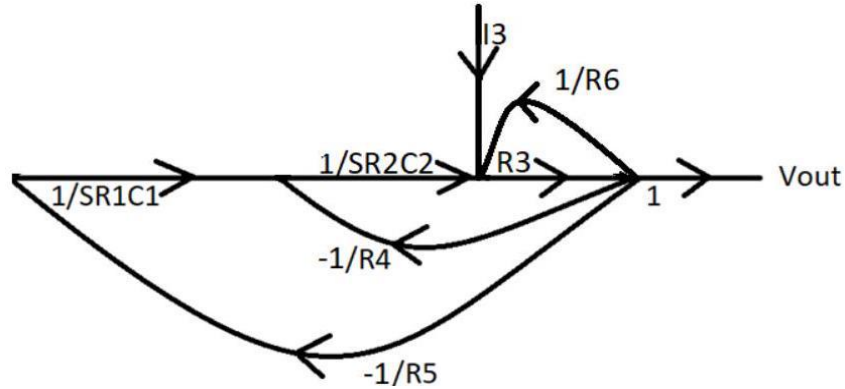


Fig 5.7: Signal flow graph of HP controlled HP shadow filter

$$\Delta_3 = 1 - \left[ \frac{-R_3}{SR_4R_2C_2} - \frac{R_3}{S^2R_5R_1R_2C_1C_2} + \frac{R_3}{R_6} \right]$$

$$\Delta_3 = \frac{S^2R_5R_4R_2R_1C_2C_1(R_6 - R_3) + S(R_6R_5R_3R_1C_1) + R_3R_4R_6}{S^2R_6R_5R_4R_2R_1C_2C_1}$$

$$\frac{V_{out}}{I_3} = \frac{S^2R_6R_5R_4R_3R_2R_1C_2C_1}{S^2R_5R_4R_2R_1C_2C_1(R_6 - R_3) + S(R_6R_5R_3R_1C_1) + R_3R_4R_6} \quad \text{Eq (6)}$$

$$\omega = \sqrt{\frac{R_3 R_6}{R_5 R_2 R_1 C_2 C_1 (R_6 - R_3)}}$$

$$\frac{\omega}{Q} = \frac{R_3 R_6}{R_4 R_2 C_2 (R_6 - R_3)}$$

$$Q = R_4 \sqrt{\frac{R_2 C_2 (R_6 - R_3)}{R_6 R_5 R_3 R_1 C_1}}$$

Equation (6) corresponds to HP controlled HP filter with R6 as positive feedback gain.

- With  $I_1$  &  $I_3$  input current with positive feedback Resistances  $R_7$  &  $R_6$  Notch shadow filter is obtained

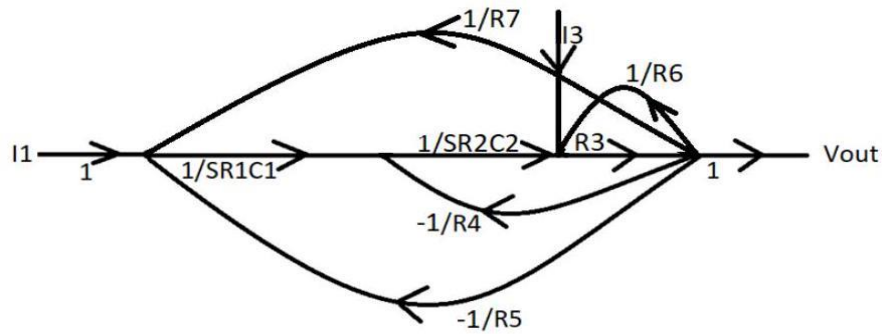


Fig 5.8: Signal flow graph of Notch controlled notch shadow filter

$$\Delta_4 = 1 - \left[ \frac{-R_3}{SR_4 R_2 C_2} - \frac{R_3}{S^2 R_5 R_1 R_2 C_1 C_2} + \frac{R_3}{S^2 R_7 R_1 R_2 C_1 C_2} + \frac{R_3}{R_6} \right]$$

$$\Delta_4 = \frac{S^2 R_7 R_5 R_4 R_2 R_1 C_2 C_1 (R_6 - R_3) + S(R_7 R_6 R_5 R_3 R_1 C_1) + R_3 R_4 R_6 (R_5 - R_7)}{S^2 R_7 R_6 R_5 R_4 R_2 R_1 C_2 C_1}$$

$$\frac{V_{out}}{I} = \frac{S^2 R_7 R_5 R_4 R_3 R_2 R_1 C_2 C_1 + R_7 R_6 R_5 R_3}{S^2 R_7 R_5 R_4 R_2 R_1 C_2 C_1 (R_6 - R_3) + S(R_7 R_6 R_5 R_3 R_1 C_1) + R_3 R_4 R_6 (R_5 - R_7)} \quad \text{Eq (7)}$$

$$\omega = \sqrt{\frac{R_3 R_6 (R_5 - R_7)}{R_7 R_5 R_2 R_1 C_2 C_1 (R_6 - R_3)}}$$

$$\frac{\omega}{Q} = \frac{R_3 R_6}{R_4 R_2 C_2 (R_6 - R_3)}$$

$$Q = R_4 \sqrt{\frac{R_2 C_2 (R_5 - R_7) (R_6 - R_3)}{R_7 R_5 R_1 C_1}}$$

Equation (7) corresponds Notch controlled notch filter with  $R_7$  &  $R_6$  as positive feedback gain.

- Band pass controlled Low pass shadow filter:



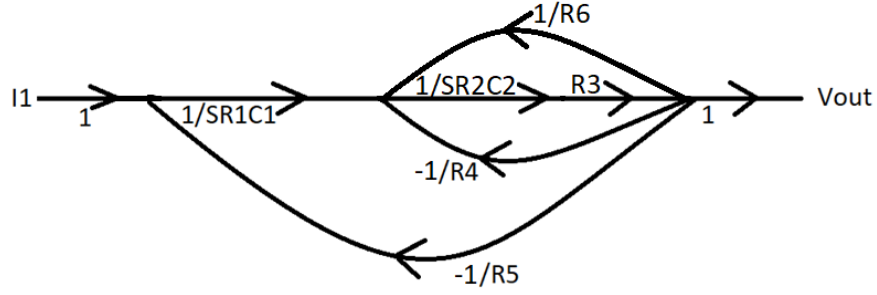


Fig 5.9: Signal flow graph of Band pass controlled Low pass shadow filter

$$\Delta_2 = \frac{S^2 R_5 R_6 R_4 R_2 R_1 C_2 C_1 + S R_3 R_5 R_1 C_1 (R_6 - R_4) + R_3 R_6 R_4}{S^2 R_6 R_5 R_4 R_2 R_1 C_2 C_1}$$

$$\frac{V_{out}}{I_1} = \frac{R_6 R_5 R_4 R_3}{S^2 R_5 R_6 R_4 R_2 R_1 C_2 C_1 + S R_3 R_5 R_1 C_1 (R_6 - R_4) + R_3 R_6 R_4} \quad \text{Eq (8)}$$

$$\omega = \sqrt{\frac{1}{R_2 R_1 C_2 C_1} \frac{R_3}{R_5}}$$

$$\frac{\omega}{Q} = \frac{R_3 (R_6 - R_4)}{R_6 R_4 R_2 C_2}$$

$$Q = \frac{R_6 R_4}{(R_6 - R_4)} \sqrt{\frac{R_2 C_2}{R_1 R_3 R_5 C_1}}$$

Equation (8) corresponds to Band pass controlled Low pass shadow filter with  $R_6$  as positive feedback gain.

- High pass controlled Low pass shadow filter:

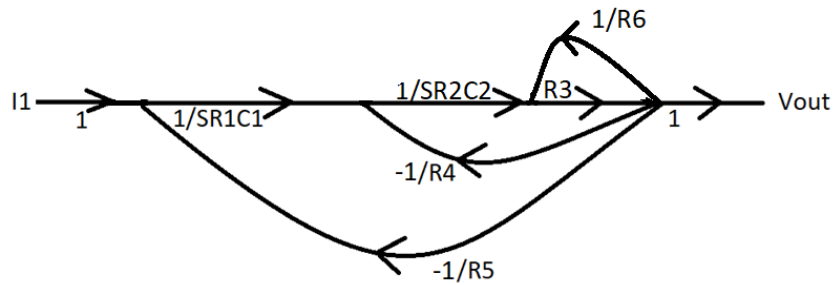


Fig 5.10: Signal flow graph of High pass controlled Low pass shadow filter

$$\Delta_3 = 1 - \left[ \frac{-R_3}{SR_4R_2C_2} - \frac{R_3}{S^2R_5R_1R_2C_1C_2} + \frac{R_3}{R_6} \right]$$

$$\Delta_3 = \frac{S^2R_5R_4R_2R_1C_2C_1(R_6 - R_3) + S(R_6R_5R_3R_1C_1) + R_3R_4R_6}{S^2R_6R_5R_4R_2R_1C_2C_1}$$

$$\frac{V_{out}}{I_1} = \frac{R_6R_5R_4R_3}{S^2R_5R_4R_2R_1C_2C_1(R_6 - R_3) + S(R_6R_5R_3R_1C_1) + R_3R_4R_6}$$

$$\omega = \sqrt{\frac{R_3R_6}{R_5R_2R_1C_2C_1(R_6 - R_3)}}$$

$$\frac{\omega}{Q} = \frac{R_3R_6}{R_4R_2C_2(R_6 - R_3)}$$

$$Q = R_4 \sqrt{\frac{R_2C_2(R_6 - R_3)}{R_6R_5R_3R_1C_1}}$$

Eq (9)

Equation (9) corresponds to High pass controlled Low pass shadow filter with  $R_6$  as positive feedback gain.

- Notch controlled Low pass shadow filter

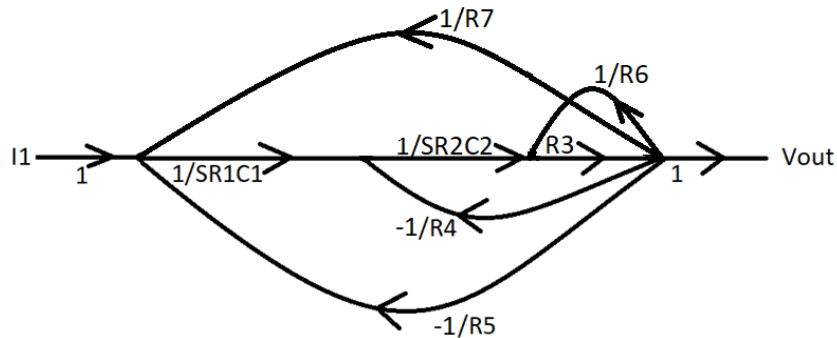


Fig 5.11: Signal flow graph of Notch controlled Low pass shadow filter

$$\Delta_4 = 1 - \left[ \frac{-R_3}{SR_4R_2C_2} - \frac{R_3}{S^2R_5R_1R_2C_1C_2} + \frac{R_3}{S^2R_7R_1R_2C_1C_2} + \frac{R_3}{R_6} \right]$$

$$\Delta_4 = \frac{S^2R_7R_5R_4R_2R_1C_2C_1(R_6 - R_3) + S(R_7R_6R_5R_3R_1C_1) + R_3R_4R_6(R_5 - R_7)}{S^2R_7R_6R_5R_4R_2R_1C_2C_1}$$

$$\frac{V_{out}}{I_1} = \frac{R_7R_6R_5R_4R_3}{S^2R_7R_5R_4R_2R_1C_2C_1(R_6 - R_3) + S(R_7R_6R_5R_3R_1C_1) + R_3R_4R_6(R_5 - R_7)}$$

$$\omega = \sqrt{\frac{R_3R_6(R_5 - R_7)}{R_7R_5R_2R_1C_2C_1(R_6 - R_3)}}$$

$$\frac{\omega}{Q} = \frac{R_3R_6}{R_4R_2C_2(R_6 - R_3)}$$

Eq(10)

Equation (10) corresponds to Notch controlled Low pass shadow filter with  $R_7$  &  $R_6$  as positive feedback gain.

- Low pass-controlled Band pass shadow filter

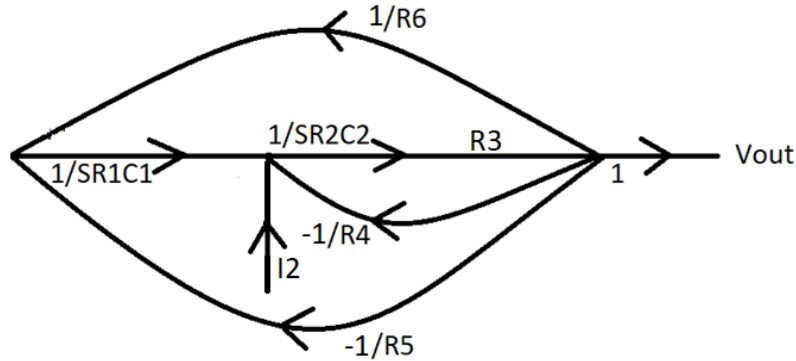


Fig 5.12: Signal flow graph of Low pass-controlled Band pass shadow filter

$$\begin{aligned} \Delta_1 &= 1 - \left[ \frac{-R_3}{SR_2C_2R_4} - \frac{R_3}{S^2R_5R_2R_1C_2C_1} + \frac{R_3}{S^2R_6R_2R_1C_2C_1} \right] \\ \Delta_1 &= \frac{S^2R_6R_5R_4R_2R_1C_2C_1 + SR_6R_5R_3R_1C_1 + R_3(R_5 - R_6)R_4}{S^2R_6R_5R_4R_2R_1C_2C_1} \\ \frac{V_{out}}{I_2} &= \frac{SR_6R_5R_4R_3R_1C_1}{S^2R_6R_5R_4R_2R_1C_2C_1 + SR_6R_5R_3R_1C_1 + R_3(R_5 - R_6)R_4} \quad \text{Eq (11)} \\ w &= \sqrt{\frac{R_3 (R_5 - R_6)}{R_5 R_6 R_2 R_1 C_2 C_1}} \\ \frac{\omega}{Q} &= \sqrt{\frac{R_3}{R_4 R_2 C_2}} \\ Q &= R_4 \sqrt{\frac{(R_5 - R_6) R_2 C_2}{R_5 R_6 R_3 R_1 C_1}} \end{aligned}$$

Equation (11) corresponds to Low pass-controlled Band pass shadow filter with  $R_6$  as positive feedback gain.

- High pass-controlled Band pass shadow filter

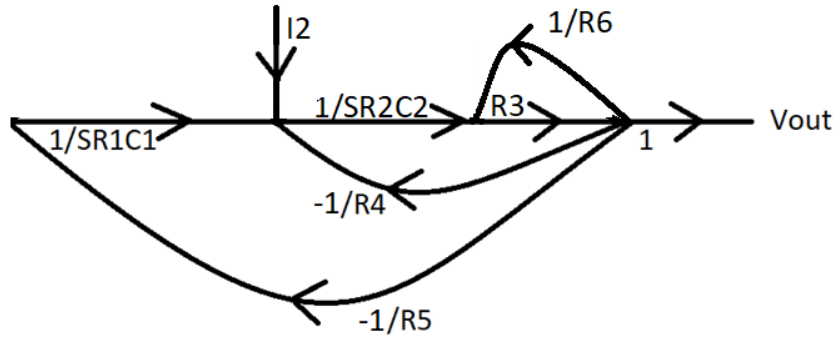


Fig 5.13: Signal flow graph of High pass-controlled Band pass shadow filter

$$\Delta_3 = 1 - \left[ \frac{-R_3}{SR_4R_2C_2} - \frac{R_3}{S^2R_5R_1R_2C_1C_2} + \frac{R_3}{R_6} \right]$$

$$\Delta_3 = \frac{S^2R_5R_4R_2R_1C_2C_1(R_6R_3) + S(R_6R_5R_3R_1C_1) + R_3R_4R_6}{S^2R_6R_5R_4R_2R_1C_2C_1}$$

$$\frac{V_{out}}{I_2} = \frac{SR_6R_5R_4R_3R_1C_1}{S^2R_5R_4R_2R_1C_2C_1(R_6 - R_3) + S(R_6R_5R_3R_1C_1) + R_3R_4R_6} \quad \text{Eq (12)}$$

$$\omega = \sqrt{\frac{R_3R_6}{R_5R_2R_1C_2C_1(R_6 - R_3)}}$$

$$\frac{\omega}{Q} = \frac{R_3R_6}{R_4R_2C_2(R_6 - R_3)}$$

$$Q = R_4 \sqrt{\frac{R_2C_2(R_6 - R_3)}{R_6R_5R_3R_1C_1}}$$

Equation (12) corresponds to High pass-controlled Band pass shadow filter with  $R_6$  as positive feedback gain.

- Notch controlled Band pass shadow filter

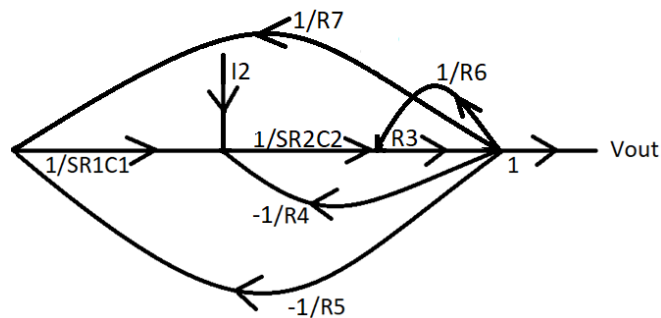


Fig 5.14: Signal flow graph of Notch controlled Band pass shadow filter

$$\begin{aligned}
\Delta_4 &= 1 - \left[ \frac{-R_3}{SR_4R_2C_2} - \frac{R_3}{S^2R_5R_1R_2C_1C_2} + \frac{R_3}{S^2R_7R_1R_2C_1C_2} + \frac{R_3}{R_6} \right] \\
\Delta_4 &= \frac{S^2R_7R_5R_4R_2R_1C_2C_1(R_6 - R_3) + S(R_7R_6R_5R_3R_1C_1) + R_3R_4R_6(R_5 - R_7)}{S^2R_7R_6R_5R_4R_2R_1C_2C_1} \\
\frac{V_{out}}{I_2} &= \frac{SR_7R_6R_5R_4R_3R_1C_1}{S^2R_7R_5R_4R_2R_1C_2C_1(R_6 - R_3) + S(R_7R_6R_5R_3R_1C_1) + R_3R_4R_6(R_5 - R_7)} \quad \text{Eq (13)} \\
\omega &= \sqrt{\frac{R_3R_6(R_5 - R_7)}{R_7R_5R_2R_1C_2C_1(R_6 - R_3)}} \\
\frac{\omega}{Q} &= \frac{R_3R_6}{R_4R_2C_2(R_6 - R_3)}
\end{aligned}$$

Equation (13) corresponds to Notch controlled Band pass shadow filter with  $R_6$  &  $R_7$  as positive feedback gain.

- Low pass controlled High pass shadow filter

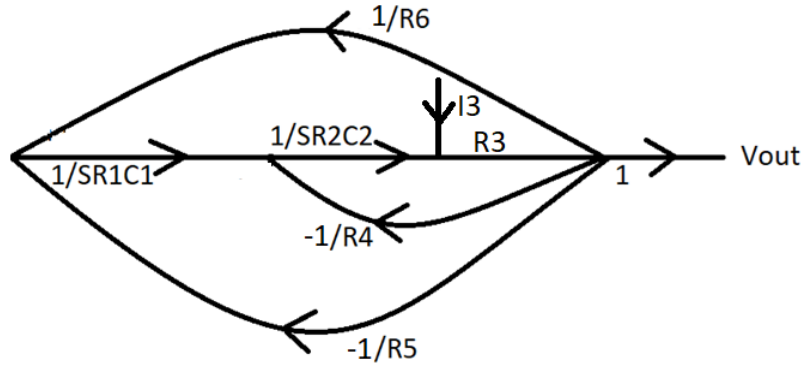


Fig 5.15: Signal flow graph of Low pass controlled High pass shadow filter

$$\begin{aligned}
\Delta_1 &= 1 - \left[ \frac{-R_3}{SR_2C_2R_4} - \frac{R_3}{S^2R_5R_2R_1C_2C_1} + \frac{R_3}{S^2R_6R_2R_1C_2C_1} \right] \\
\Delta_1 &= \frac{S^2R_6R_5R_4R_2R_1C_2C_1 + BR_6R_5R_3R_1C_1 + R_3(R_5 - R_6)R_4}{S^2R_6R_5R_4R_2R_1C_2C_1} \\
\frac{V_{out}}{I_3} &= \frac{S^2R_6R_5R_4R_3R_2R_1C_2C_1}{S^2R_6R_5R_4R_2R_1C_2C_1 + SR_6R_5R_3R_1C_1 + R_3(R_5 - R_6)R_4} \quad \text{Eq (14)} \\
w &= \sqrt{\frac{R_3(R_5 - R_6)}{R_5R_6R_2R_1C_2C_1}} \\
\frac{\omega}{Q} &= \sqrt{\frac{R_3}{R_4R_2C_2}} \\
Q &= R_4 \sqrt{\frac{(R_5 - R_6)R_2C_2}{R_5R_6R_3R_1C_1}}
\end{aligned}$$

Equation (14) corresponds to Low pass controlled High pass shadow filter with  $R_6$  as positive

feedback gain.

- Band pass controlled High pass shadow filter

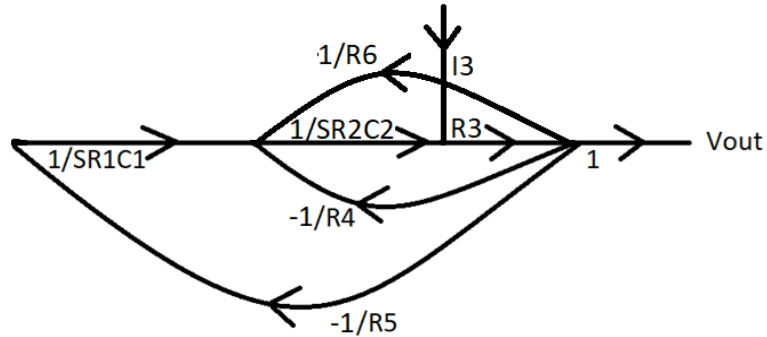


Fig 5.16: Signal flow graph of Band pass controlled High pass shadow filter

$$\Delta_2 = \frac{S^2 R_5 R_6 R_4 R_2 R_1 C_2 C_1 + S R_3 R_5 R_1 C_1 (R_6 - R_4) + R_3 R_6 R_4}{S^2 R_6 R_5 R_4 R_2 R_1 C_2 C_1}$$

$$\frac{V_{out}}{I_3} = \frac{S^2 R_6 R_5 R_4 R_3 R_2 R_1 C_2 C_1}{S^2 R_5 R_6 R_4 R_2 R_1 C_2 C_1 + S R_3 R_5 R_1 C_1 (R_6 - R_4) + R_3 R_6 R_4} \quad \text{Eq (15)}$$

$$\omega = \sqrt{\frac{1}{R_2 R_1 C_2 C_1} \frac{R_3}{R_5}}$$

$$\frac{\omega}{Q} = \frac{R_3 (R_6 - R_4)}{R_6 R_4 R_2 C_2}$$

$$Q = \frac{R_6 R_4}{(R_6 - R_4)} \sqrt{\frac{R_2 C_2}{R_1 R_3 R_5 C_1}}$$

Equation (15) corresponds to Band pass controlled High pass shadow filter with  $R_6$  as positive feedback gain.

- Notch controlled High pass shadow filter

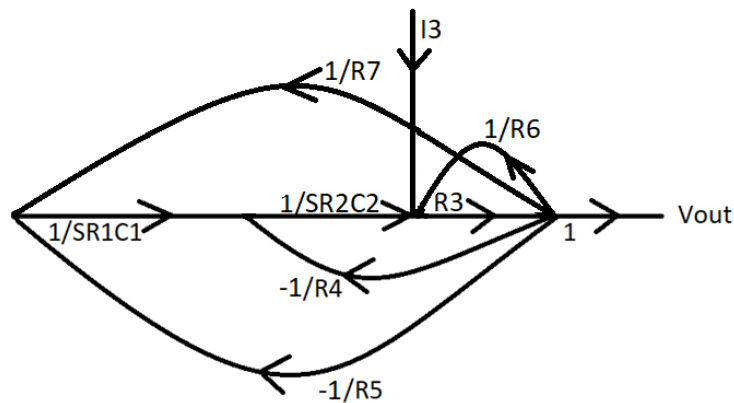


Fig 5.17: Signal flow graph of Notch controlled High pass shadow filter

$$\Delta_4 = 1 - \left[ \frac{-R_3}{SR_4R_2C_2} - \frac{R_3}{S^2R_5R_1R_2C_1C_2} + \frac{R_3}{S^2R_7R_1R_2C_1C_2} + \frac{R_3}{R_6} \right]$$

$$\Delta_4 = \frac{S^2R_7R_6R_5R_4R_2R_1C_2C_1(R_6 - R_3) + S(R_7R_6R_5R_3R_1C_1) + R_3R_4R_6(R_5 - R_7)}{S^2R_7R_6R_5R_4R_2R_1C_2C_1}$$

$$\frac{V_{out}}{I_3} = \frac{S^2R_7R_6R_5R_4R_3R_2R_1C_2C_1}{S^2R_7R_6R_5R_4R_2R_1C_2C_1(R_6 - R_3) + S(R_7R_6R_5R_3R_1C_1) + R_3R_4R_6(R_5 - R_7)}$$

$$\omega = \sqrt{\frac{R_3R_6(R_5 - R_7)}{R_7R_5R_2R_1C_2C_1(R_6 - R_3)}}$$

$$\frac{\omega}{Q} = \frac{R_3R_6}{R_4R_2C_2(R_6 - R_3)}$$

Equation (16) corresponds to Notch controlled Band pass shadow filter with  $R_6$  &  $R_7$  as positive feedback gain.

- Low pass-controlled Notch shadow filter

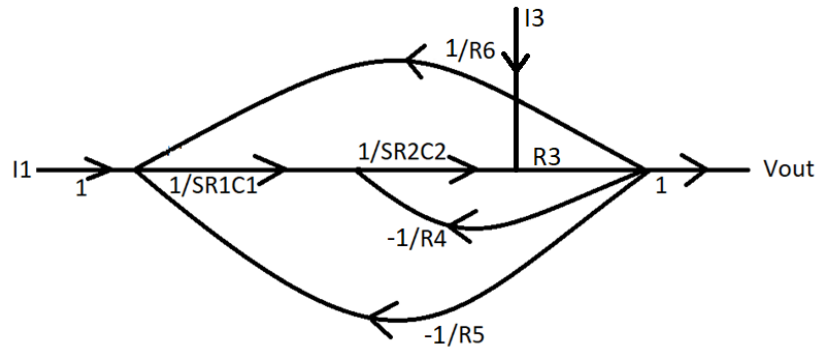


Fig 5.18: Signal flow graph of Low pass-controlled Notch shadow filter

$$\Delta_1 = 1 - \left[ \frac{-R_3}{SR_2C_2R_4} - \frac{R_3}{S^2R_5R_2R_1C_2C_1} + \frac{R_3}{S^2R_6R_2R_1C_2C_1} \right]$$

$$\Delta_1 = \frac{S^2R_6R_5R_4R_2R_1C_2C_1 + BR_6R_5R_3R_1C_1 + R_3(R_5 - R_6)R_4}{S^2R_6R_5R_4R_2R_1C_2C_1}$$

$$\frac{V_{out}}{I} = \frac{S^2R_5R_4R_3R_2R_1C_2C_1 + R_6R_5R_3}{S^2R_6R_5R_4R_2R_1C_2C_1 + SR_6R_5R_3R_1C_1 + R_3(R_5 - R_6)R_4} \quad \text{Eq (17)}$$

$$w = \sqrt{\frac{R_3(R_5 - R_6)}{R_5R_6R_2R_1C_2C_1}}$$

$$\frac{\omega}{Q} = \sqrt{\frac{R_3}{R_4R_2C_2}}$$

$$Q = R_4 \sqrt{\frac{(R_5 - R_6)R_2C_2}{R_5R_6R_3R_1C_1}}$$

Equation (17) corresponds to Low pass-controlled Notch shadow filter with  $R_6$  as positive feedback gain.

- Band pass-controlled Notch shadow filter

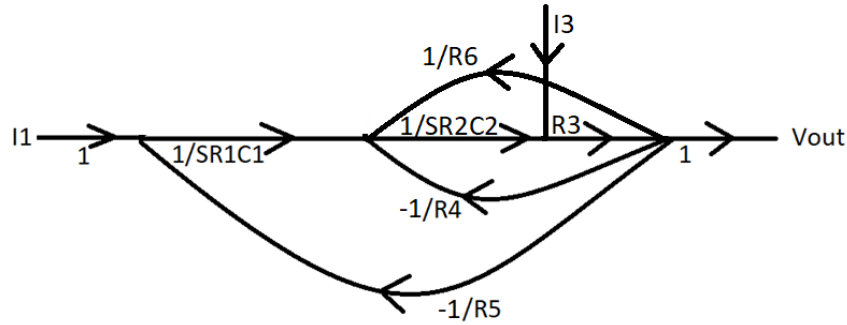


Fig 5.19: Signal flow graph of Band-pass controlled Notch shadow filter

$$\Delta_2 = \frac{S^2 R_5 R_6 R_4 R_2 R_1 C_2 C_1 + S R_3 R_5 R_1 C_1 (R_6 - R_4) + R_3 R_6 R_4}{S^2 R_6 R_5 R_4 R_2 R_1 C_2 C_1}$$

$$\frac{V_{out}}{I} = \frac{S^2 R_5 R_4 R_3 R_2 R_1 C_2 C_1 + R_6 R_5 R_3}{S^2 R_5 R_6 R_4 R_2 R_1 C_2 C_1 + S R_3 R_5 R_1 C_1 (R_6 - R_4) + R_3 R_6 R_4} \quad \text{Eq (18)}$$

$$\omega = \sqrt{\frac{1}{R_2 R_1 C_2 C_1} \frac{R_3}{R_5}}$$

$$\frac{\omega}{Q} = \frac{R_3 (R_6 - R_4)}{R_6 R_4 R_2 C_2}$$

$$Q = \frac{R_6 R_4}{(R_6 - R_4)} \sqrt{\frac{R_2 C_2}{R_1 R_3 R_5 C_1}}$$

Equation (18) corresponds to Band pass-controlled Notch shadow filter with  $R_6$  as positive feedback gain.

- High pass-controlled Notch shadow filter

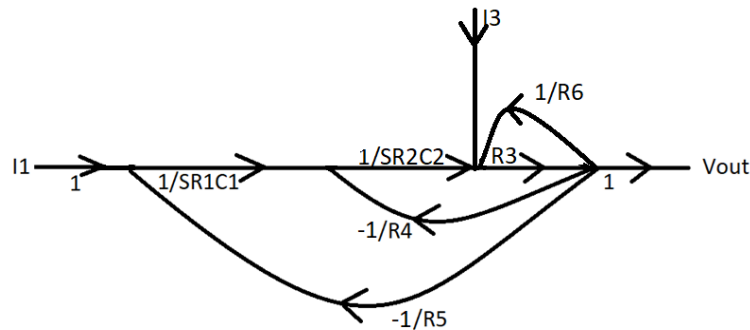


Fig 5.20: Signal flow graph of High pass-controlled Notch shadow filter



$$\Delta_2 = \frac{S^2 R_5 R_6 R_4 R_2 R_1 C_2 C_1 + S R_3 R_5 R_1 C_1 (R_6 - R_4) + R_3 R_6 R_4}{S^2 R_6 R_5 R_4 R_2 R_1 C_2 C_1}$$

$$\frac{V_{out}}{I} = \frac{S^2 R_5 R_4 R_3 R_2 R_1 C_2 C_1 + R_6 R_5 R_3}{S^2 R_5 R_6 R_4 R_2 R_1 C_2 C_1 + S R_3 R_5 R_1 C_1 (R_6 - R_4) + R_3 R_6 R_4} \quad \text{Eq (19)}$$

$$\omega = \sqrt{\frac{1}{R_2 R_1 C_2 C_1} \frac{R_3}{R_5}}$$

$$\frac{\omega}{Q} = \frac{R_3 (R_6 - R_4)}{R_6 R_4 R_2 C_2}$$

$$Q = \frac{R_6 R_4}{(R_6 - R_4)} \sqrt{\frac{R_2 C_2}{R_1 R_3 R_5 C_1}}$$

Equation (19) corresponds to High pass-controlled Notch shadow filter with  $R_6$  as positive feedback gain.

### 5.2.2. Negative feedback:

Too much praise and positive feedback can occasionally boost the system gain far too much, generating oscillatory circuit responses as the scale of the effective input signal increases, just as it might in electronic and control systems. Positive or regenerative feedback raises the gain and the risk of instability in a system, perhaps leading to self-oscillation; thus, negative feedback shadow is proposed further, keeping the system's stability in mind.

- With  $I_1$  input current with negative feedback Resistance  $R_6$

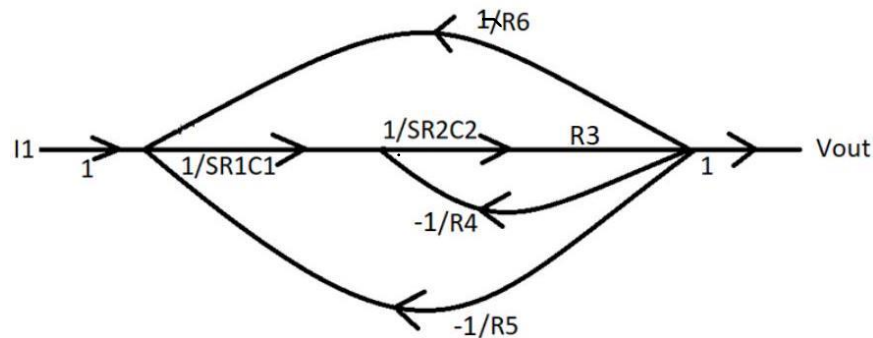


Fig 5.21: Signal flow graph of Low pass controlled low pass shadow filter

$$\Delta_1 = 1 - \left[ \frac{-R_3}{S R_2 C_2 R_4} - \frac{R_3}{S^2 R_5 R_2 R_1 C_2 C_1} - \frac{R_3}{S^2 R_6 R_2 R_1 C_2 C_1} \right]$$

$$\begin{aligned}
&= 1 - \left[ \frac{-R_3}{SR_2C_2R_4} - \frac{R_3}{S^2R_2R_1C_2R_1} \left[ \frac{1}{R_5} + \frac{1}{R_6} \right] \right] \\
&= 1 - \left[ \frac{-R_3}{SR_2C_2R_4} - \frac{R_3R_6 + R_3R_5}{S^2R_6R_5R_2R_1C_2S_1} \right] \\
\Delta_1 &= \frac{S^2R_6R_5R_4R_2R_1C_2C_1 + BR_6R_5R_3R_1C_1 + R_3(R_5 + R_6)R_4}{S^2R_6R_5R_4R_2R_1C_2C_1} \\
\frac{V_{out}}{I_1} &= \frac{R_6R_5R_4R_3}{S^2R_6R_5R_4R_2R_1C_2C_1 + SR_6R_5R_3R_1C_1 + R_3(R_5 + R_6)R_4} \quad \text{Eq (20)} \\
\omega &= \sqrt{\frac{R_3(R_5 + R_6)}{R_5R_6R_2R_1C_2C_1}} \\
\frac{\omega}{Q} &= \sqrt{\frac{R_3}{R_4R_2C_2}} \\
Q &= R_4 \sqrt{\frac{(R_5 + R_6)R_2C_2}{R_5R_6R_3R_1C_1}}
\end{aligned}$$

Equation (20) corresponds to Low pass filter with R6 as negative feedback gain.

- With  $I_2$  input current with negative feedback Resistance  $R_6$

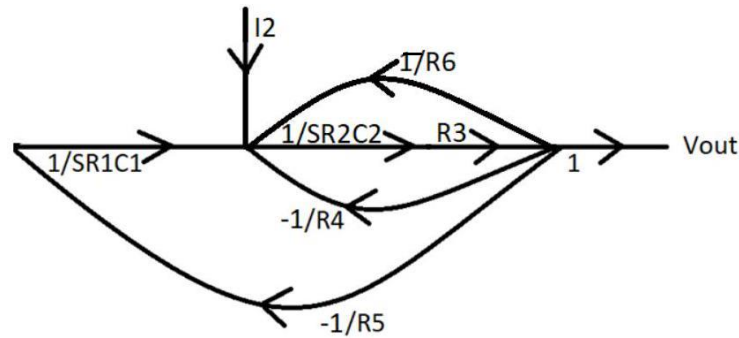


Fig 5.22: Signal flow graph of Band-pass controlled band pass shadow filter

$$\Delta_2 = 1 - \left[ \left[ -\frac{R_3}{SR_4R_2C_2} - \frac{R_3}{SR_6R_2C_2} \right] - \frac{R_3}{S^2R_5R_2R_1C_2C_1} \right]$$

$$\Delta_2 = \frac{S^2 R_5 R_6 R_4 R_2 R_1 C_2 C_1 + S R_3 R_5 R_1 C_1 (R_6 + R_4) + R_3 R_6 R_4}{S^2 R_6 R_5 R_4 R_2 R_1 C_2 C_1}$$

$$\frac{V_{out}}{I_2} = \frac{S R_6 R_5 R_4 R_3 R_1 C_1}{S^2 R_5 R_6 R_4 R_2 R_1 C_2 C_1 + S R_3 R_5 R_1 C_1 (R_6 + R_4) + R_3 R_6 R_4} \quad \text{Eq (21)}$$

$$\omega = \sqrt{\frac{1}{R_2 R_1 C_2 C_1} \frac{R_3}{R_5}}$$

$$\frac{\omega}{Q} = \frac{R_3 (R_6 + R_4)}{R_6 R_4 R_2 C_2}$$

$$Q = \frac{R_6 R_4}{(R_6 + R_4)} \sqrt{\frac{R_2 C_2}{R_1 R_3 R_5 C_1}}$$

Equation (21) corresponds to Band pass filter with R6 as negative feedback gain.

- With  $I_3$  input current with negative feedback Resistance  $R_6$

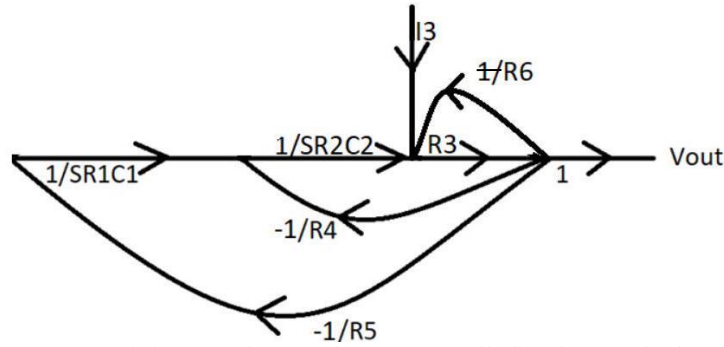


Fig 5.23: Signal flow graph of High pass controlled high pass shadow filter

$$\Delta_3 = 1 - \left[ \frac{-R_3}{S R_4 R_2 C_2} - \frac{R_3}{S^2 R_5 R_1 R_2 C_1 C_2} - \frac{R_3}{R_6} \right]$$

$$\Delta_3 = \frac{S^2 R_5 R_4 R_2 R_1 C_2 C_1 (R_6 + R_3) + S (R_6 R_5 R_3 R_1 C_1) + R_3 R_4 R_6}{S^2 R_6 R_5 R_4 R_2 R_1 C_2 C_1}$$

$$\frac{V_{out}}{I_3} = \frac{S^2 R_6 R_5 R_4 R_3 R_2 R_1 C_2 C_1}{S^2 R_5 R_4 R_2 R_1 C_2 C_1 (R_6 + R_3) + S (R_6 R_5 R_3 R_1 C_1) + R_3 R_4 R_6} \quad \text{Eq (22)}$$

$$\omega = \sqrt{\frac{R_3 R_6}{R_5 R_2 R_1 C_2 C_1 (R_6 + R_3)}}$$

$$\frac{\omega}{Q} = \frac{R_3 R_6}{R_4 R_2 C_2 (R_6 + R_3)}$$

$$Q = R_4 \sqrt{\frac{R_2 C_2 (R_6 + R_3)}{R_6 R_5 R_3 R_1 C_1}}$$

Equation (22) corresponds to High pass filter with R6 as negative feedback gain.

- With  $I_1$  &  $I_3$  input current with negative feedback Resistances  $R_7$  &  $R_6$

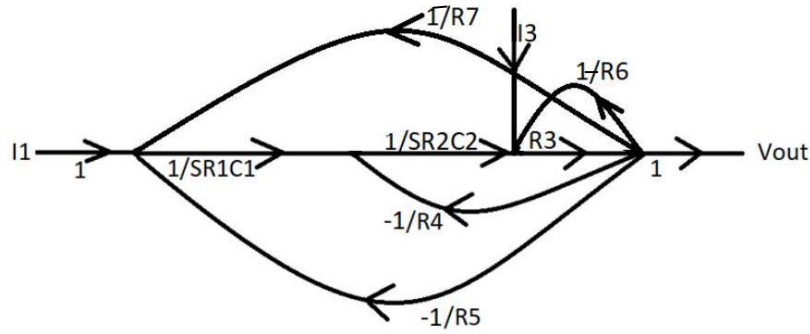


Fig 5.24: Signal flow graph of Notch controlled notch shadow filter

$$\Delta_4 = 1 - \left[ \frac{-R_3}{SR_4R_2C_2} - \frac{R_3}{S^2R_5R_1R_2C_1C_2} - \frac{R_3}{S^2R_7R_1R_2C_1C_2} - \frac{R_3}{R_6} \right]$$

$$\Delta_4 = \frac{S^2R_7R_5R_4R_2R_1C_2C_1(R_6 + R_3) + S(R_7R_6R_5R_3R_1C_1) + R_3R_4R_6(R_5 + R_7)}{S^2R_7R_6R_5R_4R_2R_1C_2C_1}$$

$$\frac{V_{out}}{I} = \frac{S^2R_7R_5R_4R_3R_2R_1C_2C_1 + R_7R_6R_5R_3}{S^2R_7R_5R_4R_2R_1C_2C_1(R_6 + R_3) + S(R_7R_6R_5R_3R_1C_1) + R_3R_4R_6(R_5 + R_7)} \quad \text{Eq (23)}$$

$$\omega = \sqrt{\frac{R_3R_6(R_5 + R_7)}{R_7R_5R_2R_1C_2C_1(R_6 + R_3)}}$$

$$\frac{\omega}{Q} = \frac{R_3R_6}{R_4R_2C_2(R_6 + R_3)}$$

$$Q = R_4 \sqrt{\frac{R_2C_2(R_5 + R_7)(R_6 + R_3)}{R_7R_5R_1C_1}}$$

Equation (23) corresponds Notch filter with  $R_7$  &  $R_6$  as negative feedback gain.

- Band pass controlled Low pass shadow filter:

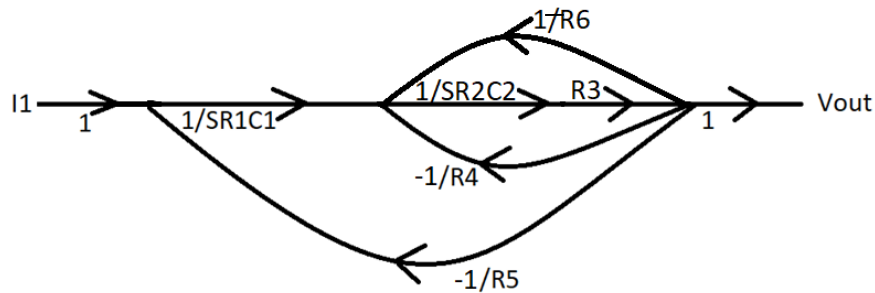


Fig 5.25: Signal flow graph of Band pass controlled Low pass shadow filter

$$\Delta_2 = \frac{S^2 R_5 R_6 R_4 R_2 R_1 C_2 C_1 + S R_3 R_5 R_1 C_1 (R_6 + R_4) + R_3 R_6 R_4}{S^2 R_6 R_5 R_4 R_2 R_1 C_2 C_1}$$

$$\frac{V_{out}}{I_1} = \frac{R_6 R_5 R_4 R_3}{S^2 R_5 R_6 R_4 R_2 R_1 C_2 C_1 + S R_3 R_5 R_1 C_1 (R_6 + R_4) + R_3 R_6 R_4} \quad \text{Eq (24)}$$

$$\omega = \sqrt{\frac{1}{R_2 R_1 C_2 C_1} \frac{R_3}{R_5}}$$

$$\frac{\omega}{Q} = \frac{R_3 (R_6 + R_4)}{R_6 R_4 R_2 C_2}$$

$$Q = \frac{R_6 R_4}{(R_6 + R_4)} \sqrt{\frac{R_2 C_2}{R_1 R_3 R_5 C_1}}$$

Equation (24) corresponds to Band pass controlled Low pass shadow filter with  $R_6$  as negative feedback gain.

- High pass controlled Low pass shadow filter:

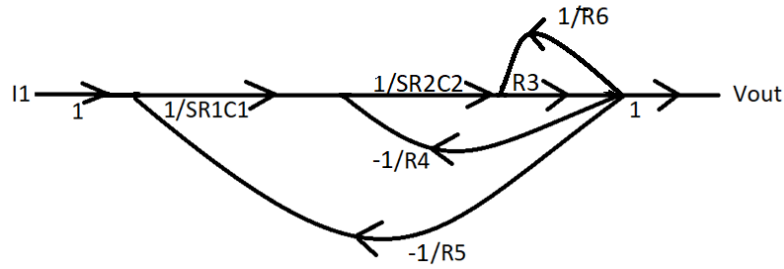


Fig 5.26: Signal flow graph of High pass controlled Low pass shadow filter

$$\Delta_3 = 1 - \left[ \frac{-R_3}{S R_4 R_2 C_2} - \frac{R_3}{S^2 R_5 R_1 R_2 C_1 C_2} - \frac{R_3}{R_6} \right]$$

$$\Delta_3 = \frac{S^2 R_5 R_4 R_2 R_1 C_2 C_1 (R_6 + R_3) + S (R_6 R_5 R_3 R_1 C_1) + R_3 R_4 R_6}{S^2 R_6 R_5 R_4 R_2 R_1 C_2 C_1}$$

$$\frac{V_{out}}{I_1} = \frac{R_6 R_5 R_4 R_3}{S^2 R_5 R_4 R_2 R_1 C_2 C_1 (R_6 + R_3) + S (R_6 R_5 R_3 R_1 C_1) + R_3 R_4 R_6} \quad \text{Eq (25)}$$

$$\omega = \sqrt{\frac{R_3 R_6}{R_5 R_2 R_1 C_2 C_1 (R_6 + R_3)}}$$

$$\frac{\omega}{Q} = \frac{R_3 R_6}{R_4 R_2 C_2 (R_6 + R_3)}$$

$$Q = R_4 \sqrt{\frac{R_2 C_2 (R_6 + R_3)}{R_6 R_5 R_3 R_1 C_1}}$$

Equation (25) corresponds to High pass controlled Low pass shadow filter with  $R_6$  as negative feedback gain.

- Notch controlled Low pass shadow filter

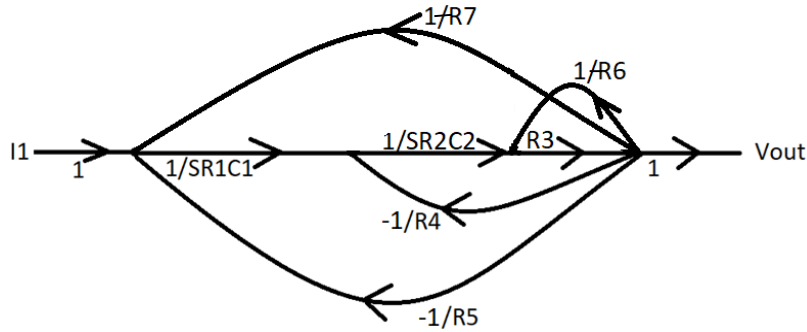


Fig 5.27: Signal flow graph of Notch controlled Low pass shadow filter

$$\Delta_4 = 1 - \left[ \frac{-R_3}{SR_4R_2C_2} - \frac{R_3}{S^2R_5R_1R_2C_1C_2} - \frac{R_3}{S^2R_7R_1R_2C_1C_2} - \frac{R_3}{R_6} \right]$$

$$\Delta_4 = \frac{S^2R_7R_5R_4R_2R_1C_2C_1(R_6 + R_3) + S(R_7R_6R_5R_3R_1C_1) + R_3R_4R_6(R_5 + R_7)}{S^2R_7R_6R_5R_4R_2R_1C_2C_1}$$

$$\frac{V_{out}}{I_1} = \frac{R_7R_6R_5R_4R_3}{S^2R_7R_5R_4R_2R_1C_2C_1(R_6 + R_3) + S(R_7R_6R_5R_3R_1C_1) + R_3R_4R_6(R_5 + R_7)} \quad \text{Eq (26)}$$

$$\omega = \sqrt{\frac{R_3R_6(R_5 + R_7)}{R_7R_5R_2R_1C_2C_1(R_6 + R_3)}}$$

$$\frac{\omega}{Q} = \frac{R_3R_6}{R_4R_2C_2(R_6 + R_3)}$$

Equation (26) corresponds to Notch controlled Low pass shadow filter with  $R_7$  &  $R_6$  as negative feedback gain.

- Low pass-controlled Band pass shadow filter

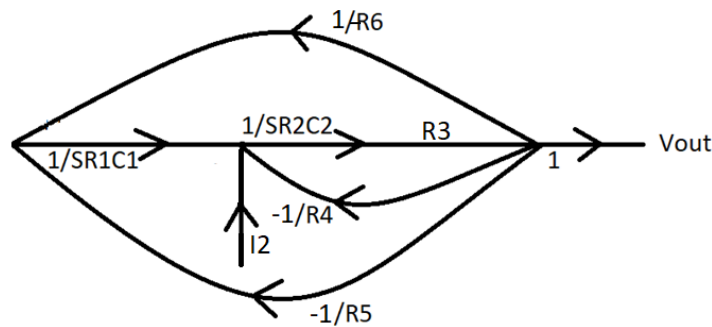


Fig 5.28: Signal flow graph of Low pass-controlled Band pass shadow filter

$$\Delta_1 = 1 - \left[ \frac{-R_3}{SR_2C_2R_4} - \frac{R_3}{S^2R_5R_2R_1C_2C_1} - \frac{R_3}{S^2R_6R_2R_1C_2C_1} \right]$$

$$\Delta_1 = \frac{S^2R_6R_5R_4R_2R_1C_2C_1 + SR_6R_5R_3R_1C_1 + R_3(R_5 + R_6)R_4}{S^2R_6R_5R_4R_2R_1C_2C_1}$$

$$\frac{V_{out}}{I_2} = \frac{SR_6R_5R_4R_3R_1C_1}{S^2R_6R_5R_4R_2R_1C_2C_1 + SR_6R_5R_3R_1C_1 + R_3(R_5 + R_6)R_4} \quad \text{Eq (27)}$$

$$w = \sqrt{\frac{R_3 (R_5 + R_6)}{R_5 R_6 R_2 R_1 C_2 C_1}}$$

$$\frac{\omega}{Q} = \sqrt{\frac{R_3}{R_4 R_2 C_2}}$$

$$Q = R_4 \sqrt{\frac{(R_5 + R_6) R_2 C_2}{R_5 R_6 R_3 R_1 C_1}}$$

Equation (27) corresponds to Low pass-controlled Band pass shadow filter with  $R_6$  as negative feedback gain.

- High pass-controlled Band pass shadow filter

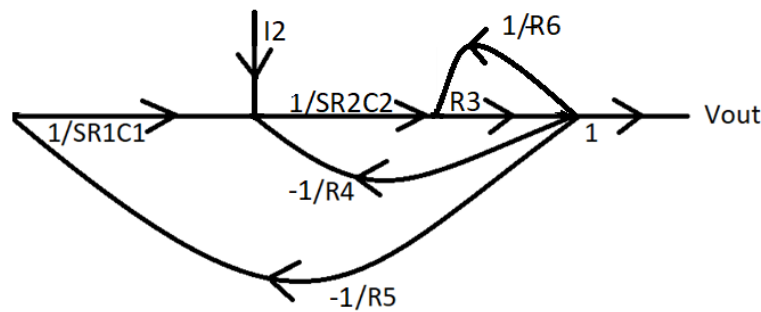


Fig 5.29: Signal flow graph of High pass-controlled Band pass shadow filter

$$\Delta_3 = 1 - \left[ \frac{-R_3}{SR_4R_2C_2} - \frac{R_3}{S^2R_5R_1R_2C_1C_2} - \frac{R_3}{R_6} \right]$$

$$\Delta_3 = \frac{S^2R_5R_4R_2R_1C_2C_1(R_6 + R_3) + S(R_6R_5R_3R_1C_1) + R_3R_4R_6}{S^2R_6R_5R_4R_2R_1C_2C_1}$$

$$\frac{V_{out}}{I_2} = \frac{SR_6R_5R_4R_3R_1C_1}{S^2R_5R_4R_2R_1C_2C_1(R_6 + R_3) + S(R_6R_5R_3R_1C_1) + R_3R_4R_6} \quad \text{Eq (28)}$$

$$\omega = \sqrt{\frac{R_3R_6}{R_5R_2R_1C_2C_1(R_6 + R_3)}}$$

$$\frac{\omega}{Q} = \frac{R_3R_6}{R_4R_2C_2(R_6 + R_3)}$$

$$Q = R_4 \sqrt{\frac{R_2C_2(R_6 + R_3)}{R_6R_5R_3R_1C_1}}$$

Equation (28) corresponds to High pass-controlled Band pass shadow filter with  $R_6$  as negative feedback gain.

- Notch controlled Band pass shadow filter

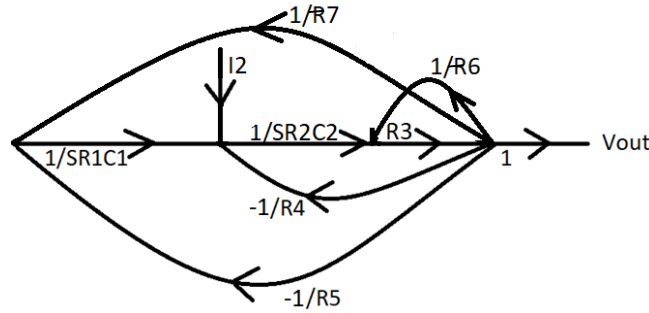


Fig 5.30: Signal flow graph of Notch controlled Band pass shadow filter

$$\Delta_4 = 1 - \left[ \frac{-R_3}{SR_4R_2C_2} - \frac{R_3}{S^2R_5R_1R_2C_1C_2} - \frac{R_3}{S^2R_7R_1R_2C_1C_2} - \frac{R_3}{R_6} \right]$$

$$\Delta_4 = \frac{S^2R_7R_5R_4R_2R_1C_2C_1(R_6 + R_3) + S(R_7R_6R_5R_3R_1C_1) + R_3R_4R_6(R_5 + R_7)}{S^2R_7R_6R_5R_4R_2R_1C_2C_1}$$

$$\frac{V_{out}}{I_2} = \frac{SR_7R_6R_5R_4R_3R_1C_1}{S^2R_7R_5R_4R_2R_1C_2C_1(R_6 + R_3) + S(R_7R_6R_5R_3R_1C_1) + R_3R_4R_6(R_5 + R_7)} \quad \text{Eq (29)}$$

$$\omega = \sqrt{\frac{R_3R_6(R_5 + R_7)}{R_7R_5R_2R_1C_2C_1(R_6 + R_3)}}$$

$$\frac{\omega}{Q} = \frac{R_3R_6}{R_4R_2C_2(R_6 + R_3)}$$

Equation (29) corresponds to Notch controlled Band pass shadow filter with  $R_6$  &  $R_7$  as negative feedback gain.



- Low pass controlled High pass shadow filter

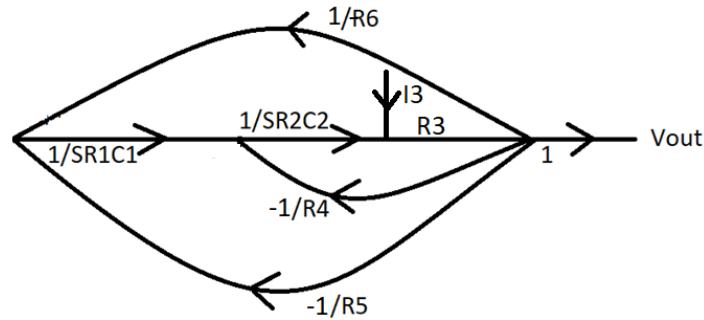


Fig 5.31: Signal flow graph of Low pass controlled High pass shadow filter

$$\Delta_1 = 1 - \left[ \frac{-R_3}{SR_2C_2R_4} - \frac{R_3}{S^2R_5R_2R_1C_2C_1} - \frac{R_3}{S^2R_6R_2R_1C_2C_1} \right]$$

$$\Delta_1 = \frac{S^2R_6R_5R_4R_2R_1C_2C_1 + BR_6R_5R_3R_1C_1 + R_3(R_5 + R_6)R_4}{S^2R_6R_5R_4R_2R_1C_2C_1}$$

$$\frac{V_{out}}{I_3} = \frac{S^2R_6R_5R_4R_3R_2R_1C_2C_1}{S^2R_6R_5R_4R_2R_1C_2C_1 + SR_6R_5R_3R_1C_1 + R_3(R_5 + R_6)R_4} \quad \text{Eq (30)}$$

$$w = \sqrt{\frac{R_3 (R_5 + R_6)}{R_5 R_6 R_2 R_1 C_2 C_1}}$$

$$\frac{\omega}{Q} = \sqrt{\frac{R_3}{R_4 R_2 C_2}}$$

$$Q = R_4 \sqrt{\frac{(R_5 + R_6) R_2 C_2}{R_5 R_6 R_3 R_1 C_1}}$$

Equation (30) corresponds to Low pass controlled High pass shadow filter with  $R_6$  as negative feedback gain.

- Band pass controlled High pass shadow filter

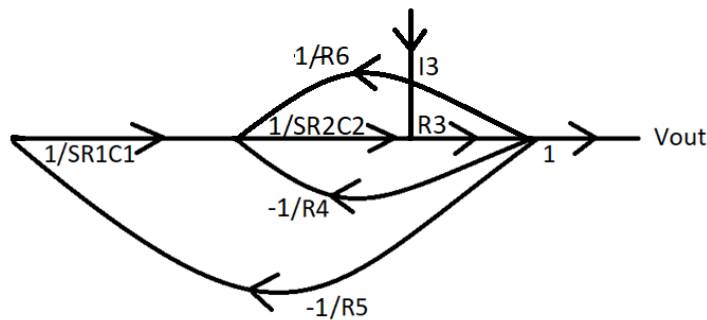


Fig 5.32: Signal flow graph of Band pass controlled High pass shadow filter

$$\Delta_2 = \frac{S^2 R_5 R_6 R_4 R_2 R_1 C_2 C_1 + S R_3 R_5 R_1 C_1 (R_6 + R_4) + R_3 R_6 R_4}{S^2 R_6 R_5 R_4 R_2 R_1 C_2 C_1}$$

$$\frac{V_{out}}{I_3} = \frac{S^2 R_6 R_5 R_4 R_3 R_2 R_1 C_2 C_1}{S^2 R_5 R_6 R_4 R_2 R_1 C_2 C_1 + S R_3 R_5 R_1 C_1 (R_6 + R_4) + R_3 R_6 R_4} \quad \text{Eq(31)}$$

$$\omega = \sqrt{\frac{1}{R_2 R_1 C_2 C_1} \frac{R_3}{R_5}}$$

$$\frac{\omega}{Q} = \frac{R_3 (R_6 + R_4)}{R_6 R_4 R_2 C_2}$$

$$Q = \frac{R_6 R_4}{(R_6 + R_4)} \sqrt{\frac{R_2 C_2}{R_1 R_3 R_5 C_1}}$$

Equation (31) corresponds to Band pass controlled High pass shadow filter with  $R_6$  as negative feedback gain.

- Notch controlled High pass shadow filter

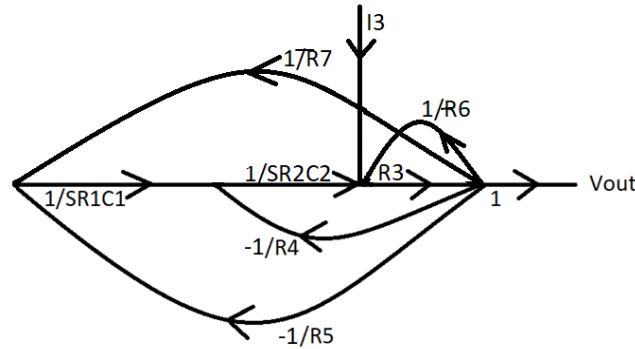


Fig 5.33: Signal flow graph of Notch controlled High pass shadow filter

$$\Delta_4 = 1 - \left[ \frac{-R_3}{S R_4 R_2 C_2} - \frac{R_3}{S^2 R_5 R_1 R_2 C_1 C_2} - \frac{R_3}{S^2 R_7 R_1 R_2 C_1 C_2} - \frac{R_3}{R_6} \right]$$

$$\Delta_4 = \frac{S^2 R_7 R_6 R_5 R_4 R_2 R_1 C_2 C_1 (R_6 + R_3) + S (R_7 R_6 R_5 R_3 R_1 C_1) + R_3 R_4 R_6 (R_5 + R_7)}{S^2 R_7 R_6 R_5 R_4 R_2 R_1 C_2 C_1}$$

$$\frac{V_{out}}{I_3} = \frac{S^2 R_7 R_6 R_5 R_4 R_3 R_2 R_1 C_2 C_1}{S^2 R_7 R_6 R_5 R_4 R_2 R_1 C_2 C_1 (R_6 + R_3) + S (R_7 R_6 R_5 R_3 R_1 C_1) + R_3 R_4 R_6 (R_5 + R_7)} \quad \text{Eq (32)}$$

$$\omega = \sqrt{\frac{R_3 R_6 (R_5 + R_7)}{R_7 R_5 R_2 R_1 C_2 C_1 (R_6 + R_3)}}$$

$$\frac{\omega}{Q} = \frac{R_3 R_6}{R_4 R_2 C_2 (R_6 + R_3)}$$

Equation (16) corresponds to Notch controlled Band pass shadow filter with  $R_6$  &  $R_7$  as negative feedback gain.

- Low pass-controlled Notch shadow filter

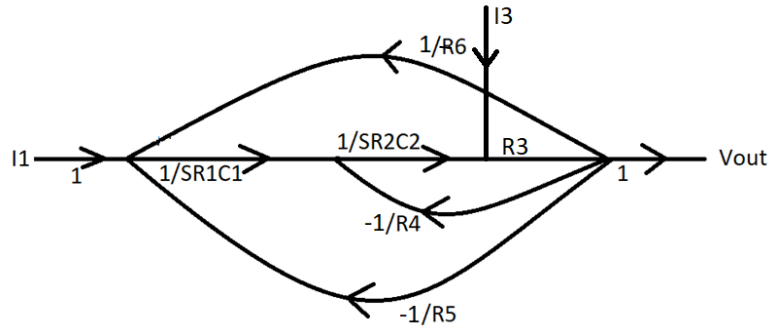


Fig 5.34: Signal flow graph of Low pass-controlled Notch shadow filter

$$\Delta_1 = 1 - \left[ \frac{-R_3}{SR_2C_2R_4} - \frac{R_3}{S^2R_5R_2R_1C_2C_1} - \frac{R_3}{S^2R_6R_2R_1C_2C_1} \right]$$

$$\Delta_1 = \frac{S^2R_6R_5R_4R_2R_1C_2C_1 + BR_6R_5R_3R_1C_1 + R_3(R_5 + R_6)R_4}{S^2R_6R_5R_4R_2R_1C_2C_1}$$

$$\frac{V_{out}}{I} = \frac{S^2R_5R_4R_3R_2R_1C_2C_1 + R_6R_5R_3}{S^2R_6R_5R_4R_2R_1C_2C_1 + SR_6R_5R_3R_1C_1 + R_3(R_5 + R_6)R_4} \quad \text{Eq (33)}$$

$$w = \sqrt{\frac{R_3 (R_5 + R_6)}{R_5 R_6 R_2 R_1 C_2 C_1}}$$

$$\frac{\omega}{Q} = \sqrt{\frac{R_3}{R_4 R_2 C_2}}$$

$$Q = R_4 \sqrt{\frac{(R_5 + R_6) R_2 C_2}{R_5 R_6 R_3 R_1 C_1}}$$

Equation (33) corresponds to Low pass-controlled Notch shadow filter with  $R_6$  as negative feedback gain.

- Band pass-controlled Notch shadow filter

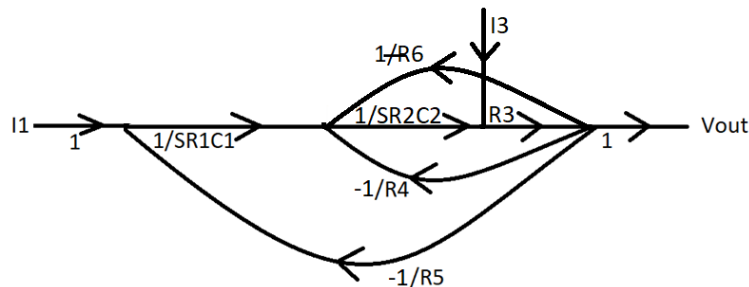


Fig 5.35: Signal flow graph of Band-pass controlled Notch shadow filter

$$\Delta_2 = \frac{S^2 R_5 R_6 R_4 R_2 R_1 C_2 C_1 + S R_3 R_5 R_1 C_1 (R_6 + R_4) + R_3 R_6 R_4}{S^2 R_6 R_5 R_4 R_2 R_1 C_2 C_1}$$

$$\frac{V_{out}}{I} = \frac{S^2 R_5 R_4 R_3 R_2 R_1 C_2 C_1 + R_6 R_5 R_3}{S^2 R_5 R_6 R_4 R_2 R_1 C_2 C_1 + S R_3 R_5 R_1 C_1 (R_6 + R_4) + R_3 R_6 R_4}$$

$$\omega = \sqrt{\frac{1}{R_2 R_1 C_2 C_1} \frac{R_3}{R_5}}$$

$$\frac{\omega}{Q} = \frac{R_3 (R_6 + R_4)}{R_6 R_4 R_2 C_2}$$

$$Q = \frac{R_6 R_4}{(R_6 + R_4)} \sqrt{\frac{R_2 C_2}{R_1 R_3 R_5 C_1}}$$

Equation (34) corresponds to Band pass-controlled Notch shadow filter with  $R_6$  as negative feedback gain.

- High pass-controlled Notch shadow filter

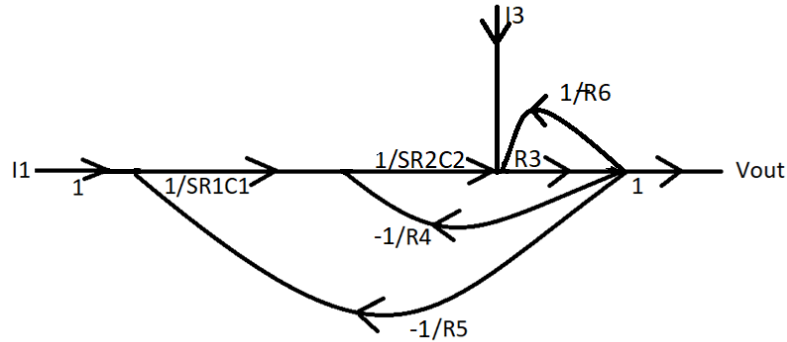


Fig 5.36: Signal flow graph of High pass-controlled Notch shadow filter

$$\Delta_2 = \frac{S^2 R_5 R_6 R_4 R_2 R_1 C_2 C_1 + S R_3 R_5 R_1 C_1 (R_6 + R_4) + R_3 R_6 R_4}{S^2 R_6 R_5 R_4 R_2 R_1 C_2 C_1}$$

$$\frac{V_{out}}{I} = \frac{S^2 R_5 R_4 R_3 R_2 R_1 C_2 C_1 + R_6 R_5 R_3}{S^2 R_5 R_6 R_4 R_2 R_1 C_2 C_1 + S R_3 R_5 R_1 C_1 (R_6 + R_4) + R_3 R_6 R_4} \quad \text{Eq (35)}$$

$$\omega = \sqrt{\frac{1}{R_2 R_1 C_2 C_1} \frac{R_3}{R_5}}$$

$$\frac{\omega}{Q} = \frac{R_3 (R_6 + R_4)}{R_6 R_4 R_2 C_2}$$

$$Q = \frac{R_6 R_4}{(R_6 + R_4)} \sqrt{\frac{R_2 C_2}{R_1 R_3 R_5 C_1}}$$

Equation (35) corresponds to High pass-controlled Notch shadow filter with  $R_6$  as negative feedback gain.

### 5.3 Summary

Table 5.1 corresponds to characteristic features of positive feedback MISO shadow filter whereas Table 5.2 corresponds to characteristic features of negative feedback MISO shadow filter. Characteristic features for different configurations of the filter are obtained by applying Mason gain formula from the signal flow graphs depicted in Figure 5. Furthermore, simplified factors can be obtained likewise as it is obtained for shadow filter beforehand.

TABLE 5.1: CHARACTERISTIC FEATURES OF POSITIVE FEEDBACK MISO SHADOW FILTER

Type of filter	Center frequency ( $\omega'_0$ )	Bandwidth ( $\Delta\omega'$ )	Quality factor ( $Q'$ )	Factors simplified	Controllability
LP controlled LP filter	$\sqrt{\frac{R_3 (R_5 - R_6)}{R_5 R_6 R_2 R_1 C_2 C_1}}$	$\sqrt{\frac{R_3}{R_4 R_2 C_2}}$	$R_4 \sqrt{\frac{(R_5 - R_6) R_2 C_2}{R_5 R_6 R_3 R_1 C_1}}$	$\omega'_0 = \omega_0 \sqrt{(1 - Aa/\omega_0^2)}$ $Q' = Q \sqrt{(1 - Aa/\omega_0^2)}$ $\Delta\omega' = \omega'_0/Q'$	$\omega'_0$ & $Q'$ controllable while $\Delta\omega'$ remains constant
BP controlled BP filter	$\sqrt{\frac{1}{R_2 R_1 C_2 C_1} \frac{R_3}{R_5}}$	$\frac{R_3(R_6 - R_4)}{R_6 R_4 R_2 C_2}$	$\frac{R_6 R_4}{(R_6 - R_4)} \sqrt{\frac{R_2 C_2}{R_1 R_3 R_5 C_1}}$	$\omega'_0 = \omega_0$ $Q' = Q/(1 - AbQ/\omega_0)$ $\Delta\omega' = \omega_0/Q'$	$\Delta\omega'$ & $Q'$ controllable while $\omega'_0$ remains constant
HP controlled HP filter	$\sqrt{\frac{R_3 R_6}{R_5 R_2 R_1 C_2 C_1 (R_6 - R_3)}}$	$\frac{R_3 R_6}{R_4 R_2 C_2 (R_6 - R_3)}$	$R_4 \sqrt{\frac{R_2 C_2 (R_6 - R_3)}{R_6 R_5 R_3 R_1 C_1}}$	$\omega'_0 = \omega_0/\sqrt{(1 - Ac)}$ $Q' = Q\sqrt{(1 - Ac)}$ $\Delta\omega' = \omega'_0/Q'$	$\omega'_0$ , $\Delta\omega'$ & $Q'$ controllable
Notch controlled notch filter	$\sqrt{\frac{R_3 R_6 (R_5 - R_7)}{R_7 R_5 R_2 R_1 C_2 C_1 (R_6 - R_3)}}$	$\frac{R_3 R_6}{R_4 R_2 C_2 (R_6 - R_3)}$	$R_4 \sqrt{\frac{R_2 C_2 (R_5 - R_7) (R_6 - R_3)}{R_7 R_5 R_1 C_1}}$	$\omega'_0 = \omega_0 \sqrt{(1 - Aa/\omega_0^2)/(1 - Ac)}$ $Q' = Q \sqrt{(1 - Aa/\omega_0^2)(1 - Ac)}$ $\Delta\omega' = \omega'_0/Q'$	$\omega'_0$ & $Q'$ controllable while $\Delta\omega'$ controllable distinctly
BP controlled LP filter	$\sqrt{\frac{1}{R_2 R_1 C_2 C_1} \frac{R_3}{R_5}}$	$\frac{R_3(R_6 - R_4)}{R_6 R_4 R_2 C_2}$	$\frac{R_6 R_4}{(R_6 - R_4)} \sqrt{\frac{R_2 C_2}{R_1 R_3 R_5 C_1}}$	$\omega'_0 = \omega_0$ $Q' = Q/(1 - AbQ/\omega_0)$ $\Delta\omega' = \omega_0/Q'$	$\Delta\omega'$ & $Q'$ controllable while $\omega'_0$ remains constant
HP controlled LP filter	$\sqrt{\frac{R_3 R_6}{R_5 R_2 R_1 C_2 C_1 (R_6 - R_3)}}$	$\frac{R_3 R_6}{R_4 R_2 C_2 (R_6 - R_3)}$	$R_4 \sqrt{\frac{R_2 C_2 (R_6 - R_3)}{R_6 R_5 R_3 R_1 C_1}}$	$\omega'_0 = \omega_0/\sqrt{(1 - Ac)}$ $Q' = Q\sqrt{(1 - Ac)}$ $\Delta\omega' = \omega'_0/Q'$	$\omega'_0$ , $\Delta\omega'$ & $Q'$ controllable
Notch controlled LP filter	$\sqrt{\frac{R_3 R_6 (R_5 - R_7)}{R_7 R_5 R_2 R_1 C_2 C_1 (R_6 - R_3)}}$	$\frac{R_3 R_6}{R_4 R_2 C_2 (R_6 - R_3)}$	$R_4 \sqrt{\frac{R_2 C_2 (R_5 - R_7) (R_6 - R_3)}{R_7 R_5 R_1 C_1}}$	$\omega'_0 = \omega_0 \sqrt{(1 - Aa/\omega_0^2)/(1 - Ac)}$ $Q' = Q \sqrt{(1 - Aa/\omega_0^2)(1 - Ac)}$ $\Delta\omega' = \omega'_0/Q'$	$\omega'_0$ & $Q'$ controllable while $\Delta\omega'$ controllable distinctly
HP controlled BP filter	$\sqrt{\frac{R_3 R_6}{R_5 R_2 R_1 C_2 C_1 (R_6 - R_3)}}$	$\frac{R_3 R_6}{R_4 R_2 C_2 (R_6 - R_3)}$	$R_4 \sqrt{\frac{R_2 C_2 (R_6 - R_3)}{R_6 R_5 R_3 R_1 C_1}}$	$\omega'_0 = \omega_0/\sqrt{(1 - Ac)}$ $Q' = Q\sqrt{(1 - Ac)}$ $\Delta\omega' = \omega'_0/Q'$	$\omega'_0$ , $\Delta\omega'$ & $Q'$ controllable
LP controlled BP filter	$\sqrt{\frac{R_3 (R_5 - R_6)}{R_5 R_6 R_2 R_1 C_2 C_1}}$	$\sqrt{\frac{R_3}{R_4 R_2 C_2}}$	$R_4 \sqrt{\frac{(R_5 - R_6) R_2 C_2}{R_5 R_6 R_3 R_1 C_1}}$	$\omega'_0 = \omega_0 \sqrt{(1 - Aa/\omega_0^2)}$ $Q' = Q \sqrt{(1 - Aa/\omega_0^2)}$ $\Delta\omega' = \omega'_0/Q'$	$\omega'_0$ & $Q'$ controllable while $\Delta\omega'$ remains constant
Notch controlled BP filter	$\sqrt{\frac{R_3 R_6 (R_5 - R_7)}{R_7 R_5 R_2 R_1 C_2 C_1 (R_6 - R_3)}}$	$\frac{R_3 R_6}{R_4 R_2 C_2 (R_6 - R_3)}$	$R_4 \sqrt{\frac{R_2 C_2 (R_5 - R_7) (R_6 - R_3)}{R_7 R_5 R_1 C_1}}$	$\omega'_0 = \omega_0 \sqrt{(1 - Aa/\omega_0^2)/(1 - Ac)}$ $Q' = Q \sqrt{(1 - Aa/\omega_0^2)(1 - Ac)}$ $\Delta\omega' = \omega'_0/Q'$	$\omega'_0$ & $Q'$ controllable while $\Delta\omega'$ controllable distinctly
LP controlled HP filter	$\sqrt{\frac{R_3 (R_5 - R_6)}{R_5 R_6 R_2 R_1 C_2 C_1}}$	$\sqrt{\frac{R_3}{R_4 R_2 C_2}}$	$R_4 \sqrt{\frac{(R_5 - R_6) R_2 C_2}{R_5 R_6 R_3 R_1 C_1}}$	$\omega'_0 = \omega_0 \sqrt{(1 - Aa/\omega_0^2)}$ $Q' = Q \sqrt{(1 - Aa/\omega_0^2)}$ $\Delta\omega' = \omega'_0/Q'$	$\omega'_0$ & $Q'$ controllable while $\Delta\omega'$ remains constant
BP controlled HP filter	$\sqrt{\frac{1}{R_2 R_1 C_2 C_1} \frac{R_3}{R_5}}$	$\frac{R_3(R_6 - R_4)}{R_6 R_4 R_2 C_2}$	$\frac{R_6 R_4}{(R_6 - R_4)} \sqrt{\frac{R_2 C_2}{R_1 R_3 R_5 C_1}}$	$\omega'_0 = \omega_0$ $Q' = Q/(1 - AbQ/\omega_0)$ $\Delta\omega' = \omega_0/Q'$	$\Delta\omega'$ & $Q'$ controllable while $\omega'_0$ remains constant
Notch controlled HP filter	$\sqrt{\frac{R_3 R_6 (R_5 - R_7)}{R_7 R_5 R_2 R_1 C_2 C_1 (R_6 - R_3)}}$	$\frac{R_3 R_6}{R_4 R_2 C_2 (R_6 - R_3)}$	$R_4 \sqrt{\frac{R_2 C_2 (R_5 - R_7) (R_6 - R_3)}{R_7 R_5 R_1 C_1}}$	$\omega'_0 = \omega_0 \sqrt{(1 - Aa/\omega_0^2)/(1 - Ac)}$ $Q' = Q \sqrt{(1 - Aa/\omega_0^2)(1 - Ac)}$ $\Delta\omega' = \omega'_0/Q'$	$\omega'_0$ & $Q'$ controllable while $\Delta\omega'$ controllable distinctly
LP controlled Notch filter	$\sqrt{\frac{R_3 (R_5 - R_6)}{R_5 R_6 R_2 R_1 C_2 C_1}}$	$\sqrt{\frac{R_3}{R_4 R_2 C_2}}$	$R_4 \sqrt{\frac{(R_5 - R_6) R_2 C_2}{R_5 R_6 R_3 R_1 C_1}}$	$\omega'_0 = \omega_0 \sqrt{(1 - Aa/\omega_0^2)}$ $Q' = Q \sqrt{(1 - Aa/\omega_0^2)}$ $\Delta\omega' = \omega'_0/Q'$	$\omega'_0$ & $Q'$ controllable while $\Delta\omega'$ remains constant

<i>BP controlled Notch filter</i>	$\sqrt{\frac{1}{R_2 R_1 C_2 C_1} \frac{R_3}{R_5}}$	$\frac{R_3(R_6 - R_4)}{R_6 R_4 R_2 C_2}$	$\frac{R_6 R_4}{(R_6 - R_4)} \sqrt{\frac{R_2 C_2}{R_1 R_3 R_5 C_1}}$	$Q' = \frac{\omega'_0}{Q} = \frac{\omega_0}{(1 - AbQ/\omega_0)}$ $\Delta\omega' = \omega_0/Q'$	$\Delta\omega' & Q'$ controllable while $\omega'_0$ remains constant
<i>HP controlled Notch filter</i>	$\sqrt{\frac{R_3 R_6}{R_5 R_2 R_1 C_2 C_1 (R_6 - R_3)}}$	$\frac{R_3 R_6}{R_4 R_2 C_2 (R_6 - R_3)}$	$R_4 \sqrt{\frac{R_2 C_2 (R_6 - R_3)}{R_6 R_5 R_3 R_1 C_1}}$	$\omega'_0 = \omega_0 \sqrt{(1 - Ac)}$ $Q' = Q \sqrt{(1 - Ac)}$ $\Delta\omega' = \omega'_0/Q'$	$\omega'_0, \Delta\omega' & Q'$ controllable

TABLE 5.2: CHARACTERISTIC FEATURES OF NEGATIVE FEEDBACK MISO SHADOW FILTER

Type of filter	Center frequency ( $\omega'_0$ )	Bandwidth ( $\Delta\omega'$ )	Quality factor ( $Q'$ )	Factors simplified	Controllability
<i>LP controlled LP filter</i>	$\sqrt{\frac{R_3 (R_5 + R_6)}{R_5 R_6 R_2 R_1 C_2 C_1}}$	$\sqrt{\frac{R_3}{R_4 R_2 C_2}}$	$R_4 \sqrt{\frac{(R_5 + R_6) R_2 C_2}{R_5 R_6 R_3 R_1 C_1}}$	$\omega'_0 = \omega_0 \sqrt{(1 + Aa/\omega_0^2)}$ $Q' = Q \sqrt{(1 + Aa/\omega_0^2)}$ $\Delta\omega' = \omega'_0/Q'$	$\omega'_0 & Q'$ controllable while $\Delta\omega'$ remains constant
<i>BP controlled BP filter</i>	$\sqrt{\frac{1}{R_2 R_1 C_2 C_1} \frac{R_3}{R_5}}$	$\frac{R_3(R_6 + R_4)}{R_6 R_4 R_2 C_2}$	$\frac{R_6 R_4}{(R_6 + R_4)} \sqrt{\frac{R_2 C_2}{R_1 R_3 R_5 C_1}}$	$Q' = \frac{\omega'_0}{Q} = \frac{\omega_0}{(1 + AbQ/\omega_0)}$ $\Delta\omega' = \omega_0/Q'$	$\Delta\omega' & Q'$ controllable while $\omega'_0$ remains constant
<i>HP controlled HP filter</i>	$\sqrt{\frac{R_3 R_6}{R_5 R_2 R_1 C_2 C_1 (R_6 + R_3)}}$	$\frac{R_3 R_6}{R_4 R_2 C_2 (R_6 + R_3)}$	$R_4 \sqrt{\frac{R_2 C_2 (R_6 + R_3)}{R_6 R_5 R_3 R_1 C_1}}$	$\omega'_0 = \omega_0 \sqrt{(1 + Ac)}$ $Q' = Q \sqrt{(1 + Ac)}$ $\Delta\omega' = \omega'_0/Q'$	$\omega'_0, \Delta\omega' & Q'$ controllable
<i>Notch controlled notch filter</i>	$\sqrt{\frac{R_3 R_6 (R_5 + R_7)}{R_7 R_5 R_2 R_1 C_2 C_1 (R_6 + R_3)}}$	$\frac{R_3 R_6}{R_4 R_2 C_2 (R_6 + R_3)}$	$R_4 \sqrt{\frac{R_2 C_2 (R_5 + R_7) (R_6 + R_3)}{R_7 R_5 R_1 C_1}}$	$\omega'_0 = \omega_0 \sqrt{\left(1 + \frac{Aa}{\omega_0^2}\right) / (1 + Ac)}$ $Q' = Q \sqrt{\left(1 + \frac{Aa}{\omega_0^2}\right) (1 + Ac)}$ $\Delta\omega' = \omega'_0/Q'$	$\omega'_0 & Q'$ controllable while $\Delta\omega'$ controllable distinctly
<i>BP controlled LP filter</i>	$\sqrt{\frac{1}{R_2 R_1 C_2 C_1} \frac{R_3}{R_5}}$	$\frac{R_3(R_6 + R_4)}{R_6 R_4 R_2 C_2}$	$\frac{R_6 R_4}{(R_6 + R_4)} \sqrt{\frac{R_2 C_2}{R_1 R_3 R_5 C_1}}$	$Q' = \frac{\omega'_0}{Q} = \frac{\omega_0}{(1 + AbQ/\omega_0)}$ $\Delta\omega' = \omega_0/Q'$	$\Delta\omega' & Q'$ controllable while $\omega'_0$ remains constant
<i>HP controlled LP filter</i>	$\sqrt{\frac{R_3 R_6}{R_5 R_2 R_1 C_2 C_1 (R_6 + R_3)}}$	$\frac{R_3 R_6}{R_4 R_2 C_2 (R_6 + R_3)}$	$R_4 \sqrt{\frac{R_2 C_2 (R_6 + R_3)}{R_6 R_5 R_3 R_1 C_1}}$	$\omega'_0 = \omega_0 \sqrt{(1 + Ac)}$ $Q' = Q \sqrt{(1 + Ac)}$ $\Delta\omega' = \omega'_0/Q'$	$\omega'_0, \Delta\omega' & Q'$ controllable
<i>Notch controlled LP filter</i>	$\sqrt{\frac{R_3 R_6 (R_5 + R_7)}{R_7 R_5 R_2 R_1 C_2 C_1 (R_6 + R_3)}}$	$\frac{R_3 R_6}{R_4 R_2 C_2 (R_6 + R_3)}$	$R_4 \sqrt{\frac{R_2 C_2 (R_5 + R_7) (R_6 + R_3)}{R_7 R_5 R_1 C_1}}$	$\omega'_0 = \omega_0 \sqrt{\left(1 + \frac{Aa}{\omega_0^2}\right) / (1 + Ac)}$ $Q' = Q \sqrt{\left(1 + \frac{Aa}{\omega_0^2}\right) (1 + Ac)}$ $\Delta\omega' = \omega'_0/Q'$	$\omega'_0 & Q'$ controllable while $\Delta\omega'$ controllable distinctly
<i>HP controlled BP filter</i>	$\sqrt{\frac{R_3 R_6}{R_5 R_2 R_1 C_2 C_1 (R_6 + R_3)}}$	$\frac{R_3 R_6}{R_4 R_2 C_2 (R_6 + R_3)}$	$R_4 \sqrt{\frac{R_2 C_2 (R_6 + R_3)}{R_6 R_5 R_3 R_1 C_1}}$	$\omega'_0 = \omega_0 \sqrt{(1 + Ac)}$ $Q' = Q \sqrt{(1 + Ac)}$ $\Delta\omega' = \omega'_0/Q'$	$\omega'_0, \Delta\omega' & Q'$ controllable
<i>LP controlled BP filter</i>	$\sqrt{\frac{R_3 (R_5 + R_6)}{R_5 R_6 R_2 R_1 C_2 C_1}}$	$\sqrt{\frac{R_3}{R_4 R_2 C_2}}$	$R_4 \sqrt{\frac{(R_5 + R_6) R_2 C_2}{R_5 R_6 R_3 R_1 C_1}}$	$\omega'_0 = \omega_0 \sqrt{(1 + Aa/\omega_0^2)}$ $Q' = Q \sqrt{(1 + Aa/\omega_0^2)}$ $\Delta\omega' = \omega'_0/Q'$	$\omega'_0 & Q'$ controllable while $\Delta\omega'$ remains constant
<i>Notch controlled BP filter</i>	$\sqrt{\frac{R_3 R_6 (R_5 + R_7)}{R_7 R_5 R_2 R_1 C_2 C_1 (R_6 + R_3)}}$	$\frac{R_3 R_6}{R_4 R_2 C_2 (R_6 + R_3)}$	$R_4 \sqrt{\frac{R_2 C_2 (R_5 + R_7) (R_6 + R_3)}{R_7 R_5 R_1 C_1}}$	$\omega'_0 = \omega_0 \sqrt{\left(1 + \frac{Aa}{\omega_0^2}\right) / (1 + Ac)}$ $Q' = Q \sqrt{\left(1 + \frac{Aa}{\omega_0^2}\right) (1 + Ac)}$ $\Delta\omega' = \omega'_0/Q'$	$\omega'_0 & Q'$ controllable while $\Delta\omega'$ controllable distinctly
<i>LP controlled HP filter</i>	$\sqrt{\frac{R_3 (R_5 + R_6)}{R_5 R_6 R_2 R_1 C_2 C_1}}$	$\sqrt{\frac{R_3}{R_4 R_2 C_2}}$	$R_4 \sqrt{\frac{(R_5 + R_6) R_2 C_2}{R_5 R_6 R_3 R_1 C_1}}$	$\omega'_0 = \omega_0 \sqrt{(1 + Aa/\omega_0^2)}$ $Q' = Q \sqrt{(1 + Aa/\omega_0^2)}$ $\Delta\omega' = \omega'_0/Q'$	$\omega'_0 & Q'$ controllable while $\Delta\omega'$ remains constant
<i>BP controlled HP filter</i>	$\sqrt{\frac{1}{R_2 R_1 C_2 C_1} \frac{R_3}{R_5}}$	$\frac{R_3(R_6 + R_4)}{R_6 R_4 R_2 C_2}$	$\frac{R_6 R_4}{(R_6 + R_4)} \sqrt{\frac{R_2 C_2}{R_1 R_3 R_5 C_1}}$	$Q' = \frac{\omega'_0}{Q} = \frac{\omega_0}{(1 + AbQ/\omega_0)}$ $\Delta\omega' = \omega_0/Q'$	$\Delta\omega' & Q'$ controllable while $\omega'_0$ remains constant
<i>Notch controlled HP filter</i>	$\sqrt{\frac{R_3 R_6 (R_5 + R_7)}{R_7 R_5 R_2 R_1 C_2 C_1 (R_6 + R_3)}}$	$\frac{R_3 R_6}{R_4 R_2 C_2 (R_6 + R_3)}$	$R_4 \sqrt{\frac{R_2 C_2 (R_5 + R_7) (R_6 + R_3)}{R_7 R_5 R_1 C_1}}$	$\omega'_0 = \omega_0 \sqrt{\left(1 + \frac{Aa}{\omega_0^2}\right) / (1 + Ac)}$ $Q' = Q \sqrt{\left(1 + \frac{Aa}{\omega_0^2}\right) (1 + Ac)}$ $\Delta\omega' = \omega'_0/Q'$	$\omega'_0 & Q'$ controllable while $\Delta\omega'$ controllable distinctly

			$\Delta\omega' = \omega'_0/Q'$		
<i>LP controlled Notch filter</i>	$\sqrt{\frac{R_3(R_5 + R_6)}{R_5 R_6 R_2 R_1 C_2 C_1}}$	$\sqrt{\frac{R_3}{R_4 R_2 C_2}}$	$R_4 \sqrt{\frac{(R_5 + R_6) R_2 C_2}{R_5 R_6 R_3 R_1 C_1}}$	$\omega'_0 = \omega_0 \sqrt{(1 + Aa/\omega_0^2)}$ $Q' = Q \sqrt{(1 + Aa/\omega_0^2)}$ $\Delta\omega' = \omega'_0/Q'$	$\omega'_0$ & $Q'$ controllable while $\Delta\omega'$ remains constant
<i>BP controlled Notch filter</i>	$\sqrt{\frac{1}{R_2 R_1 C_2 C_1} \frac{R_3}{R_5}}$	$\frac{R_3(R_6 + R_4)}{R_6 R_4 R_2 C_2}$	$\frac{R_6 R_4}{(R_6 + R_4)} \sqrt{\frac{R_2 C_2}{R_1 R_3 R_5 C_1}}$	$\omega'_0 = \omega_0$ $Q' = Q/(1 + AbQ/\omega_0)$ $\Delta\omega' = \omega_0/Q'$	$\Delta\omega'$ & $Q'$ controllable while $\omega'_0$ remains constant
<i>HP controlled Notch filter</i>	$\sqrt{\frac{R_3 R_6}{R_5 R_2 R_1 C_2 C_1 (R_6 + R_3)}}$	$\frac{R_3 R_6}{R_4 R_2 C_2 (R_6 + R_3)}$	$R_4 \sqrt{\frac{R_2 C_2 (R_6 + R_3)}{R_6 R_5 R_3 R_1 C_1}}$	$\omega'_0 = \omega_0/\sqrt{(1 + Ac)}$ $Q' = Q\sqrt{(1 + Ac)}$ $\Delta\omega' = \omega'_0/Q'$	$\omega'_0$ , $\Delta\omega'$ & $Q'$ controllable

# CHAPTER 6

## SIMULATION AND RESULT

### 6.1 SIMULATION RESULTS

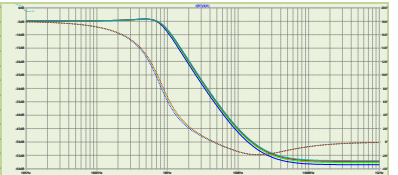
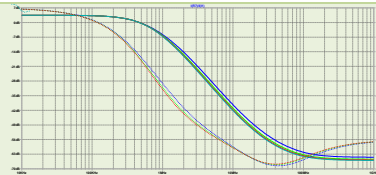
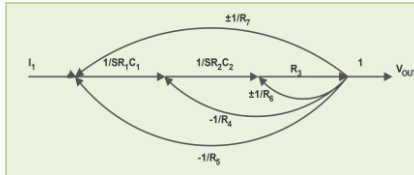
The proposed filter was created with the OTRA framework structure on 180 nm technology using LTspice schematic software with power supplies are given as  $V_{DD} = -V_{SS} = 1.5 \text{ V}$ . Capacitor  $C_1$  and  $C_2$  are of  $4\text{pF}$ . Other circuit components are taken as  $R_1 = R_3 = R_4 = R_5 = 50\text{k}\Omega$ ,  $R_2 = 28\text{k}\Omega$ . A variable resistor  $R_6$  with varying resistance between  $60\text{k}\Omega$  to  $200\text{k}\Omega$  is used to feedback the output to the input terminal for all of the controlled inputs. For notch-controlled filters one more resistor  $R_7 = 100\text{k}\Omega$  is used along with the  $R_6$  resistor to feedback the output to low pass input terminal as  $R_6$  is used to feedback the output to high pass input terminal. Varying values of  $\omega_0$  and  $Q'$  for different values of amplifier gain ( $R_6$ ) are demonstrated in Table 5.3.

TABLE 5.3: SIGNAL FLOW GRAPH AND FREQUENCY RESPONSE OF FILTERS

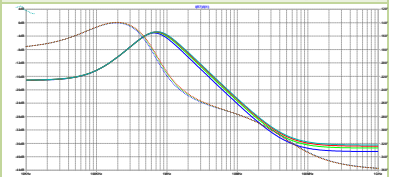
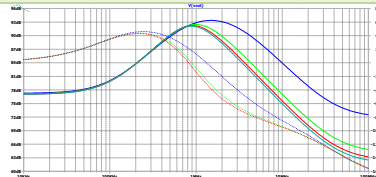
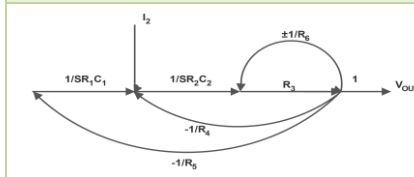
Type of filter	Signal flow graph	Positive feedback response	Negative feedback response
LP controlled LP filter			
BP controlled BP filter			
HP controlled HP filter			
Notch controlled notch filter			
BP controlled LP filter			
HP controlled LP filter			



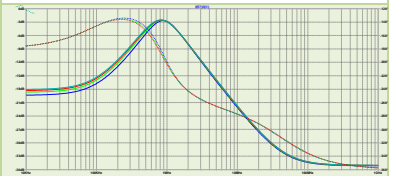
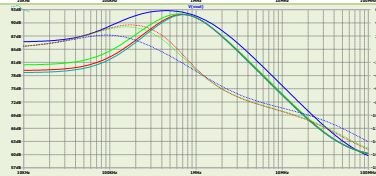
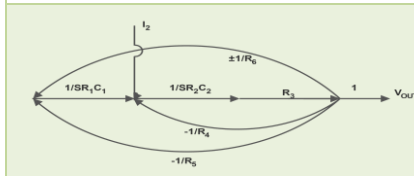
Notch  
controlle  
d LP  
filter



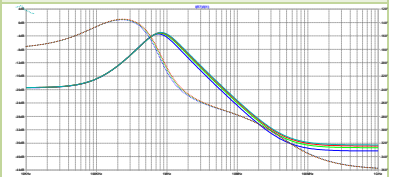
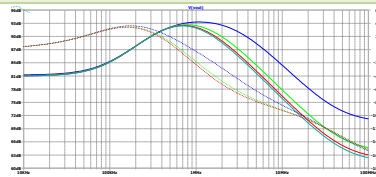
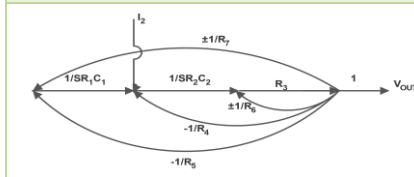
HP  
controlle  
d BP  
filter



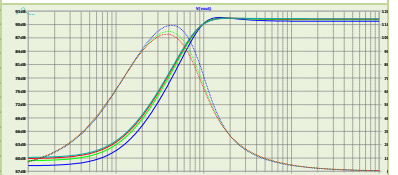
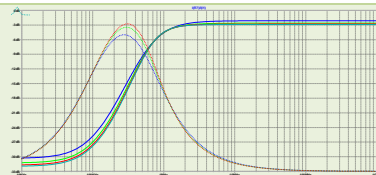
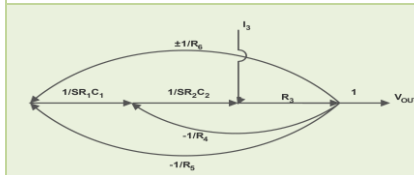
LP  
controlle  
d BP  
filter



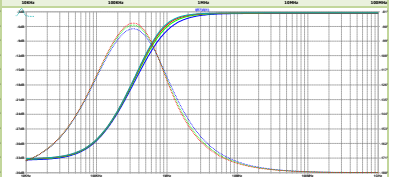
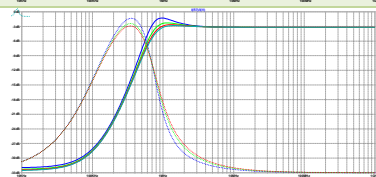
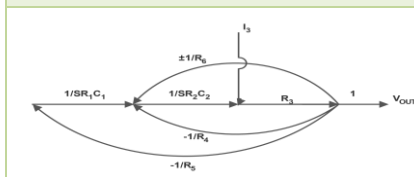
Notch  
controlle  
d BP  
filter



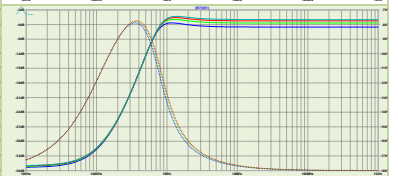
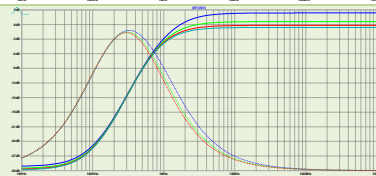
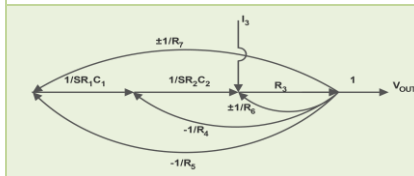
LP  
controlle  
d HP  
filter



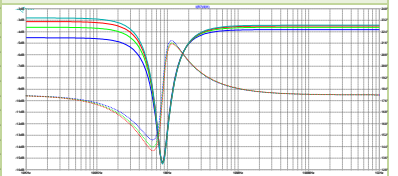
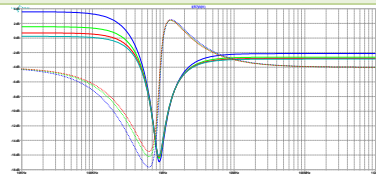
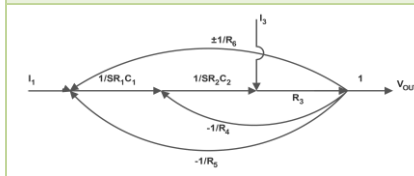
BP  
controlle  
d HP  
filter



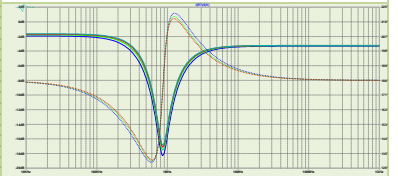
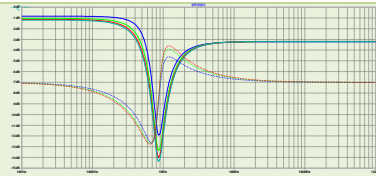
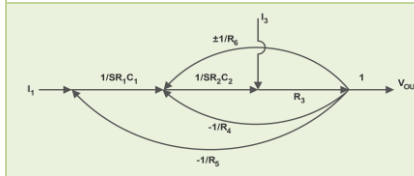
Notch  
controlle  
d HP  
filter



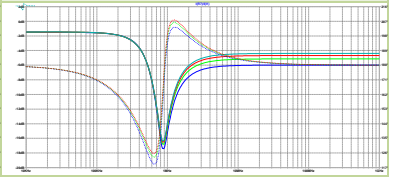
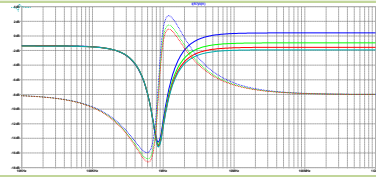
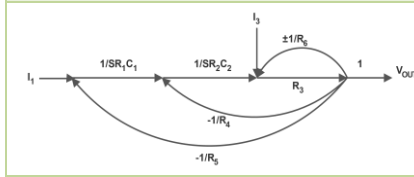
LP  
controlle  
d Notch  
filter



BP  
controlle  
d Notch  
filter



HP  
controlle  
d Notch  
filter



Color index: -- 60kΩ, --110kΩ, --160kΩ, --200kΩ

## **6.2 SUMMARY**

The filter output parameters of the LP, HP, BP, and Notch filters, as well as their characteristic features, can be controlled by varying the feedback gain by manipulating the feedback resistor values in an OTRA-based MISO shadow filter configuration. SPICE simulations are used to prove the feasibility of the proposed shadow filter output for various synergies of LP, BP, HP, and Notch filters. For the identical configuration, it was also discovered that the frequency response of a negative feedback filter was comparatively fitter than that of a positive feedback filter. The proposed structure can also be used to fine-tune various responses. These filters can be used in multi-grade transceivers as reconfigurable filters.

## **CHAPTER 7**

### **CONCLUSION AND FUTURE WORK**

This thesis describes the development of a new Current mode shadow filter based on OTRA. A brief history of filters and their importance in electronic circuits is presented in the introductory chapter, which serves as motivation for the work. Following that, the work's specific goal is presented. In Chapter 2, SPICE simulations are used to realize and characterize the OTRA block. In Chapter 3, OTRA-based applications are realized and simulated, from which it can be concluded that the OTRA provides electronic tuning capability of its trans-resistance gain by adjusting its bias current or voltage, and can be implemented using both bipolar and CMOS technologies. Additionally, circuits implemented with the OTRA do not require a resistor, making them ideal for any integrated circuit implementation. Chapter 4 presents a review of the existing literature on shadow filter design. In Chapter 5, a new feedback mode shadow filter is proposed. LP controlled LP filter, LP controlled BP filter, LP controlled HP filter, LP controlled notch filter, BP controlled LP filter, BP controlled BP filter, BP controlled HP filter, BP controlled notch filter, HP controlled LP filter, HP controlled BP filter, HP controlled HP filter, HP controlled notch filter, notch-controlled LP filter, notch controlled BP filter, notch controlled HP filter, notch controlled notch filter, notch controlled notch filter. The following are the benefits of the proposed voltage mode shadow filter:

- i) A MISO configuration is used, which eliminates the need for a separate summing amplifier.
- ii) ii) By adjusting the gains of the external Resistance, the parameters of this filter can be easily controlled electronically.
- iii) iii) No component-matching or inverting inputs are required in order to realize the filter responses. The proposed filter's responses are validated using a TSMC 180 nm CMOS process, and the results agree with the theoretical values.

The generalization of the OTRA-based shadow filter so that any multiple input single output filter can be easily converted to a shadow filter without the use of summing circuits is one of the future goals.

## REFERENCES

- [1] T. L. Deliyannis, Y. Sun, J. K. Fidler, "Continuous-Time Active Filter Design", New York CRC Press LLC, 1999.
- [2] M. Kumngern, B. Knobnob, K. Dejhan, "Electronically tunable high input impedance voltage-mode universal biquadratic filter based on simple CMOS OTAs", AEU International Journal of Electronics and Communications, vol. 64, pp. 934-939, 2010.
- [3] H. P. Chen, S. S. Shen, J.P. Wang, "Electronically tunable versatile voltage-mode universal filter", AEU International Journal of Electronics and Communications, vol. 62, pp. 316-319, 2008.
- [4] Chen, J. J., Tsao H. W., Chen, C. C. Operational transresistance amplifier Using CMOS Technology. Electronics Letters. 1992, vol. 28, no. 22, p. 2087–2088.
- [5] Chen J. J., Tsao H. W., Liu S. and Chui W., Parasitic-capacitance-insensitive current-mode filters using operational transresistance amplifiers, IEE Proc. Circuits Devices and Systems 1995, vol. 142, no. 3, p. 186–192.
- [6] Salama K. N., Soliman A. M., CMOS operational transresistance amplifier for analog signal processing. Microelectron J. 1999, vol. 30, issue 3, p. 235–45.
- [7] Mostafa H. and Soliman A.M., A modified CMOS realization of the operational transresistance amplifier Frequenz, 2006, vol. 60, p. 70-76.
- [8] Kafrawy A. K. and Soliman A. M., "New CMOS Operational Transresistance Amplifier", International Conference on Microelectronics, 2008, p. 31-34.
- [9] Kafrawy A. K. and Soliman A. M., A modified CMOS differential operational transresistance amplifier (OTRA), Int. J. Electron. Commun. 2009, (AEU) vol. 63, p. 1067-1071.
- [10] Toker A., Özoğuz S., Cicekoglu O. and Acar C., Current-mode allpass filters using current differencing buffered amplifier and new high-Q bandpass filter configuration, IEEE Tran. Circuits Syst. II, Analog Digital Signal Process. Sep. 2000, vol. 47, no. 9, p. 949–954.
- [11] Riewruja V., Parnklang J. and Julprapa A., Current Tunable Cmos Operational Transresistance Amplifier, ISIE 2001, vol. 2, p. 1328–1338.
- [12] Ravindran A., Salva A., Younus Md. I. and Ismail M., A 0.8V CMOS filter based on a novel low voltage OTRA, IEEE 2002, vol. III p. 368-371.
- [13] Brodie J., A notch filter employing current differencing operational amplifier, International Journal of Electronics, 1976, vol. 41, no. 5, p. 501–508.
- [14] National Semiconductor Corp., Designing with a New Super Fast Dual Norton Amplifier, Linear Applications Data Book, 1981.

- [15] National Semiconductor Corp., The LM3900: A New Current Differencing ^ Quad of the Input Amplifiers, Linear Applications Data Book, 1986.
- [16] Chen J. J., Tsao H. W. and Liu S. I., Voltage-mode MOSFET-C filters using operational transresistance amplifiers (OTRAs) with reduced parasitic capacitance effect, IEE Proc.-circuits Devices Sys., October 2001, vol. 148, no.5, p. 242-249.
- [17] Cam U., Cakri C. and Cicekoglu O., Novel Transmission Type First Order All- Pass Filter Using Single OTRA, Int. J. Electron. Commun. 2004 (AEU), vol. 58, p. 296- 298.
- [18] Kiling S. and Cam U., Operational Transresistance Amplifier Based First-Order allpass Filter with an Application Example, the 47th IEEE International Midwest Symposium on Circuits and Systems, 2004, p. I-65 to I-68.
- [19] Kiling S. and Cam U., Transimpedance Type Fully Integrated Biquadratic Filters Using Operational Transresistance Amplifiers, Analog Integrated Circuits and Signal Processing, 2006, vol. 47, p. 193-198.
- [20] Gokcen A. and Cam U., MOS-C single amplifier biquads using the Operational Transresistance Amplifiers, Int. J. Electron. Commun. 2009, (AEU), vol. 63, p. 660- 664.
- [21] Kaçar F., Operational Transresistance Amplifier Based Current-Mode All-pass Filter Topologies, Applied Electronics, 2009, p. 149–152.
- [22] Pandey R. and Bothra M., Multiphase Sinusoidal Oscillators Using Operational Trans-Resistance Amplifier, IEEE Symposium on Industrial Electronics and Applications, 2009, p. 371-376.
- [23] Cam U., A Novel Single-Resistance-Controlled Sinusoidal Oscillator Employing Single Operational Transresistance Amplifier, Analog Integrated Circuits and Signal Processing, 2002, vol. 32, p. 183–186.
- [24] Salama K. N. and Soliman A. M., Novel oscillators using the Operational Transresistance Amplifiers, Microelectronics Journal, 2000, vol. 31, p. 39-47.
- [25] Lo Y. K. and Chien H. C., Single OTRA-based current-mode monostable multivibrator with two triggering modes and a reduced recovery time, IET Circuits Devices Syst., 2007, vol. 1, no. 3, p. 257–261.
- [26] Lo Y. K. and Chien H. C., Current-Mode Monostable Multivibrators Using OTRAs, IEEE Transactions on Circuits and Systems, Nov. 2006, vol. 53, no. 11, p. 1274- 1278.
- [27] Hou C.L., Chien H.C. and Lo Y.K., Square wave generators employing OTRAs, IEE Proc.-Circuits Devices Syst., Dec. 2005, vol. 152, no. 6, p. 718-722.
- [28] Lo Y. K., Chien H. C. and Chiu H. J., Current-input OTRA Schmitt trigger with dual hysteresis modes, Int. J. Circ. Theor. Appl., 2009.

- [29] Kacar F., Cam U., Cicekoglu O., Kuntman H. and Kuntman A., New parallel immittance simulator realizations using single OTRA. 2002,
- [30] Cam U., Kacar F., Cicekoglu O., Kuntman H. and Kuntman A., Novel Grounded Parallel Immittance Simulator Topologies Employing Single OTRA. 2003, *Int. J. Electron. Commun. (AEU)*, vol. 57, no. 4, p. 287-290.
- [31] Cam U., Kacar F., Cicekoglu O., Kuntman H. and Kuntman A., Novel Two OTRA- Based Grounded Immittance Simulator Topologies. 2004, *Analog Integrated Circuits and Processing*, vol. 39, p.169-175.
- [32] Sánchez-López C., Fernández F.V. and Tlelo-Cuautle E., Generalized admittance matrix models of OTRAs and COAs. *Microelectronics Journal*, August 2010, vol. 41, issue 8, p. 502-505.
- [33] Mostafa, H., & Soliman, A. M. (2006). A modified CMOS realization of the operational transresistance amplifier (OTRA). *Frequenz*. 60(3–4), 70–77.
- [34] Y. Lakys, A. Fabre, “Shadow filters: New family of second-order filters”, *Electronics Letters*, vol. 46, pp. 276–277, 2010.
- [35] Anurag, Rashika & Pandey, Rajeshwari & Pandey, Neeta & Singh, Mandeep & Jain, Manish. (2015). OTRA based shadow filters. 1-4.
- [36] Annu Dabas, Neha Arora (2014). TUNABLE FILTERS USING OPERATIONAL TRANSRESISTANCE AMPLIFIER. *International Journal of Electrical and Electronics Engineering (IJEEER)* ISSN(P): 2250-155X; ISSN(E): 2278-943X Vol. 4, Issue 4, 103-112.
- [37] Chadha, Ujjwal & Arora, Tajinder. (2016). SIMO and MISO universal filters employing OTRA. 47-52. 10.1201/9781315364094-10.
- [38] Roy, S.C.. (2014). ‘Shadow’ Filters - A New Family of Electronically Tunable Filters. *IETE Journal of Education*. 51. 75-78. 10.1080/09747338.2010.10876070.